VNIVERSITAT DE VALÈNCIA

Doctorat en Neurociències
Bàsiques i Aplicades

# NONAPEPTIDERGIC SYSTEMS IN THE BRAIN OF THE MOUSE

## Mapping the Distribution of Vasopressin and Oxytocin in the Social and Maternal Brain

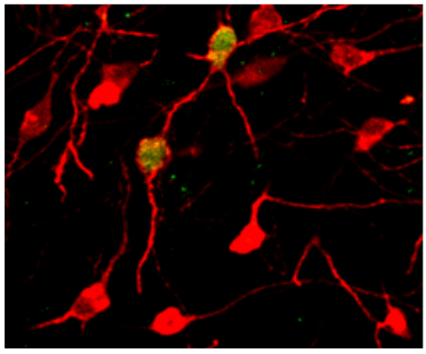

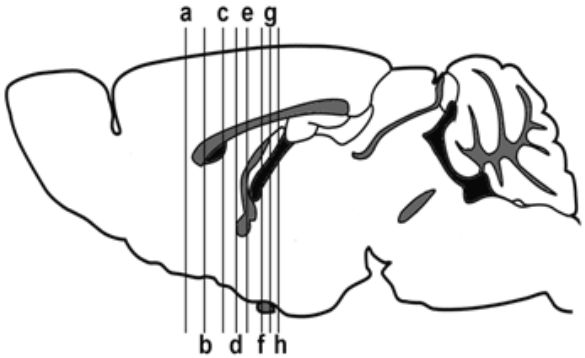


TESIS DOCTORAL
**Marcos Otero García**
DIRIGIDA POR
**Fernando Martínez García**

VNIVERSITAT DE VALÈNCIA

Departament de Biologia Funcional
i Antropologia Física

# SISTEMAS NONAPEPTIDÉRGICOS EN EL ENCÉFALO DEL RATÓN

## Cartografiando la Distribución de Vasopresina y Oxitocina en el Cerebro Social y Maternal

**Doctorado en Neurociencias Básicas y Aplicadas**

Doctorando: **Marcos Otero García**

Director de Tesis: **Fernando Martínez García**

Burjassot, 2015

Fernando Martínez García, Catedràtic de Fisiologia del Departament de Biologia Funcional i Antropologia Física de la Universitat de València, actualment en comissió de serveis a la Unitat Predepartamental de Medicina de la Universitat Jaume I (UJI) de Castelló

*Fernando Martinez-Garcia, Professor of Physiology at the Department of Functional Biology and Physical Anthropology of the University of València, currently at the Predepartmental Unit of Medicine of the Universitat Jaume I (UJI) in Castelló*

**C e r t i f i q u e / *H e r e b y c e r t i f y***

Que **En Marcos Otero García**, llicenciat en Biologia per la *Universitat de València*, ha realitzat sota la meua direcció el treball titulat ***"SISTEMAS NONAPEPTIDÉRGICOS EN EL ENCÉFALO DEL RATÓN. Cartografiando la Distribución de Vasopresina y Oxitocina en el Cerebro Social y Maternal"*** per a l'obtención del grau de Doctor en Neurociències Bàsiques i Aplicades.

*That **Mr. Marcos Otero García**, BSc in Biology at the University of València, has performed, under my supervisión the work entitled: "NONAPEPTIDERGIC SYSTEMS IN THE BRAIN OF THE MOUSE. Mappingthe Distribution of Vasopressin and Oxytocin in the Social and Maternal Brain" to obtain the PhD in Basic and Applied Neurosciences.*

La qual cosa signe a Burjassot, el dia 8 de Juny de 2015

*What I sign as required in Burjassot, on June the 8th 2015*

Fernando Martínez García, PhD

Durante la realización de esta tesis, el autor ha sido beneficiario de una beca del Programa de Formación de Profesorado Universitario del Ministerio de Educación y Ciencia; FPU (AP2009-4256).

Este trabajo se ha enmarcado en los proyectos financiados por:

- Ministerio de Educación y Ciencia-FEDER *Papel de las vias amigdalo-estriatales en el procesamiento del valor reforzante de las feromonas sexuales y sus componentes* (BFU2007-67912-C02-01)
- Ministerio de Economia y Competitividad-FEDER *Señales vomeronasales y control amigdalino del comportamiento sociosexual: un modelo experimental de la neurobiologia del comportamiento social y sus alteraciones* (BFU2013-47688-P)
- Junta de Comunidades de Castilla-La Mancha/FEDER *Alteraciones en los sistema quimiosensoriales en las enfermedades de Alzheimer y Parkinson* (PEIC11-0045-4490)
- Vicerectorado de Investigación de la Universitat Jaume I de Castelló

## ACKNOWLEDGMENTS

It is not easy to acknowledge all the people that have made possible this doctoral thesis and do it fairly, briefly and without forgetting anyone, but I will try.

First of all, thanks to Fernando, who gave me the opportunity to join the lab and has been more than a mentor, even a father; thanks for contributing so to my personal growth. If I had a mother in this big family of science it would be Dori, without whom the lab simply couldn't run; thanks for your always honest advice. Thanks to Quique, for his help, support and kindness. Thanks to Carmen and Joana, for being excellent teachers and friends.

I'm especially thankful to Ana and Lluis, who began the work that gave way to this thesis; you've been the best mates and I hope I won't forget all we've learned together. Thanks to Hugo and his big heart, big mind, and even bigger laughs. Thanks to Beña for her support and undaunted advice. Thanks to Paco for all what he taught me. And thanks to Mike Ludwig for his kindness and support during the stay-abroad, and to the members of his lab.

Of course, thanks to my parents and my brother who have unconditionally supported me since before the beginning, and thanks to Nuria and to the rest of my family for their encouragement. This little journey wouldn't have been possible without the support of both my scientific and biological families.

Finally, thanks to my friends for their indispensable help, for bearing my spiels, cheering me up and even feeding me. I'd like to thank also all the people that helped me at some point along the way but my fickle memory may not remember at this final stretch.

# INDEX

## ABBREVIATIONS

| | |
|---|---|
| **10N** | dorsal motor nucleus of the vagus |
| **12N** | hypoglossal nucleus |
| **3V** | 3rd ventricle |
| **4n** | trochlear nerve or its root |
| **4V** | 4$^{th}$ ventricle |
| **A1** | A1 noardrenaline cells |
| **AC** | anterior commissural nucleus |
| **AC** | anterior commissural nucleus |
| **aca** | anterior commissure, anterior part |
| **Acb** | accumbens nucleus |
| **AcbC** | accumbens nucleus, core |
| **AcbSh** | accumbens nucleus, shell |
| **ACo** | anterior cortical amygdaloid nucleus |
| **acp** | anterior commissure, posterior part |
| **AD** | anterodorsal thalamic nucleus |
| **ADP** | anterodorsal preoptic nucleus |
| **AH** | anterior hypothalamic area |
| **AHA** | anterior hypothalamic area, anterior part |
| **AHP** | anterior hypothalamic area, posterior part |
| **AIP** | agranular insular cortex, posterior part |
| **AM** | anteromedial thalamic nucleus |
| **Amb** | ambiguus nucleus |
| **AN** | accessory nuclei |
| **AP** | area postrema |
| **APir** | amygdalopiriform transition area |
| **Aq** | aqueduct (Sylvius) |
| **Arc** | arcuate hypothalamic nucleus |
| **AStr** | amygdalostriatal transition area |
| **AV** | anteroventral thalamic nucleus |
| **AVP** | arginine-vasopressin |
| **AVPe** | anteroventral periventricular nucleus |
| **AVP-ir** | arginine-vasopressin immunoreactive |
| **AVV** | anteroventral thalamic nucleus, ventral part |
| **BAC** | bed nucleus of the anterior commissure |
| **BAOT** | bed nucleus of the accessory olfactory |
| **Bar** | Barrington's nucleus |
| **BL Amy** | basolateral amygdala |
| **BLA** | basolateral amygdaloid nucleus, anterior |
| **BLV** | basolateral amygdaloid nucleus, ventral |
| **BMA** | basomedial amygdaloid nucleus, anterior |
| **BST** | bed nucleus of the stria terminalis |
| **BSTA** | bed nucleus of the stria terminalis, anterior part |
| **BSTIA** | bed nucleus of the stria terminalis, intraamygdaloid division |

| | |
|---|---|
| **BSTLD** | bed nucleus of the stria terminalis, lateral division, dorsal part |
| **BSTLP** | bed nucleus of the stria terminalis, lateral division, posterior part |
| **BSTLV** | bed nucleus of the stria terminalis, lateral division, ventral part |
| **BSTMA** | bed nucleus of the stria terminalis, medial division, anterior part |
| **BSTMP** | bed nucleus of the stria terminalis, medial division, posterior part |
| **BSTMPI** | bed nucleus of the stria terminalis, medial division, posterointermediate part |
| **BSTMPL** | bed nucleus of the stria terminalis, medial division, posterolateral part |
| **BSTMPM** | bed nucleus of the stria terminalis, medial division, posteromedial part |
| **BSTMV** | bed nucleus of the stria terminalis, medial division, ventral part |
| **BSTS** | bed nucleus of the stria terminalis, supracapsular part |
| **cc** | corpus callosum |
| **CC** | central canal |
| **Ce** | central amygdaloid nucleus |
| **CeC** | central amygdaloid nucleus, capsular part |
| **CeL** | central amygdaloid nucleus, lateral division |
| **CeM** | central amygdaloid nucleus, medial division |
| **CeMAD** | central amygdaloid nucleus, medial division, anterodorsal part |
| **CeMAV** | central amygdaloid nucleus, medial division, anteroventral part |
| **CGPn** | central gray of the pons |
| **Cl** | claustrum |
| **CL** | centrolateral thalamic nucleus |
| **CM** | central medial thalamic nucleus |
| **cp** | cerebral peduncle, basal part |
| **CPu** | caudate putamen (striatum) |
| **cst** | commissural stria terminalis |
| **Cu** | Cuneate nucleus |
| **CxA** | cortex-amygdala transition zone |
| **D3V** | dorsal 3rd ventricle |
| **DEn** | dorsal endopiriform nucleus |
| **DG** | dentate gyrus |
| **DLPAG** | dorsolateral periaqueductal gray |
| **DM** | dorsomedial hypothalamic nucleus |
| **DMPAG** | dorsomedial periaqueductal gray |
| **DMTg** | dorsomedial tegmental nucleus |
| **DP** | dorsal peduncular cortex |
| **DpMe** | deep mesencephalic nucleus |
| **DRC** | dorsal raphe nucleus, caudal part |
| **DRI** | dorsal raphe nucleus, interfascicular part |
| **DTg** | dorsal tegmental nucleus |
| **DTgP** | dorsal tegmental nucleus, pericentral part |
| **DTM** | dorsal tuberomammillary nucleus |
| **DTT** | dorsal tenia tecta |
| **ECu** | external cuneate nucleus |
| **EW** | Edinger-Westphal nucleus |
| **f** | fornix |

| | |
|---|---|
| **F** | nucleus of the fields of Forel |
| **FG** | fluorogold |
| **fi** | fimbria of the hippocampus |
| **fmi** | forceps minor of the corpus callosum |
| **fr** | fasciculus retroflexus |
| **GrDG** | granular layer of the dentate gyrus |
| **Gus** | gustatory thalamic nucleus |
| **HDB** | nucleus of the horizontal limb of the diagonal band |
| **Hip** | Hippocampus |
| **I** | intercalated nuclei of the amygdala |
| **IAD** | interanterodorsal thalamic nucleus |
| **ic** | internal capsule |
| **ICj** | islands of Calleja |
| **ICjM** | islands of Calleja, major island |
| **ICjvm** | islands of Calleja, ventromedial island |
| **icp** | inferior cerebellar peduncle |
| **icv** | intracerebroventricular |
| **IG** | indusium griseum |
| **IL** | infralimbic cortex |
| **IM** | intercalated amygdaloid nucleus, main part |
| **In** | intercalated nucleus of the medulla |
| **IO** | inferior olive |
| **IOD** | inferior olive, dorsal nucleus |
| **IPAC** | interstitial nucleus of the posterior limb of the anterior commissure |
| **IPACL** | lateral interstitial nucleus of the posterior limb of the anterior commissure |
| **IPACM** | medial interstitial nucleus of the posterior limb of the anterior commissure |
| **IRt** | intermediate reticular nucleus |
| **KF** | Ko¨lliner-Fuse nucleus |
| **La** | lateral amygdaloid nucleus |
| **LA** | lateroanterior hypothalamic nucleus |
| **LaDL** | lateral amygdaloid nucleus, dorsolateral part |
| **LaVL** | lateral amygdaloid nucleus, ventrolateral part |
| **LaVM** | lateral amygdaloid nucleus, ventromedial part |
| **LC** | locus coeruleus |
| **LDTg** | laterodorsal tegmental nucleus |
| **LDTgV** | laterodorsal tegmental nucleus, ventral part |
| **LEnt** | lateral entorhinal cortex |
| **LGP** | lateral globus pallidus |
| **LH** | lateral hypothalamic area |
| **LHb** | lateral habenular nucleus |
| **lo** | lateral olfactory tract |
| **LPBE** | lateral parabrachial nucleus, external part |
| **LPBS** | lateral parabrachial nucleus, superior part |
| **LPBV** | lateral parabrachial nucleus, ventral part |
| **LPMR** | lateral posterior thalamic nucleus, mediodorsal part |

| | |
|---|---|
| **LPO** | lateral preoptic area |
| **LRt** | lateral reticular nucleus |
| **LS** | lateral septum |
| **LSD** | lateral septal nucleus, dorsal part |
| **LSI** | lateral septal nucleus, intermediate part |
| **LSV** | lateral septal nucleus, ventral part |
| **LV** | lateral ventricle |
| **mAC** | mouse accessory nuclei |
| **maopt** | medial accessory optic tract |
| **MCLH** | magnocellular nucleus of the lateral hypothalamus |
| **MCPO** | magnocellular preoptic nucleus |
| **MD** | mediodorsal thalamic nucleus |
| **MdD** | medullary reticular nucleus, dorsal part |
| **MdV** | medullary reticular nucleus, ventral part |
| **Me** | medial amugdaloid nucleus |
| **Me5** | mesencephalic trigeminal nucleus |
| **MeA** | medial amugdaloid nucleus, anterior part |
| **MeAD** | medial amygdaloid nucleus, anterior dorsal part |
| **MeAV** | medial amygdaloid nucleus, anteroventral part |
| **MeEA** | medial extended amygdala |
| **MePD** | medial amygdaloid nucleus, posterodorsal part |
| **MePV** | medial amygdaloid nucleus, posteroventral part |
| **mfb** | medial forebrain bundle |
| **MGP** | medial globus pallidus (entopeduncular nucleus) |
| **MHb** | medial habenular nucleus |
| **Mid** | midbrain |
| **ml** | medial lemniscus |
| **mlf** | medial longitudinal fasciculus |
| **MnPO** | median preoptic nucleus |
| **MPA** | medial preoptic area |
| **MPB** | medial parabrachial nucleus |
| **MPO** | medial preoptic nucleus |
| **MPOL** | medial preoptic nucleus, lateral part |
| **MPOM** | medial preoptic nucleus, medial part |
| **MS** | medial septal nucleus |
| **mt** | mamillothalamic tract |
| **mtg** | mamillotegmental tract |
| **MTu** | medial tuberal nucleus |
| **MVe** | medial vestibular nucleus |
| **mvStP** | medioventral striato-pallidum |
| **NADPHd** | Nicotinamide adenine dinucleotide phosphate diaphorase |
| **Ns** | nigrostriatal bundle |
| **O** | nucleus O |
| **opt** | optic tract |
| **OT** | oxytocin |

| | |
|---|---|
| **OT-ir** | oxytocin-like immunoreactive (referring to immunostaining using antibodies raised against oxytocin or against its specific neurophysin) |
| **PaAP** | paraventricular hypothalamic nucleus, anterior parvicellular |
| **PAG** | periaqueductal gray |
| **PaL** | paraventricular hypothalamic nucleus, lateral part |
| **PaM** | paraventricular hypothalamic nucleus, medial part |
| **PaPo** | paraventricular hypothalamic nucleus, posterior part |
| **PaV** | paraventricular hypothalamic nucleus, ventral part |
| **PB** | phosphate buffer |
| **PBS** | phosphate buffered saline |
| **PC** | paracentral thalamic nucleus |
| **Pc** | posterior commissure |
| **PCom** | nucleus of the posterior commissure |
| **Pe** | periventricular hypothalamic nucleus |
| **PeF** | perifornical nucleus |
| **PF** | parafascicular thalamic nucleus |
| **PH** | posterior hypothalamic area |
| **Pir** | piriform cortex |
| **PLCo** | posterolateral cortical amygdaloid nucleus |
| **PMCo** | posteromedial cortical amygdaloid nucleus |
| **PMD** | premammillary nucleus, dorsal part |
| **PMn** | paramedian reticular nucleus |
| **PMnR** | paramedian raphe nucleus |
| **PMV** | premamillary nucleus, ventral part |
| **PnC** | pontine reticular nucleus, caudal part |
| **PO** | periolivary region |
| **Pr5** | principal sensory trigeminal nucleus |
| **PRh** | perirhinal cortex |
| **PrL** | prelimbic cortex |
| **PSTh** | parasubthalamic nucleus |
| **PT** | paratenial thalamic nucleus |
| **PV** | paraventricular thalamic nucleus |
| **PVA** | paraventricular thalamic nucleus, anterior part |
| **Py** | pyramidal cell layer of the hippocampus |
| **Rad** | stratum radiatum of the hippocampus |
| **Re** | reuniens thalamic nucleus |
| **RI** | rostral interstitial nucleus of the medial longitudinal fasciculus |
| **RLi** | rostral linear nucleus of the raphe |
| **RMg** | raphe magnus nucleus |
| **RPF** | retroparafascicular nucleus |
| **RRF** | retrorubral field |
| **rs** | rubrospinal tract |
| **Rt** | reticular thalamic nucleus |
| **SBN** | social brain network |
| **SCh** | suprachiasmatic nucleus |

| | |
|---|---|
| **SCO** | subcommissural organ |
| **scp** | superior cerebellar peduncle |
| **SFi** | septofimbrial nucleus |
| **SFO** | subfornical organ |
| **Shi** | septohippocampal nucleus |
| **SHy** | septohypothalamic nucleus |
| **SI** | substantia innominata |
| **SL** | semilunar nucleus |
| **SLu** | stratum lucidum, hippocampus |
| **SM** | nucleus of the stria medullaris |
| **sm** | stria medullaris of the thalamus |
| **SN** | substantia nigra |
| **Sol** | nucleus of the solitary tract |
| **sol** | solitary tract |
| **SON** | supraoptic nucleus |
| **SOR** | supraoptic nucleus, retrochiasmatic part |
| **SP** | substance P |
| **sp5** | spinal trigeminal tract |
| **st** | stria terminalis |
| **StA** | striatal part of the preoptic area |
| **Str** | striatum |
| **Su3** | supraoculomotor periaqueductal gray |
| **Su5** | supratrigeminal nucleus |
| **SubB** | subbrachial nucleus |
| **SubC** | subcoeruleus nucleus |
| **TBS** | TRIS buffered saline |
| **TC** | tuber cinereum area |
| **Te** | terete hypothalamic nucleus |
| **Tu** | olfactory tubercle |
| **Unc** | uncinate fasciculus |
| **V1aR** | arginine-vasopressin receptor type 1a |
| **V1bR** | arginine-vasopressin receptor type 1b |
| **VA** | ventral anterior thalamic nucleus |
| **VDB** | nucleus of the vertical limb of the diagonal band |
| **VEn** | ventral endopiriform nucleus |
| **VLPO** | ventrolateral preoptic nucleus |
| **VM** | ventromedial thalamic nucleus |
| **VMH** | ventromedial hypothalamic nucleus |
| **VMHC** | ventromedial hypothalamic nucleus, central part |
| **VMHDM** | ventromedial hypothalamic nucleus, dorsomedial part |
| **VMHVL** | ventromedial hypothalamic nucleus, ventrolateral part |
| **VMPO** | ventromedial preoptic nucleus |
| **VOLT** | vascular organ of the lamina terminalis |
| **VP** | ventral pallidum |
| **vsc** | ventral spinocerebellar tract |

| | |
|---|---|
| **VTA** | ventral tegmental area |
| **VTg** | ventral tegmental nucleus |
| **VTM** | ventral tuberomammillary nucleus |
| **VTT** | ventral tenia tecta |
| **Xi** | xiphoid thalamic nucleus |
| **ZI** | zona incerta |

# INTRODUCTION

## 1. Social behaviour

Social behaviour is defined as the interactions that occur between two or more individuals of the same species. Social behaviour likely evolved as a survival response to selective pressures, increasing survival of the individuals engaging in it. For example, cooperative interactions can facilitate obtaining food or increase the protection against predators, ease traveling (e.g. bird flocks) and improve breeding. These benefits can arise from the specialization of tasks, which is carried to the extreme by eusocial species of the Hymenoptera and Isoptera orders, but also by rodents like mole-rats (*Heterocephalus glaber* and *Fukomys damarensis*) (O'Riain & Faulkes, 2008; Wilson & Hölldobler, 2005). Eusocial animals have cooperative brood care, division of labour into reproductive and non-reproductive groups and overlapping generations of adults alive at the same time within a colony. In contraposition to eusociality, there is the term presociality, which can be divided in three categories as originally purposed by C.D. Michener for insects: subsociality, solitary but social and parasociality (Michener, 1969). Subsocial animals care for their young during a given length of time, but they don't associate with other adults. If adults gather occasionally, for breeding or sleeping, they are classified as solitary-but-social species. Finally, parasocial animals always share a cooperative dwelling. Parasocial species include communal (share a single nest but care of their own young), quasisocial (share nest and brood care) and semisocial (share nest and brood care, have division of labour, but adult generations do not overlap).

Although the classification of sociality was originally intended for insects, it can be applied to other animal taxa. In fact, social behaviour is exhibited by an extraordinary wide variety of animals, including invertebrates, fish, birds and mammals. Within a given species, social behaviour is diverse as it can serve different purposes. Depending on the aim of a particular social behaviour, it can be broadly categorised as agonistic, affiliative, sexual or parental.

One of the disadvantages of social aggregation is the reduction of available resources per individual. Agonistic behaviours emerge for the competition for resources that are often limited, including food, shelter and mates. The term agonistic (competitive) behaviour includes all intraspecific conducts adapted to situations involving physical conflict (aggression, threats, displays, retreats, placating aggressors and conciliation) and consists of three kinds of behaviours: threat, aggression and submission. These three behaviours are functionally and physiologically interrelated and, though they can be displayed alone, normally occur sequentially (McGlone, 1986). Some authors define two types of agonistic behaviour, offensive and defensive, on the basis of differences in motor patterns, functions and outcomes

(Blanchard & Blanchard, 1988). In the case of mice, even though males are more aggressive, both males and females display offensive and defensive behaviours.

Affiliative social behaviours foster the development and maintenance of social relationships and bonds. In most animals, these behaviours are commonly observed in the context of specific types of long-lasting social relationships, such as mother-infant bonding and sexual pair-bonding, and involve extensive body contact and frequent communication (Stoesz, Hare, & Snow, 2013).

Sexual behaviour plays a main role in reproduction and is highly dimorphic between sexes. In mammals, it is organized in two main phases, anticipatory and consummatory. In the case of males, penile erection, seminal emission and ejaculation characterize the consummatory phase, while vaginal lubrication, clitoris erection and orgasm are typical of the female sexual response. These consummatory responses are preceded by an anticipatory phase which includes motivation towards and searching of an adequate partner (Agmo, 1997; Pfaus, 1999).

Parental behaviour is the collection of behaviours aimed to increase offspring survival. These behaviours are most frequently displayed by the mother and termed maternal behaviours. However, in many species male progenitors show similar nurturing behaviours called paternal behaviours. If older conspecifics also take care of the brood, these conducts are labelled alloparental behaviour. In the case of mice and rats, maternal behaviours can be pup directed, which include retrieval, nursing, grouping, licking and tactile stimulation. Non-pup directed behaviours include nest building, placentophagia and defence of the young. If the latter is directed towards a conspecific, this defensive behaviour is called maternal aggression. Maternal behaviour is of particular interest in social neurobiology due to its long-term impact in child's future stress reactivity and developing personality. Moreover, maternal behaviour is inherited in part through epigenetic mechanisms, shaping the parenting style of the next generation (e.g. Francis et al. 1999; Fleming et al. 2002).

For a long time, social behaviour seemed too intricate to be studied and understood at a mechanistic level. However, technical advances in neuroscience research and the use of animal models are now unvealing complex brain networks at morphological, connective and neurochemical levels. In the case of socio-sexual behaviours, their expression depends on internal physiological regulators (like hormonal state) and on external sensory cues. However, most socio-sexual behaviours (such as mating or aggression) are innate, so the circuitry underlying them is hard-wired into the genome.

The mouse (*Mus musculus*), widely used in neuroscience research, has a rich social life. Like other rodents, their social communication and behaviour depend on recognizing conspecifics and assessing their gender, age/maturity, hormonal status and/or hierarchy. Since mice are macrosmatic animals, they obtain most information from conspecifics via chemical signals, which drive their social interactions. These chemical signals can be detected via the olfactory and/or the vomeronasal system, and they parallel the role that visual and auditory cues play in social communication in humans. Specifically, in mice and other rodents, chemicals excreted or secreted by an individual elicit stereotyped reactions in other individuals, thus fulfilling the classical definition of pheromones (Karlson & Luscher, 1959). Previous work from our group aimed at identifying the olfactory or vomeronasal nature of the pheromones that mediate sexual attraction in female mice. Thus, early studies demonstrated that females reared in complete absence of adult males or their odours consistently preferred male-soiled bedding to female soiled-bedding when they had unrestricted access to the bedding, but not when they had restricted access to the volatile odorants emanating from the bedding (Moncho-Bogani et al. 2002). This result suggested that male mice secreted some involatile pheromones that were innately attractive to the females. These putative pheromones acted as effective reinforcers in a conditioned place preference paradigm (Martinez-Ricos, Agustin-Pavon, Lanuza, & Martinez-Garcia, 2007). Lesions of the accessory olfactory bulb abolished both attraction and place preference, demonstrating that the putative pheromones were detected by the vomeronasal system (Martinez-Ricos, Agustin-Pavon, Lanuza, & Martinez-Garcia, 2008).

More recent work has identified some of these male pheromones that are detected by the vomeronasal system. For example, a peptidic compound of the lacrimal secretion of males, ESP1, induces female receptivity (Haga et al., 2010), whereas darcin, a major urinary protein (MUP), is responsible for female attraction (Roberts et al. 2010), and induces conditioned place preference (Roberts et al, 2012).

Further, our group recently demonstrated that darcin promotes maternal aggression in lactating dams (Martín-Sánchez et al, 2015), in contrast to its attractive properties for virgin females. Similarly, MUPs are responsible for agonistic aggression between males (Chamero et al., 2007). In summary, these data reveal that chemosignals play a key role in modulating social behaviour in mice, and suggest that brain nuclei processing olfactory and vomeronasal information will be part of the brain network which controls social behaviour, as we discuss below.

## 2. The sociosexual brain and the amygdala

Social behaviours are under the control of a specific brain functional system, which is named the "socio-sexual brain network" (SBN), as originally proposed by Newman (1999). The SBN is composed of at least six nodes: the medial extended amygdala (medial amygdala plus medial bed nucleus of the stria terminalis), the lateral septum, the preoptic area, the anterior hypothalamus, the ventromedial hypothalamus and the midbrain (particularly the periaqueductal gray and various motor areas of the tegmentum; Fig A). All these nodes possess a few important features: each of the nodes has been implicated in the control of various forms of social behaviour, they are reciprocally interconnected and each area contains receptors for sex steroids (allowing the steroid modulation of behaviours like inter-male aggression and male or female sexual behaviours). Other brain areas are also important for socio-sexual behaviours, but this network proposed by Newman should be regarded as the "hub" of the social brain. In this model, each kind of social behaviour would not be regulated by a segregated linear system. Instead, each node of the network can respond to a variety of stimuli and each behavioural response is associated with a distinct pattern of response across the network (see Fig A). The model has its limitations, but it is supported by ample experimental data. In accordance with its adaptive importance, this network shows a high degree of conservation during evolution and is present in virtually all studied vertebrates (Goodson, 2005).

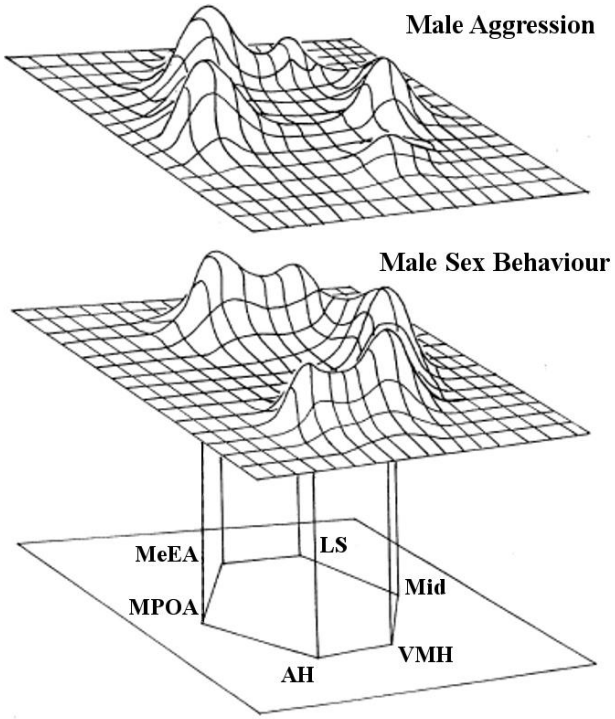


**Fig. A. The social behaviour network** as proposed by Newman (1999) –modified from the original paper-. The network is composed of six nodes: the medial extended amygdala (MeEA), lateral septum (LS), medial preoptic area (MPOA), anterior hypothalamus (AH), ventromedial hypothalamus (VMH) and midbrain (Mid). Schematic representations of early gene expression data show distinctive activation patterns across the nodes of the network, for two different behavioural outputs (male aggression and male sexual behaviour).

In the case of rodents, as stated above, olfactory and vomeronasal

cues (e.g. pheromones) play a key role in modulating socio-sexual interactions. This modulation takes place via direct and indirect olfactory and vomeronasal inputs to the SBN, which reach primarily the amygdala. As indicated above (see Fig. A), the medial extended amygdala is an important node of the SBN (Canteras, 2002; Newman, 1999). In fact, the medial extended amygdala is enriched in cells expressing receptors for oestrogens and androgens (Mitra et al., 2003; Simerly, Chang, Muramatsu, & Swanson, 1990), which are also present in other nuclei of the amygdala. The amygdala contains all the secondary vomeronasal centres of the brain and many secondary and tertiary olfactory centres (Martínez-García, Novejarque, Gutiérrez-Castellanos, & Lanuza, 2012), as well as convergent chemosensory information onto specific nuclei of the amygdala (Gutierrez-Castellanos, Martinez-Marcos, Martinez-Garcia, & Lanuza, 2010). These direct inputs from the olfactory bulbs, together with an intricate set of intra-amygdaloid connections, provide the medial extended amygdala, with updated information of the chemical composition of the environment, including the presence of pheromones and chemosignals.

Anatomical data in mice indicate that the posteromedial cortical amygdala, which constitutes the vomeronasal cortex (Gutiérrez-Castellanos, Pardo-Bellver, Martínez-García, & Lanuza, 2014), the medial amygdala and several olfactory and associative centres of the amygdala, project directly to specific regions of the medial aspect of the ventral striato-pallidum (mvStP; Ubeda-Banon et al. 2008; Novejarque et al. 2011; Pardo-Bellver et al. 2012). This is important since the ventral striatum is the core of the circuitry for motivated behaviours. For instance, specific portions of the nucleus accumbens shell and ventral pallidum mediate an opioid-dependent increase in food intake, whereas a distinct, small area of the nucleus accumbens is specifically involved in processing the hedonic impact of sweet taste (Pecina & Berridge, 2000, 2005). Therefore, the inputs from the chemosensory amygdala suggest that the anteromedial ventral striato-pallidum might include a region for pheromone-motivated behaviours, which would be crucial for the control of intraspecific interactions, e.g. deciding whether attacking or, on the contrary, expressing affiliative, parental or sexual behaviour towards conspecifics. In fact, independently replicated lesion studies indicate that the mvStP is necessary for the hedonic value of sexual chemosignals (Agustin-Pavon, Martinez-Garcia, & Lanuza, 2014; DiBenedictis, Olugbemi, Baum, & Cherry, 2014) and broad evidence from experiments in monogamous voles indicates that this region is crucial for pair-bond formation (Larry J Young & Wang, 2004).

In sexually reproducing species, social and sexual behaviours differ between genders. Accordingly, the neural circuitry on which they depend, the SBN, is also sexually dimorphic.

Sex-specific differences in the SBN are a consequence of both the organizational and activational effects of gonadal steroid hormones. During perinatal development, testosterone produced by the testes bind to steroid receptors in brain cells, regulating the survival of cells (e.g. protecting them against programmed apoptosis) as well as the transcription of key genes, thus leading to the development the dimorphic neural circuits (Geert J. de Vries, 2008; Morris, Jordan, & Breedlove, 2004; X. Xu et al., 2012). An organizational effect of oestrogens in females cannot be completely discarded, however (Brock, Baum, & Bakker, 2011).

Some of the genes whose expression is controlled by this organizational effect of testosterone are those coding receptors for gonadal steroids. Consequently, the SBN shows a dimorphic expression of gonadal steroid receptors. The socio-sexual behaviour in the adult individuals is, therefore, largely under activational control by sexual steroids.

## 3. Nonapeptides and the regulation of sociality

Besides the expression of receptors for sexual steroids and their reciprocal connectivity, the areas comprising the SBN share another distinctive feature: they are enriched in nonapeptidergic innervation and nonapeptide receptors. Rodents and other mammals express two closely related nonapeptides, arginine-vasopressin (AVP) and oxytocin (OT). Both peptides consist of nine aminoacids only differing at the 3rd and 8th positions (see Fig B), being the difference in the 8$^{th}$ position their most distinguishing feature.

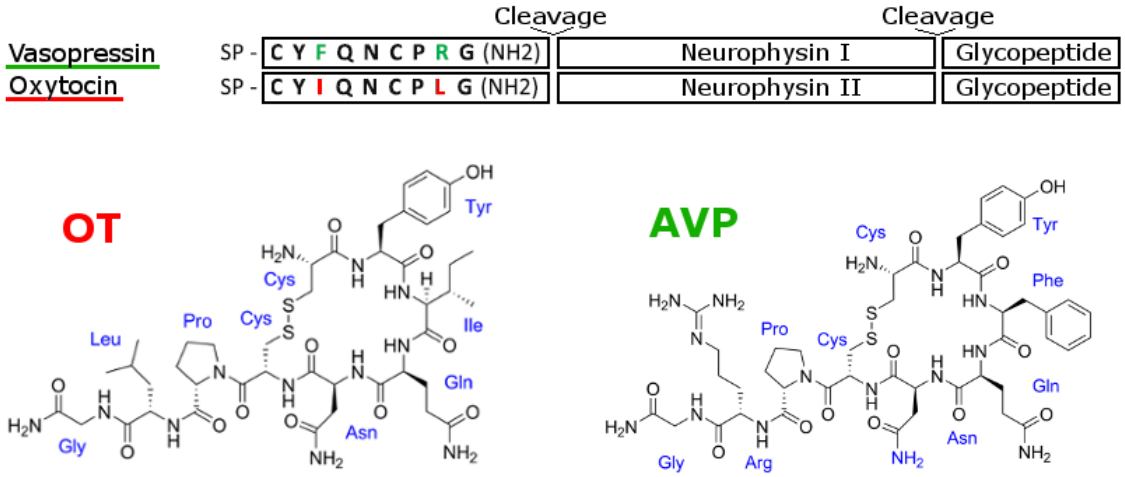


**Fig. B. Basic structure of AVP and OT pro-hormones and molecular structure of the nonapeptides.** On top, the basic structure of arginine-vasopressin and oxytocin prohormones: signalling peptide (SP) – cysteine, tyrosine, isoleucine(OT)/phenylalanine(AVP), glutamine, asparagine, cysteine, proline, leucine(OT)/arginine(AVP), glycine – cleavage site (glycine, lysine, arginine) – specific neurophysin (112aa) – monobasic cleavage site (alanine) – glycopeptide (39aa). Below, secondary structure of OT and AVP showing the disulphide bond between cysteines.

In mice, rats and humans, the OT and AVP genes are located on the same chromosome separated by a short (3.5–12 kbp) intergenic region but are in opposite transcriptional orientations. A comparative cladistic analysis reflects that both genes derive from a single one through gene-duplication, no far before vertebrate divergence (H. Caldwell & Young 3rd, 2006). The ancestral nonapeptide can be found in species as distant as snails and annelids. Most invertebrates have only one OT/AVP homolog whereas most vertebrates have two. However, the function of nonapeptides is highly conserved and non-mammalian homologues of AVP and OT fulfil similar roles in their respective species (Choleris, Pfaff, & Kavaliers, 2013).

The nonapeptides AVP and OT are first synthesized as precursor peptides of 145 and 106 amino acids, respectively. The pro-hormones (precursor peptides) consist of a signalling peptide, followed by the nonapeptide sequence, a specific carrier protein (neurophysin) and the COOH-terminal glycopeptide (see Fig B). Neurophysins (NP) are specific for each nonapeptide (neurophysin-I for AVP and neurophysin-II for OT) and remarkably well conserved. The signal peptide is removed during co-translation processing in the endoplasmic reticulum, together with initial glycosylation and formation of disulphide bonds. Further processing and cleavage of the nonapeptide, neurophysin and glycopeptide takes place inside the storing vesicles. In consequence, AVP and OT are always co-stored and co-released with their respective carrier neurophysins, their glycopeptides and residual cleavage products (for a review see Burbach et al. 2001).

In rodents and humans, nonapeptides exert their actions through four identified receptors: V1aR, V1bR, V2R for AVP and OTR. The most abundant nonapeptide receptors in the CNS are OTR and V1aR, while V1bR appears in few brain areas and V2R expression is virtually restricted to peripheral tissues (Gimpl, Fahrenholz, & Gene, 2001; Verbalis, 2010). All known nonapeptide receptors belong to the G protein-coupled superfamily (see Fig C). Oxytocin and vasopressin receptors can be coupled to different G proteins, leading to different signalling cascades. Depending on the G protein, the signalling pathways trigger diverse cellular events including calcium mobilization (Wiegand & Gimpl, 2012), regulation of rectifying currents (Gravati et al., 2010; Ogier, Tribollet, Suarez, & Raggenbass, 2006), inward sodium-dependent currents (Alberi, Dreifuss, & Raggenbass, 1997; Raggenbass, Goumaz, Sermasi, Tribollet, & Dreifuss, 1991). This may lead to different physiological effects depending on the target cell. For instance, OT promotes contraction in uterine smooth muscle (Alberi et al., 1997) and cell proliferation in stem cells leading to cardiomyogenesis (Danalache, Gutkowska, Ślusarz, Berezowska, & Jankowski, 2010).

In this respect, it is important to keep in mind that nonapeptide-receptor binding is quite unspecific. Thus, despite what the nomenclature suggests, AVP binds with similar affinity to OTR as it does to AVP receptors. On the other hand, OT shows more specificity for OTR, but it can still bind AVP receptors with a 100-fold lower affinity (see Manning et al. 2012 and reference therein).

Within the CNS, V1aR and OTR are the prevalent ones and their activation by OT and AVP appears involved in the direction of social and non-social behaviours and reproductive functions, including olfaction and sensory processing, fear and anxiety, stress-copying and homeostasis, and learning and memory (Carter, Grippo, Pournajafi-Nazarloo, Ruscio, & Porges, 2008; Donaldson & Young, 2008; Meyer-Lindenberg, Domes, Kirsch, & Heinrichs, 2011; Neumann & Landgraf, 2012; Stoop, 2012).

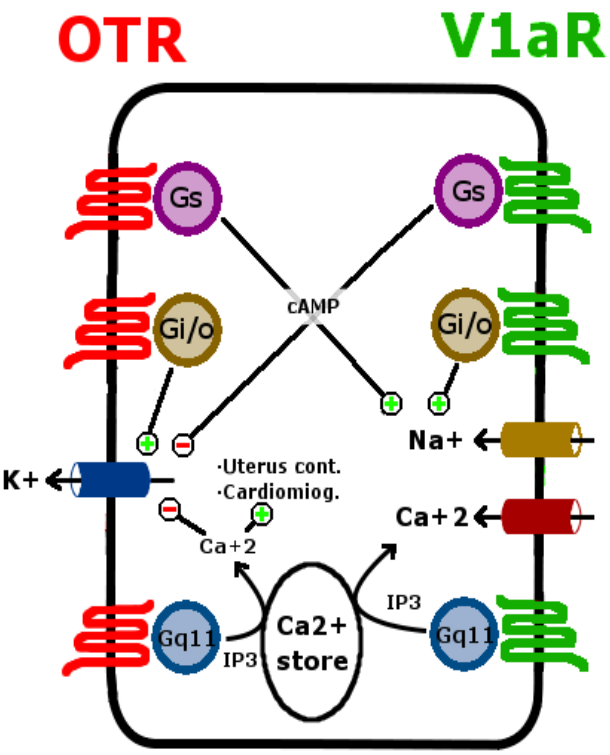


**Fig. C. Intracellular pathways activated by OT or AVP depending on which specific G proteins are activated when binding to the oxytocin receptor (OTR) and vasopressin V1a receptor (V1aR)** (adapted from Stoop 2012). Binding to OTR can activate adenylate cyclase via Gs protein, leading to sustained sodium-dependent inward currents (Alberi et al 1997). When OTR are coupled to Gq/11 proteins, they can activate the phospholipase Cβ pathway and mobilize intracellular calcium; this appears to inhibit inward rectifying currents in neurons (Gravati et al., 2010), induce uterine smooth muscle contraction (Alberi et al., 1997) and promote cardiomyogenesis (Danalache et al., 2010). OTR activation can also induce inward rectifying currents when coupled to Gi/o protein (Gravati et al., 2010). V1aR activation can also induce inward sodium-dependent currents (Raggenbass et al., 1991), suppress potassium currents (Ogier et al., 2006) and change intracellular calcium concentration, depending on the G protein to which the receptor is coupled.

Furthermore, the expression of nonapeptides and their receptors in the SNB suggests a pivotal role of OT and AVP transmission in the control of chemosensory-mediated social recognition. In fact, expression of AVP receptor V1aR in the septal area appears necessary for social recognition in mice (Bielsky, Hu, Ren, Terwilliger, & Young, 2005). In addition, knock out mice for V1bR, show deficits in social motivation and aggression (S. R. Wersinger, Caldwell, Christiansen, & Young, 2007; Scott R. Wersinger et al., 2004). Also in mice, OT receptor activation in the medial amygdala results necessary and sufficient for social recognition

(Ferguson, Aldag, Insel, & Young, 2001). In voles, research indicates that variations in the distribution of oxytocin receptors and vasopressin V1a receptors are responsible for differences in social attachment and pair bonding (Donaldson & Young, 2008). In an excellent review, Thomas Insel (2010) explains how highly affiliative species have nonapeptide receptors in forebrain circuits related to reward or reinforcement. A well-known example is the case of voles, where mate preference depends on the expression of V1aR in the ventral striato-pallidum (M M Lim & Young, 2004). This finding further stresses the importance of the projections of the vomeronasal amygdala to the ventral striato-pallidum (see above) in social interactions, and points to a crucial position of the ventral striato-pallidum in the control of social behaviour.

Regarding the effects of gonadal steroids on OT and AVP systems, sexual hormones have effects at both pre- and postsynaptic levels. This steroid modulation occurs in medial amygdala and other SBN areas, leading to a fine adjusting of social recognition, hence tuning social and reproductive functions in a sex-specific manner (Gabor, Phan, Clipperton-Allen, Kavaliers, & Choleris, 2012).

Genetic studies in mammals point to a role of the genetic locus AVP1RA (which codes for the V1aR) in the modulation social behaviour, linking variations in this locus to social behavioural diversity. In voles, differences in a microsatellite of the AVP1RA predict differences in receptor distribution and behavioural traits (E. A. D. Hammock & Young, 2005). In humans, variations of AVP1RA microsatellites are also associated to differences in traits relevant for social interactions (Israel et al., 2009; Prichard, Mackinnon, Jorm, & Easteal, 2007), including partner bonding and fidelity (Walum et al., 2008). Allelic variants of the V1aR gene have also been associated with autism (Kim et al., 2002; Wassink et al., 2004). Interestingly, OT administration can increase social cognition and attenuate repetitive behaviour in autistic patients (Bartz & Hollander, 2008).

Most studies in humans analysing the effects of nonapeptides in social cognition have used intranasal administration of AVP and OT. There is no experimental evidence proving that OT or AVP trespass the blood-brain barrier or reach the brain after intranasal or intravenous administration (Neumann & Landgraf, 2012). In addition, the administered doses of OT and AVP are usually very high and their effects could represent pharmacological artefacts. However, the reported behavioural outcomes of intranasal administration are consistent and could be explained by peripheral effects or yet unknown mechanisms. Apparently, OT delivery has pro-social effects in humans. Intranasal OT administration increases the capacity of

recognizing facial expressions (Domes, Heinrichs, Michel, Berger, & Herpertz, 2007) and promotes trust and cooperative interactions (Kosfeld, Heinrichs, Zak, Fischbacher, & Fehr, 2005). The mechanism of OT effects may imply decreased amygdala activity resulting in lower fear and anxiety, thus facilitating social interaction (Baumgartner, Heinrichs, Vonlanthen, Fischbacher, & Fehr, 2008; Kosfeld et al., 2005; Petrovic, Kalisch, Singer, & Dolan, 2008). On the other hand, the effects of intranasal AVP seem sexually dimorphic, promoting agonistic responses in males and affiliative reactions in females. Intranasal AVP administration in human males decreased the perceived friendliness of faces and promoted agonistic facial patterns. In contrast, human females rated faces as friendlier and showed affiliative facial motor patterns (Thompson, George, Walton, Orr, & Benson, 2006). This evidence is consistent with a sexually dimorphic AVP system.

## 4. Central nonapeptidergic systems: complex neuromodulation for complex functions

Oxytocin and vasopressin have a dual role, acting both as central neurotransmitters/neuromodulators and as peripheral neurohormones. The main physiological sources of AVP and OT are the neurosecretory hypothalamic cell groups. These hypothalamic neurosecretory neurons release nonapeptides into the bloodstream at the level of the posterior pituitary gland. As a hormone, OT promotes uterine contraction during parturition and milk ejection during lactation. In contrast, AVP increases blood pressure via antidiuretic and vasoconstrictor effects. Experimental evidence indicates that nonapeptides cannot cross back the blood-brain barrier (Neumann & Landgraf, 2012). Nonetheless, they are likely released within the brain. In fact, OT and AVP are known to be released from the soma and dendrites of neuroendocrine cells (Ludwig & Leng, 2006; Sabatier, Shibuya, & Dayanithi, 2004; Tobin, Leng, & Ludwig, 2012) and from axonal processes by synaptic mechanisms. This can also be related to the existence of intra- or extra-hypothalamic nonapeptidergic cells showing important central projections to key centres of the SBN.

When acting as neurotransmitters at synaptic sites, oxytocin and vasopressin are released by calcium-dependent exocytosis from the storage vesicles (Brownstein, Russell, & Gainer, 1980) and bind to neuropeptide receptors (Liu et al., 1994) but the peptides are not recycled at synapse and may diffuse and act upon distant neurons (Zoli & Agnati, 1996). Nonapeptides (OT and AVP) can also be released extra-synaptically by exocytosis. By spreading through the extracellular fluid they can bind receptors in large numbers of target cells and mediate long duration events in broad areas (Landgraf & Neumann, 2004; Trueta & De-Miguel, 2012). This extra-synaptic signalling, termed volume transmission, makes nonapeptide signalling not

primarily dependent on the topology of the wiring but on the chemistry and concentration of the neuropeptides and the distribution of its receptors within the brain.

Landgraf and Neumann (2004) argue that the efficacy of nonapeptidergic long-term neuromodulation may rely on the combination of synaptic point-to-point communication, with more diffuse, slower and long-lasting modes of signalling. Volume transmission of OT and AVP has been studied mainly in the magnocellular neurons of the supraoptic nucleus (SON, Pow & Morris 1989), where release of OT and AVP can occur independently of electrical activity. Due to positive feedback effects, release of the nonapeptides can be sustained for long intervals (e.g. 90 min; Ludwig & Leng 2006), which combined with their long half-life in the brain (around 20 min; Mens et al. 1983), would allow an effective peptidergic signal reaching as far as 4-5 mm from its site of origin (Engelmann, Wotjak, Ebner, & Landgraf, 2000). The hypothalamic paraventricular and supraoptic nuclei are considered the main source of volume transmitted AVP and OT, mainly via dendritic release and passive diffusion (Ludwig & Leng, 2006).

The importance of volume transmission in nonapeptidergic other central systems, like the SBN nodes, is stressed by the fact that the anatomical distribution of OT and AVP receptors often shows mismatches with the corresponding nonapeptidergic innervation. Such mismatches can be attributed not just to extra-synaptic signalling through volume transmission, but also to receptor promiscuity.

Local synaptic circuits and volume transmission are of particular importance in the modulatory actions of nonapeptides in different areas of the central nervous system, including several nodes of the SBN. Thus, in a recent review, Stoop (2012) discussed the close interplay between AVP and OT modulatory actions in different functional systems of the brain, including relay stations of the olfactory systems, key nuclei for social recognition and mating (medial amygdala), as well as in the central amygdala, where they may be involved in the decrease of anxiety associated to motherhood (Knobloch et al., 2012).

## 5. Previous data and justification of the work

Rodents have been extensively used for the research of the neurobiology of social behaviour (Bosch, 2011; Nephew & Bridges, 2008; Takahashi & Miczek, 2013; Toth & Neumann, 2013). The large amount of neuroanatomical data available from rats confirm that SBN and mesolimbic reward system (as defined by Newman 1999 and O'Connell & Hofmann 2012), show a remarkable density of receptors for AVP and/or OT (Veinante & Freund-Mercier, 1997)

as well as important innervation by AVPergic fibres (DeVries, Buijs, Van Leeuwen, Caffe, & Swaab, 1985). Regarding OT, although OT-ir cell bodies have been mapped (e.g. (Hou-Yu, Lamme, Zimmerman, & Silverman, 1986)), data on the distribution of OT fibres are scarce, even for the rat.

Mice are becoming the species-of-choice for the research on social neurobiology. This is so due to two main reasons. On the one hand, pheromones mediating social interactions are being identified for the mouse (Chamero et al., 2007; Isogai et al., 2011; Nodari et al., 2008; Roberts et al., 2010) and, on the other hand, the use of genetically engineered mice is generating very useful data for understanding the neural basis of social behaviour (Bielsky et al., 2005; H K Caldwell, Wersinger, & Young 3rd, 2008; Dölen, Darvishzadeh, Huang, & Malenka, 2013; Egashira et al., 2007; Jin et al., 2007; Nishimori et al., 2008; Pobbe et al., 2012). However, neuroanatomical data are fragmentary and scarce in mice, as compared to rats. Concerning nonapeptides, several good descriptions of the distribution of AVP have recently been published, although in the specific strain of inbred mice C57BL/6 (Rood & De Vries 2011). It is especially interesting to compare this with other strains differing in some aspects of their social behaviour. For instance, in a comparative behavioural analysis of different mice strains it was found that Swiss CD1 (ICR) outbred mice showed much higher rates of inter-male attack, infanticide, inter-female attack and maternal aggression but, interestingly, the lower anxiety than inbred lines like C57BL (Parmigiani, Palanza, Rodgers, & Ferrari, 1999). Therefore, there is a need for a fine, detailed description of the vasopressinergic systems in the brain of several genetic lines of mice, focusing in the key areas that primarily drive their social behaviour. In fact, it has been shown that the distribution of OT and VP receptors in limbic regions (including specific nodes of the SBN) appears highly variable even between closely related species in relation to variations in their socio-sexual behaviour (e. g. the above mentioned case of voles; Young et al. 1999).

Consequently, the first aim of the present work is to provide a detailed anatomical description of vasopressinergic elements in the brain of CD1 mice, paying special attention to the nodes of the SBN. We will also analyse the presence of sexual dimorphism (described in other species) and the hormonal control of AVP expression, focusing on the ventral striato-pallidum.

As mentioned previously, research works in various rodents have shown that the mvStP area participates in the expression of sexually dimorphic social behaviours. This striato-pallidal area is of special importance because of the above discussed pheromonal and olfactory inputs, connectivity and anatomical location between the SBN and mesolimbic reward system. A

specific aim of this work is to characterise the AVPergic innervation of the striato-pallidum of mice, and look for the site-of-origin of its innervation.

In the case of OT, there is a single previous description of its distribution in the brain of the mouse (Castel & Morris, 1988) using immunohistochemistry for the accompanying neurophysin (type II). A reanalysis of this issue in the light of new anatomical and functional data is urgently needed. In addition, data on the distribution of nonapeptide receptors using radiolabelled AVP (Dubois-Dauphin, Barberis, & De Bilbao, 1996) and OT agonists (Insel et al. 1993; Hammock & Levitt, 2013) have reinforced the view (see above) that there is a clear mismatch between nonapeptides and their receptors. In this scenario, identifying precisely the site of release of both nonapeptides and their relative density in each node of the SBN would be crucial to understand its functionality (Merighi, Polak, Fumagall, & Theodosis, 1989; Stoop, 2012). Therefore, it would be very interesting to compare the distribution of AVP and OT. Accordingly, the fourth aim of this work is to directly compare the distribution with OT and AVP in the same sections of the brain of mice by means of a double immunohistochemistry. We must consider that although AVP and OT are usually presumed to be expressed in different, segregated populations of neurons, there is evidence indicating that the majority of magnocellular neurons co-express both peptide messenger RNAs in varying amounts (Glasgow et al., 1999; Xi, Kusano, & Gainer, 1999). This co-expression is functionally relevant as demonstrated by the fact that it is regulated during physiologically relevant conditions like water deprivation (Telleria-Diaz, Grinevich, & Jirikowski, 2001) or maternity (Mezey & Kiss, 1991). However, the basal pattern of co-expression of both peptides in neurosecretory and centrally-projecting cells and their processes is still lacking.

## 6. Specific aims of the work

1. Describe the distribution of AVP in the brain of CD1 mice and analyse the presence of sexual dimorphism and the hormonal control of AVP expression. We focus on the ventral striato-pallidum as a possible centre where chemosignals might influence social behaviour.
2. Trace the origin of the sexually dimorphic innervation of the ventral striato-pallidum, in an attempt to further understand its relationship with the SBN.
3. Provide a detailed description of the distribution of OT in the brain of CD1 mice.
4. Perform a direct comparison of the distribution of AVP and OT in the same material, and analyse the presence of neural elements where both nonapeptides are co-expressed.

# MATERIAL AND METHODS

For this work, we used 62 adult mice of CD1 strain (9–16 weeks of age; Harlan, Barcelona, Spain; Janvier-Europe, Le Genest Saint Isle, France) (n=39 for Experiment 1; n=5 for experiment 2; n=12 for experiment 3; n=6 for experiment 4; Harlan, Barcelona, Spain; Janvier-Europe, Le Genest Saint Isle, France). Animals were treated throughout according to the European Communities Council Directive of November 24th, 1986 97 (86/609/EEC) and procedures were approved by the Committee of Ethics on Animal Experimentation of the University of València.

## 1. Experiment 1. Distribution of AVP immunoreactivity in the cerebral hemispheres of mice and analysis of its sexual dimorphism

For this experiment we processed 24 adult males and 15 adult females for immunohistochemistry of AVP. Six animals (3 males and 3 females) received previous colchicine injections to improve cell body immunostaining. The remaining animals received no colchicine and some of them were used for quantification. A group of males (n=9) was orchidectomised and also used for quantification to analyse the testosterone-dependence of the expression of AVP. To precisely locate the AVP-immunoreactive (AVP-ir) elements in the brain we processed parallel series of sections for: a) Nissl staining; b) combination of AVP-immunohistochemistry with NADPH diaphorase histochemistry; c) substance P immunohistochemistry; and d) NeuN immunohistochemistry.

### *1.1. Colchicine injections*

In order to boost the immunolabelling of AVP-ir cell bodies, we performed intracerebroventricular (icv) injections of colchicine in three males and three females. Colchicine is a polycyclic toxic compound that inhibits microtubule polymerization by binding to tubulin. This results in the disruption of axonal transport and accumulation of AVP in neuronal somata.

For the icv administration of colchicine, animals were first anaesthetized with isofluorane by introducing them in a chamber where 3% isofluorane (Esteve Veterinaria, Barcelona, Spain) in oxygen was delivered at 0,8 L/min. Then, animals were fixed in a stereotaxic frame provided with a mask through which 1,5% isofluorane was delivered at 0.6L/min for anaesthesia maintenance. A subcutaneous injection of 25µl of butorphanol tartrate 1% (Torbugesic, Fort Dodge, Girona, Spain) was given for pain control and sedation. Once anaesthetized, animals received hydraulic injections of 1,25-1,85 µL of colchicine (20 µg/µL in saline solution) in the lateral ventricle next to the BST (AP: -0,2mm; Lateral: +0,9 mm; 1,85 mm deep from surface) from a silicon glue-sealed, 30 µm-diameter tip capillary, at a continuous rate of 0,08-0,15

µL/min. Forty-eight hours after surgery, animals were perfused and their brains were removed, postfixed and sectioned as indicated above. One or two of the five parallel series obtained were then processed for AVP immunohistochemistry, and the rest frozen in 30% sucrose in PB for subsequent use.

### *1.2. Orchidectomy*

Previous data in several vertebrates indicate that the AVP innervation of several centers of the cerebral hemispheres (e.g. the septum) is sexually dimorphic. To explore if this is also true for the medioventral striato-pallidum (mvStP) we assessed the density of AVP-ir fibers in the mvStP of intact (n=9) and castrated (n=9) males, as well as of adult intact females (n=9). Males were randomly assigned to the group intact and castrated. Males assigned to the group "castrated" were gonadectomized via a single midline incision on the scrotal sac. For surgery, animals received pentobarbital anaesthesia (i.p. injection of 6,5 µL/g of body weight of the solution reported by Shipley & Adamek (1984). Atropine (0.4mg/kg i.p.) was administered to prevent cardio-respiratory depression and buprenorphine (Buprex, Schering-Plough; 0.02 mg/kg, s.c.) to provide postsurgical analgesia. After castration, animals were allowed to recover for at least three weeks to ensure that their testosterone levels were low. After that, all the males and females were perfused and their brains processed for AVP immunohistochemistry.

### *1.3. Perfusion, fixation and sectioning*

Animals were deeply anaesthetized using an overdose of pentobarbital (i.p. injection of 9 µL/g of body weight of the pentobarbital-based solution reported by Shipley & Adamek (1984) and transcardially perfused with saline solution (5,5 ml) followed by 66 ml of 4% paraformaldehyde in 0.1M phosphate buffer pH 7.4, at a rate of 5,5 ml/min. Brains were carefully removed from the skull, postfixed in the same fixative for 4 h and placed into 30% sucrose (in 0.01M phosphate buffered saline, pH 7.6, PBS) until they sank. The brains were then frozen and 40-µm-thick coronal sections were obtained with a freezing microtome (Microm HM-450, Walldorf, Germany). Free-floating sections were collected in five parallel series. The first and third series were collected in TBS at 4ºC for immunocytochemical detection of vasopressin, whereas the second series was mounted and processed for Nissl staining or immunohistochemistry for the neuron-specific marker NeuN. The remaining series were frozen in phosphate buffered 30% sucrose (0.1 M pH 7.4) for their eventual use in subsequent experiments. In some specimens the fourth series (adjacent to the one processed for AVP-immunostaining) was processed for immunohistochemistry for substance P (SP) or

histochemistry for NADPH diaphorase (NADPHd) that were helpful to delineate the architecture of the regions showing AVP immunoreactivity, especially in the ventral striato-pallidum and amygdala. In one specimen that received a colchicine injection (see below) AVP-immunostaining was combined with NADPH-d in the same section, to better locate the AVP immunoreactive cell bodies in the architecture of the amygdala.

### *1.4. Immunohistochemistry*

Unless indicated otherwise, for immunohistochemistry we employed the indirect ABC procedure (see Table 1). Briefly, sections were incubated sequentially in: (i) 1 % hydrogen peroxide ($H_2O_2$) in 0.05M TRIS buffered saline pH 7.6 (TBS) for 30 min at room at 25ºC, for endogenous peroxidase inactivation; (ii) the primary antibody diluted as indicated in Table 1 in TBS with 0.3% Triton X-100, 1% bovine serum albumin (BSA), 4% normal serum of the species in which the secondary antibody was raised, overnight at 4ºC; (iii) diluted biotinylated secondary antibody (Table 1), in TBS, 90 min at room temperature (25ºC); and (iv) avidin-biotin-peroxidase complex (ABC Elite kit or ABC standard kit; Vector Laboratories) in TBS with 0.2% Triton X-100, for 90 min at room temperature. After each step, sections were washed in TBS (4 x 10 min). After ABC incubation, sections were rinsed in TBS (2 x 15 min) and TRIS buffer 0.05M pH 8 (TB, 2 x 10 min), prior to the histochemical detection of the resulting peroxidase activity. This was done by incubation in in 0.003% $H_2O_2$, and 0.025% 3,3'-diaminobenzidine (Sigma) in TB for about 5 min. Sections were rinsed thoroughly in TB and mounted onto gelatinized slides, dehydrated in alcohols, cleared with xylene and coverslipped with Entellan.

Table 1. Antibodies and immunoprocedure of experiment 1 and 2

| **Primary antibody** | **Dilution** | **Secondary antibody** | **Dilution** |
|---|---|---|---|
| **Rabbit anti-Vasopressin IgG** (Millipore Cat#AB1565) | 1:10,000 | Biotinylated goat anti-rabbit IgG (Vector Labs, BA-1000) | 1:200 |
| Antigen: Full-length vasopressin Inmunogen: Synthetic vasopressin conjugated to thyroglobulin | 1:2,500 | Alexa Fluor 546-conjugated Goat anti-rabbit IgG (Molecular Probes, A-11071) | 1:300 |
| **Mouse anti-NeuN IgG** (Millipore Cat#MAB377) | 1:5,000 | Biotinylated horse anti-mouse IgG (Vector Labs, BA-2000) | 1:300 |
| **Rabbit anti-Substance P IgG** (Millipore Cat#AB1566) | 1:10,000 | Biotinylated goat anti-rabbit IgG (Vector Labs, BA-1000) | 1:200 |

### *1.5. NADPH diaphorase histochemistry and its combination with AVP immunostaining*

For histochemical detection of NADPH diaphorase we slightly modified the protocol by Barbaresi, Quaranta, Amoroso, Mensà, & Fabri (2012). Briefly, sections were incubated in the dark for about 90 minutes at 37º C in TBS with 0.3% Triton X-100 containing 1 mg/mL nicotinamide adenine dinucleotide phosphate (b-NADPH) and 0.25 mg/mL nitro blue tetrazolium (NBT; both from Sigma, St. Louis, MO). Staining was checked periodically and the reaction was stopped by rinsing the sections in TBS. For double staining, two series of the brain of a male that had received an intracerebroventricular injection of colchicine were thawed. The immunohistochemical detection of AVP was performed first as explained above and, after rinsing thoroughly with TBS, NADPH-d was performed on the same tissue. Sections were finally rinsed in TB and mounted onto gelatinized slides, dehydrated in alcohols, cleared with xylene and coverslipped with Entellan.

### *1.6. Study of Histological preparations*

Histological preparations where studied using a microscope Leitz DMRB (Leica AG, Germany) with a digital camera (Leica DFC300 FX), obtaining photomicrographs of specific areas within the sections. Background was subtracted and the resulting images processed with ImageJ to improve brightness and contrast, with no further processing. Figures were elaborated using GIMP free software.

### *1.7. Data analysis: AVP immunoreactive terminal fields*

To compare the AVP-ir systems among intact males, castrated males and intact females, we performed a quantitative analysis of the AVP-ir innervation of a centre for which sexual dimorphism has been already documented, the lateral septum, of the terminal field in the mvStP and in another region of the ventral striatum, the core of nucleus accumbens. Using the stereotaxic atlas of (Paxinos & Franklin, 2001) frames were selected as indicated with dotted lines in figures 1b (accumbens core), 1c (ventral striato-pallidum), 1d (lateral septum) and 1l (posterodorsal medial amygdala).

Photographs of these frames were taken in both hemispheres using a microscope Leitz DMRB (Leica AG, Germany) with a digital camera (Leica DFC300 FX). Background light was subtracted, and the histogram normalized, using Image J. Then the green channel was selected from the RGB colour image and it was binarized using the same thresholding rule for all the animals: pixels whose grey level was lower than 80% of the mode of the histogram were selected as

belonging to immunolabeled fibres. The area fraction that these pixels represent in all the frames of a given structure (both cerebral hemispheres) was registered for each animal.

### *1.8. Data analysis: AVP immunoreactive cell bodies*

In the same animals, the sections through the bed nucleus of the *stria terminalis* (both hemispheres) were photographed. A person who was blind to the experimental group, counted the number of AVP-immunoreactive cell bodies in all the photographs using the "cell-counter" plug-in for Image J. This allowed assessing the number of AVP-ir cell bodies in the intra and extra-amygdaloid bed nucleus of the stria terminalis of the intact and castrated males and of the females.

### *1.9. Statistical analysis*

We analysed the data on area fraction of AVP-ir innervation and on the number of AVP-ir cell bodies with the SPSS software package. After checking for normality (Kolmogorov–Smirnov test with Lilliefors' correction) and the homogeneity of the variance (Levene's test) a one-way ANOVA was used to check inter-group (intact male, castrated male, female) differences in the amount of labelling in each location (lateral septum, ventral striato-pallidum, nucleus accumbens, intra-amygdaloid BST and extra-amygdaloid BST). When we obtained positive results, these differences were further explored using post-hoc pair-wise comparisons (Bonferroni or Games-Howell).

In addition, an analysis of possible correlations among the different measurements (AVP-ir innervation fraction in different regions and AVP-ir cell bodies in the intra- and extra-amygdaloid BST) was performed using the whole set of data of all three groups of mice (intact and castrated males, and females) using Pearson's coefficient.

## 2. Experiment 2. Origin of the AVP-ir innervation of the ventral striato-pallidum

The presence of positive correlation between the density of innervation (area fraction) in the mvStP and the density of AVP-ir cell bodies in the BST (see Results), suggests that there is an AVPergic projection from the BST to the mvStP. Experiment 2 is designed to check this possibility by means of two different experimental approaches.

On the one hand we combined retrograde tracing of the afferents to the ventral striato-pallidum with AVP-immunofluorescence. We used a fluorescent neuroanatomical tracer, Fluorogold, to look for double labelled AVP-FG cells. We focused on the cell groups that showed sexual dimorphism in the BST.

In a second group of animals we performed unilateral lesions the BST region using a fibre-sparing excitotoxic drug, ibotenic acid. Then we analysed the effects of this lesion in the AVP-ir terminal fields in the striato-pallidum and other areas by comparing their density in the injected and non-injected brain hemisphere.

### *2.1. Retrograde tracing of ventral striatopallidal afferents with Fluorogold*

Fluorogold (FG, hydroxystilbamidine, Biotium, Hayward, CA) is a florescent dye that bounds to nucleic acids. It is commonly used as retrograde tracer and although it is also transported anterogradelly, at long survival times (more than 2 days) it accumulates in the neuronal soma where it remains for several months.

For the retrograde tracing experiment, FG was stereotactically injected in the mvStP by iontophoresis from a 2% solution in saline. Injections were aimed at regions of the mvStP involving the anteromedial islands of Calleja. To do so, we adapted the coordinates of the stereotaxic atlas (Paxinos & Franklin, 2001) to the brain of male CD1 mice (relative to Bregma: AP -1.42mm, L 0.2mm, 4mm deep from surface). For these injections the pipette was introduced in a lateral coordinate (2 mm) with an angle of 25 degrees, to avoid leakage of the tracer in the rostral lateral septum along the pipette trajectory.

Animals (male mice, n=5) were deeply anaesthetized with sodium pentobarbital and treated with atropine and buprenorphine as in Experiment 2. Once anaesthetized, animals were placed on a stereotaxic frame (David Kopf Instruments 963-A, Tujunga CA, EE.UU), a hole was drilled in the skull and a micropipette (tip 10-20 µm-thick, inner diameter) filled with the tracer solution was introduced down to the target nucleus with a constant retaining current (-0.9 µA). Then the tracer was delivered by passing pulses (7s ON- 7s OFF) of a +5 µA for 5-10 minutes with a current injector connected to the pipette (Midgard Precision Current Source, Stoelting). Ten minutes after the end of the injection, the pipette was carefully withdrawn with a retaining current to avoid tracer leakage along the pipette track.

### *2.2. Immunofluorescence for AVP and image acquisition*

After 5-7 days of survival, animals were perfused and their brains treated and cut as in Experiments 1. Free-floating sections were collected in five parallel series. After checking for the location of the FG injection, two of the series were processed for AVP immunofluorescence. Sections were incubated overnight at 4ºC in the primary antibody diluted, as specified in Table 1, in TBS with 0.3 Triton X-100 plus 2% normal serum. After 3 rinses in TBS, sections were incubated in the secondary antibody for 2 hours at room

temperature in the dark, rinsed again, mounted on gelatine-coated slides and cover-slipped with fluorescent mounting medium (Dako, Carpinteria, CA).

Photographs of fluorescent material were obtained in a Leitz microscope DMRB with epifluorescence (Leica EL-6000) using filters specific for FG (Leica, A) and rhodamine (Leica N2.1). Brightness and contrast were adjusted using ImageJ. No additional processing was performed.

### *2.3. Excitotoxic lesions of the BST*

A second approach for testing the origin of the AVP-ir innervation of the mvStP in the BST consists in performing unilateral lesions of the BST and checking if this results in a decrease in the density of AVP-ir fibres in the mvStP ipsilateral to the lesion, as compared to the contralateral hemisphere. In order to ablate neuronal somata without affecting fibres of passage, we employed ibotenic acid as excitotoxic agent. Due to its structural similarity with glutamate, ibotenic acid acts as a non-selective glutamate receptor agonist, provoking considerable neuronal death and minimum damage to crossing axons.

We carried out unilateral excitotoxic lesions in 12 male mice that were operated under isofluorane anaesthesia as for colchicine injections in Experiment 1. Once anesthetized and placed in the stereotaxic frame, animals received hydraulic injections of 150 nl of ibotenic acid (60 mM in PBS) in the BSTMP (AP: -2.25mm from Bregma; Lateral: 0.85mm from midline, 4.85mm deep from surface) from a silicon glue-sealed capillary containing the solution of ibotenic acid. The general surgical procedure was similar to FG injections. Leakage of ibotenic acid to the cerebrospinal fluid could cause epileptic seizures. Thus, to avoid the capillary entrance to the ventricles, we used a postero-anterior angle of 23 degrees. The drug solution was injected at a flow of 50nL/min in 1 min steps separated by 2-minute non-injection periods. After the injection the micropipette was left in place for further 10 minutes before withdrawal. Seven days after surgery, the animals were perfused and their brains postfixed and sectioned as in previous experiment. Two parallel series of coronal sections were processed for NeuN (to delineate the lesion) and for AVP immunohistochemistry, respectively, using the same procedure as in Experiment 1.

### *2.4. Data analysis: quantification of AVP immunoreactivity and statistics*

Finally, the number of AVP-ir cell bodies in intra- and “extramygdaloid” portions of the BST, as well as the density of AVP-ir fibres in the lateral septum, medial amygdala and mvStP, were evaluated in both hemispheres with the same methodology described in Experiment 1.

Statistics analysis was performed to check the hypothesis that there was a decrease of AVP-ir cell bodies in the BST of the injected *vs* the contralateral cerebral hemisphere, which is correlated with a decrease in density of AVP-ir fibres in the terminal fields of the lateral septum and mvStP. To do so, a Student's t test for related measurement comparing both hemispheres was followed by a Pearson's correlation analysis of cell bodies *vs* fibre density in the terminal fields.

### 3. Experiment 3. Distribution of OT immunoreactivity in the cerebral hemispheres

For the description of the distribution of oxytocin (OT) immunoreactivity, we obtained permanent immunolabeled preparations from 10 virgin females and 2 virgin males of CD1 strain. Animals where euthanatized and their brains processed as in Experiment 1, but the sections collected in four parallel series instead of five. One or two of the four series of each specimen were processed for the immunodetection of OT, employing the indirect ABC immunoperoxidase procedure as in Experiment 1 (For antibodies and dilutions see Table 2).

Histological preparations were studied and the figures elaborated using the same methodology as in Experiment 1.

Table 2. Antibodies and immunoprocedure of experiment 3

| **Primary antibody** | **Dilution** | **Secondary antibody** | **Dilution** |
|---|---|---|---|
| **Mouse anti-oxytocin, monoclonal** (Dr. Harold Gainer, NIH Cat#PS38)<br>Antigen: Oxytocin-specific neurophysin<br>Inmunogen: Rat posterior pituitary extract, KLH coupled | 1:600 | Biotinylated goat anti-mouse IgG (Vector Labs, BA-9200) | 1:200 |
| **Rabbit anti-Oxytocin IgG** (Millipore Cat#AB911)<br>Antigen: Full-length oxytocin<br>Inmunogen: Synthetic oxytocin conjugated to thyroglobulin | 1:25,000 | Biotinylated goat anti-rabbit IgG (Vector Labs, BA-1000) | 1:200 |

### 4. Experiment 4. Distribution of OT+AVP co-localization

For simultaneous immunolabelling of oxytocin and vasopressin we employed combined immunofluorescence. We used two out of four parallel series obtained from three virgin

females and three virgin males. Sections were incubated sequentially in: (i) 1% Sodium borohydride in TBS at room temperature (RT, approximately 25ºC) for 30 minutes (ii) 0.05M TRIS buffered saline pH 7.6 (TBS) with 0.3% Triton X-100, 1% bovine serum albumin (BSA) and 4% normal serum of the species in which the secondary antibody was raised, at RT for 1 hour; (iii) primary antibodies, diluted as indicated in Table 3, in TBS with 0.2% Triton X-100, 1% BSA and 4% normal goat serum (the species in which both secondary antibodies were raised) for 48h at 4ºC; (iv) fluorescent-labelled secondary antibodies diluted as indicated in Table 3, in TBS, for 90 min at room temperature. After each step, sections were washed in TBS (except between step ii and iii).

To reveal the cytoarchitecture of the brain in the same sections, prior to mounting, sections were counterstained by bathing them for 5 min in 600nM DAPI (4 ',6-diamino-2-fenilindol) at room temperature. Sections were finally rinsed thoroughly in TB and mounted onto gelatinized slides and cover-slipped with fluorescence mounting medium (Dako, Glosrup, Denmark).

Immunofluorescence was analysed with an Olympus FV1000 Confocal Microscope System, mounted on an inverted microscope. Triple scans were made to identify DAPI, Alexa Fluor 488 (AVP) and Rhodamine Red X (OT). Excitation wavelengths were 405 nm for DAPI, 488 nm for Alexa Fluor 488 and 559 nm for Rhodamine Red X. Emission wavelengths were 461, 520 and 591 respectively. Z-sections with a distance between 1.5 and 4 microns of separation were taken at x100, x200 and x600 magnifications through the regions of interest. To minimize channel spill-over the images were sequentially acquired, and saved as OIF and TIF files. The stacks obtained were further processed with ImageJ to optimize brightness and contrast. No manipulation of individual image elements was performed. Figures were elaborated with GIMP software.

Table 3. Antibodies and immunoprocedure of experiment 4

| **Primary antibody** | **Dilution** | **Secondary antibody** | **Dilution** |
|---|---|---|---|
| **Mouse anti-oxytocin, monoclonal** (Dr. Harold Gainer, NIH Cat#PS38) | 1:200 | Rhodamine Red X-conjugated goat anti-mouse IgG (Invitrogen R6393) | 1:250 |
| **Rabbit anti-Vasopressin IgG** (Millipore Cat#AB1565) | 1:2,500 | Alexa Fluor 488-conjugated Goat anti-rabbit IgG (Jackson ImmunoResearch, 111-545-003) | 1:300 |

# RESULTS

## 1. Distribution of AVP immunoreactivity in the cerebral hemispheres of mice and analysis of its sexual dimorphism.

### *1.1. Distribution of AVP immunoreactivity*

Our data clearly support the observations by (Rood and de Vries 2011) in C57BL/6 mice, indicating that few, if any, differences exist between C57BL/6J and CD1 (Swiss) mice concerning the distribution of AVP in the brain. We will focus our description on the details relative to the distribution of cell bodies and fibres immunoreactive for AVP in the cerebral hemispheres, with special reference to the innervation of the ventral striato-pallidal telencephalon and amygdaloid formation (including the bed nucleus of the stria terminalis). For the description of the results we will follow the atlas by (Paxinos & Franklin, 2001). We will describe and illustrate the distribution of vasopressin immunoreactive (AVP-ir) cell bodies and processes based on our material of indirect (ABC) immunoperoxidase.

#### *1.1.1. Distribution of AVP-ir cell bodies*

Like in previous descriptions in mice and other rodent species, in our material the most intensely immunostained cells for AVP correspond to the magnocellular neurosecretory cell groups of the hypothalamus (supraoptic, suprachiasmatic and paraventricular nuclei; see Fig. 1f-h), with few cells intermingled with them (the accessory nuclei by (Castel and Morris 1988)). In addition, the cerebral hemispheres contain two groups of faintly immunoreactive somata. Most of the AVP-ir cell bodies are sparsely distributed in the caudal aspect of the bed nucleus of the stria terminalis proper (Fig. 1e-h). There, the use of NADPHd histochemistry allows a precise chemoarchitectonic analysis of the distribution of AVP-ir cell bodies (Fig. 2a-c). Most labelled cells are observed in the intermediate subdivision of the medial posterior BST (BSTMPI) where they are intermingled with the NADPHd-positive neurons typical of this subnucleus (Figs. 2a-b) and no cells are doubly labelled. The lateral subdivision of the medial posterior BST (BSTMPL) also contains a remarkable population of AVP-ir cells (Figs. 2a; 3a'-b') and a few cells are also found in the posterior division of the lateral BST (BSTLP; Fig. 1e-f). Another group of AVP-ir cells are seen in the medial portion of the medial posterior BST (BSTMPM) where they are located next to the fornix (see Fig. 3a'-b').

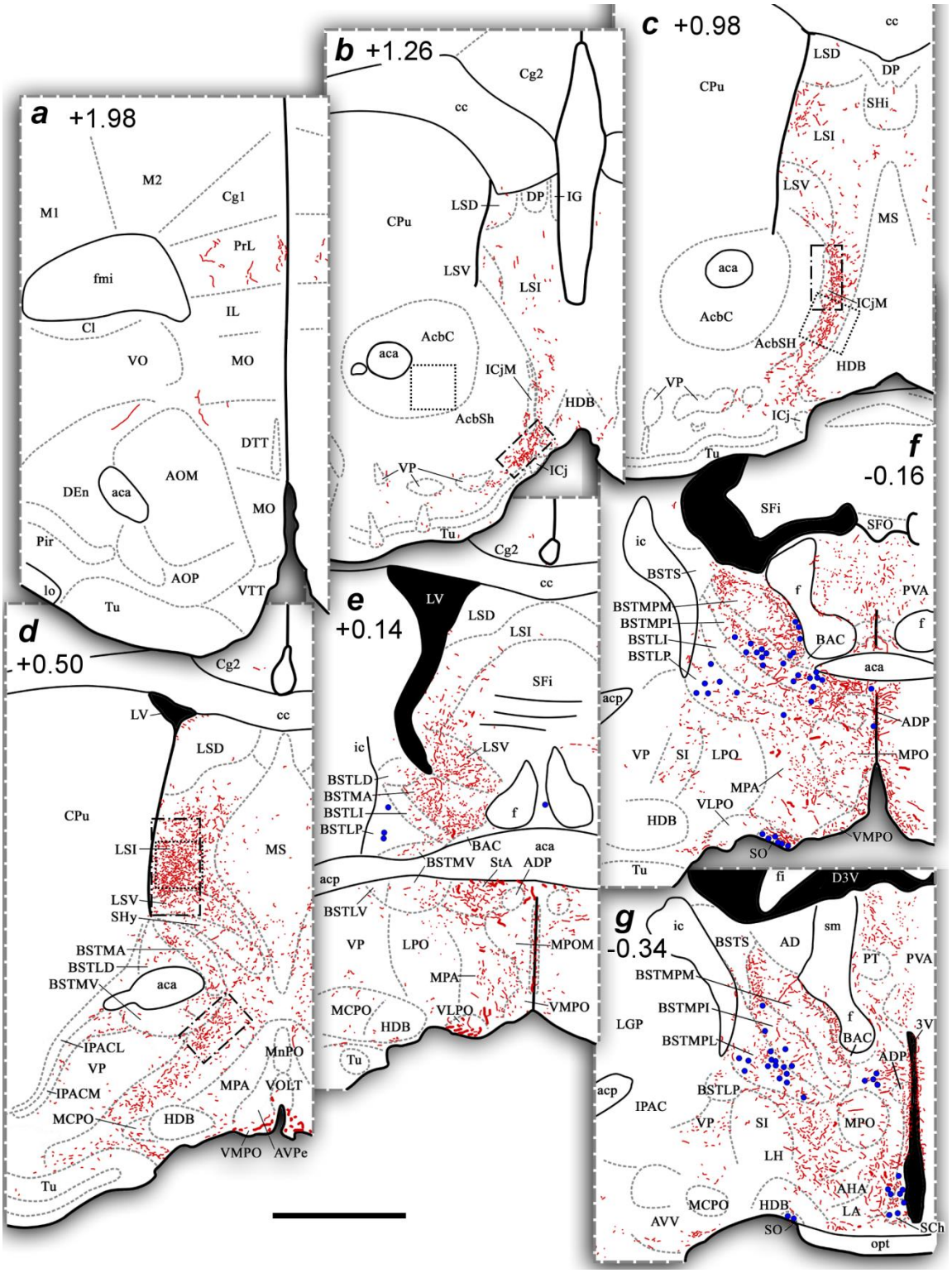
a +1.98
M2
M1
Cg1
PrL
fmi
IL
Cl
VO
MO
DTT
AOM
DEn
aca
MO
Pir
AOP
VTT
lo
Tu
b +1.26
Cg2
cc
LSD
DP
IG
CPu
LSV
LSI
AcbC
aca
ICjM
AcbSh
HDB
VP
ICj
Tu
c +0.98
cc
LSD
DP
CPu
SHi
LSI
LSV
MS
aca
ICjM
AcbC
AcbSH
HDB
VP
ICj
Tu
d +0.50
Cg2
LV
cc
LSD
CPu
LSI
MS
LSV
SHy
BSTMA
BSTLD
BSTMV
aca
IPACL
VP
MnPO
IPACM
MPA
VOLT
MCPO
HDB
VMPO
AVPe
Tu
e +0.14
LV
LSD
LSI
cc
Cg2
SFi
ic
LSV
BSTLD
BSTMA
BSTLI
BSTLP
f
BAC
aca
BSTMV
StA
ADP
acp
BSTLV
VP
LPO
MPOM
MPA
MCPO
HDB
VLPO
VMPO
Tu
f -0.16
SFi
SFO
ic
BSTS
f
PVA
BSTMPM
BSTMPI
BSTLI
BSTLP
BAC
f
aca
acp
ADP
VP
SI
LPO
MPO
MPA
VLPO
HDB
VMPO
SO
Tu
fi
D3V
g -0.34
ic
BSTS
AD
sm
PT
PVA
BSTMPM
BSTMPI
LGP
f
BAC
3V
BSTMPL
ADP
acp
BSTLP
IPAC
VP
SI
MPO
LH
AHA
MCPO
HDB
LA
AVV
SO
SCh
opt

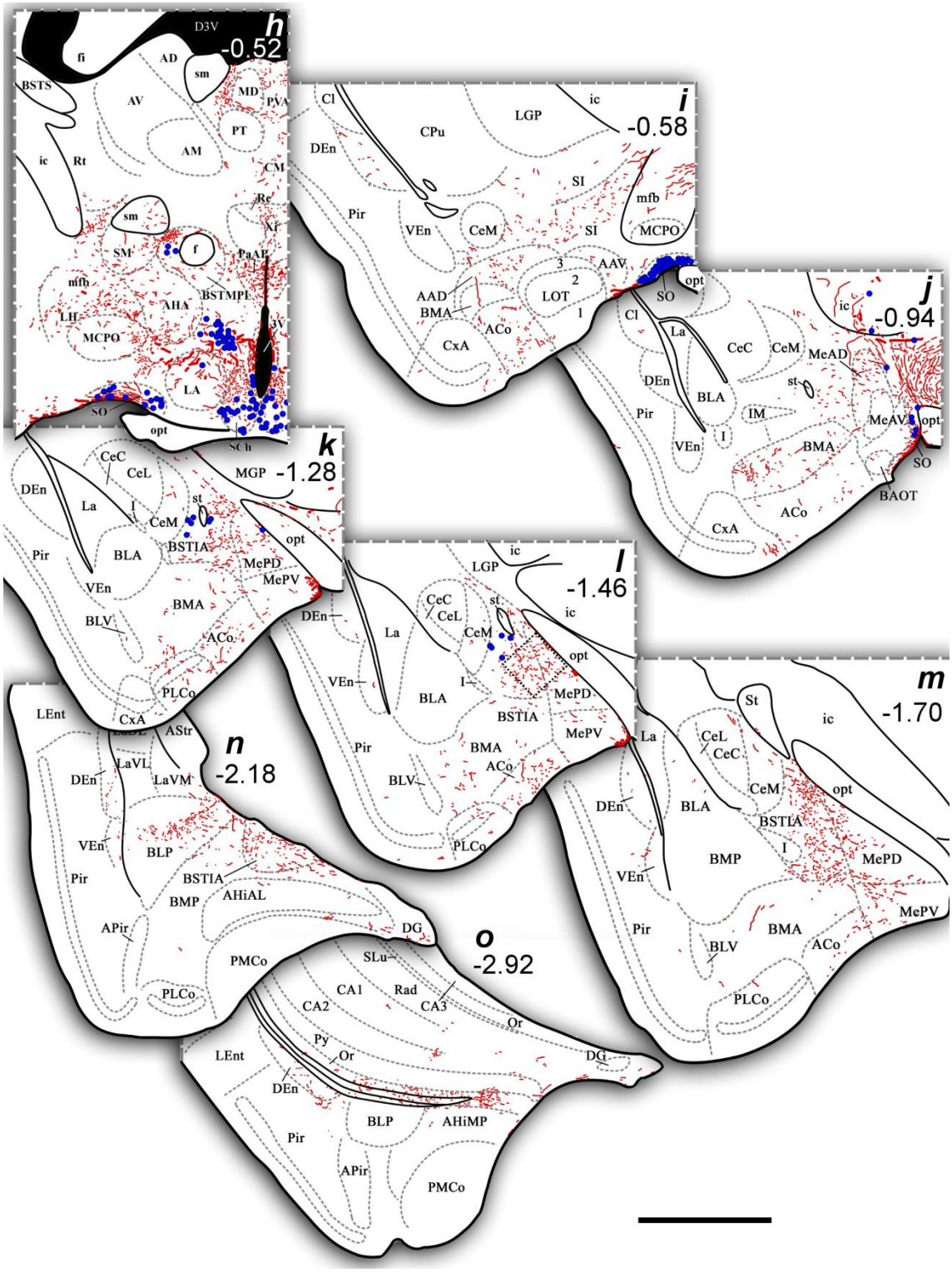


**Fig. 1. Vasopressin immunoreactivity (AVP-ir) in the telencephalon of male mice**. Semi-schematic camera lucida drawings of specific regions of selected coronal sections through the left cerebral hemisphere (***a-o*** from rostral to caudal) of a representative case (M1102), in which immunoreactive fibers are represented by thin lines (red), while AVP-ir cell bodies are shown as solid circles (blue). The antero-posterior level of each section is indicated as the distance from Bregma in millimeters. Scale bar, 1mm.

A few, intensely immunolabelled neurons are also observed in what appears as the caudal aspect of the ventral medial BST (BSTMV) according to the atlas by (Paxinos and Franklin 2001). A close examination of the full series of sections through the BST/preoptic area suggests, however, that these cells are not part of the BSTMV but very likely belong to the nucleus of the anterior commissure (AC) and the anterodorsal preoptic area (ADP). In fact, whereas the BSTMV shows a low density of faintly stained cells with the NADPH-d histochemistry (not shown), this caudal location is characterized by a cluster of intensely stained NADPHd-positive cells. Many of these cells are also AVP-ir, so that this is the only location of the BST-preoptic continuum where doubly labelled cells (NADPHd-AVP-ir) are observed (see arrows in Fig. 2c). Henceforth we name this AVP-ir cell group the AC/ADP.

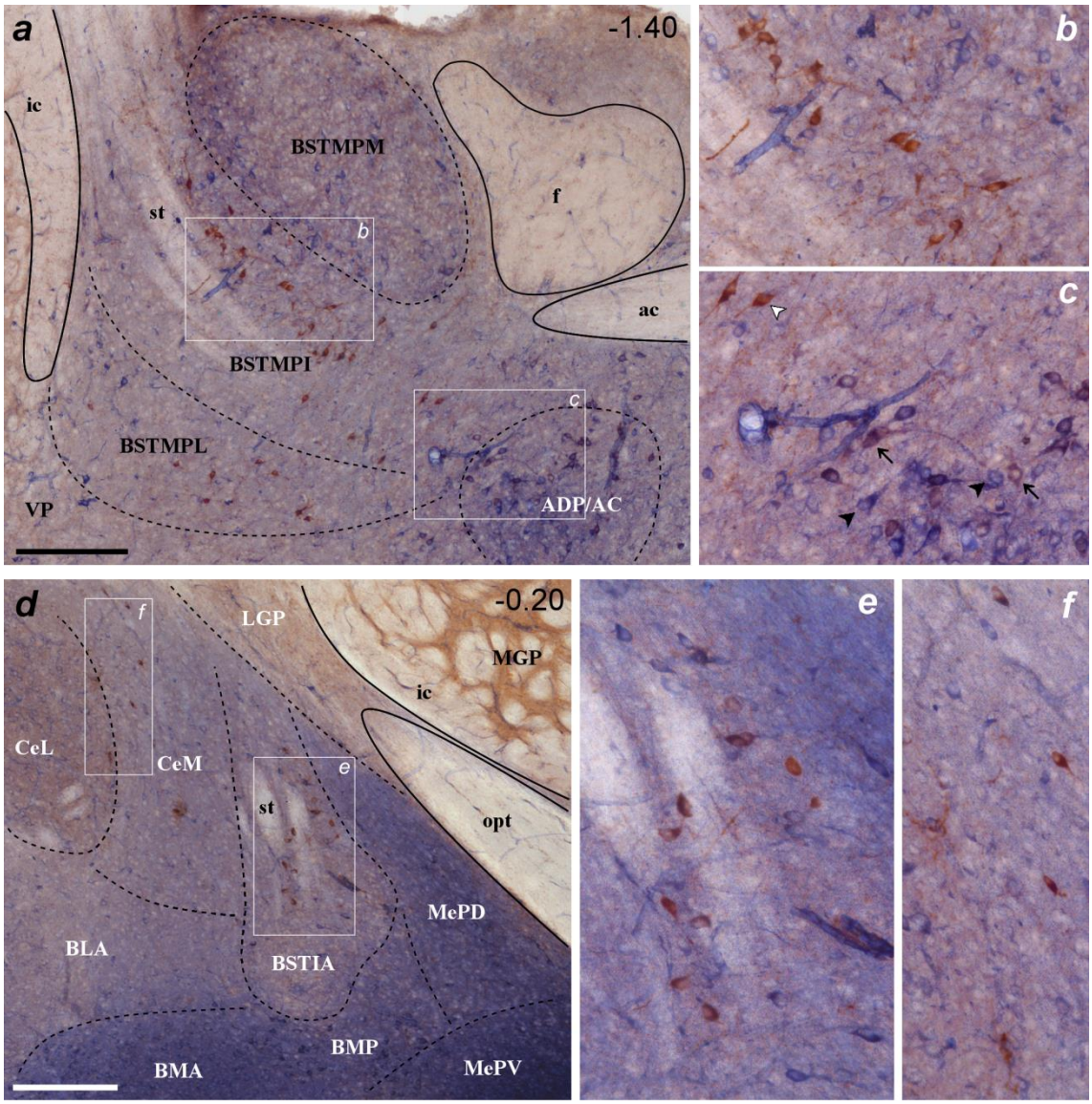

**Fig. 2. Architecture of the AVP-ir cell groups of the cerebral hemispheres of mice**. Coronal sections of a male mouse that had received an icv injection of colchicine were processed for the simultaneous detection of AVP (immunostaining, brown) and NADPH diaphorase (histochemistry, blue). ***a.*** In the BST, most AVP-ir cells are grouped in the BSTMPI and a few are also seen in the BSTMPL. Within the BSTMPI, AVP-ir cells coexist with NADPHd-positive neurons, but no double labeling is observed (***b***). In the lower right corner of ***a***, a dense cluster of doubly labeled cells (NADPHd + AVP) is observed within the ADP/AC. The framed area is shown at higher magnification in ***c***, where black arrowheads point to NADPHd-positive cells, the white arrowhead to an AVP-ir neuron belonging to the BSTMPI and the black arrows to doubly labeled neurons, belonging to the AC/ADP. ***d.*** A section through the amygdala shows the main intraamygdaloid cell group immunoreactive for AVP to be located lateral to the MePD, in an area showing a distinct, faint staining (as compared to the Me) for NADPHd. This area corresponds to the BSTIA, as cells are interspersed with the bundles composing the stria terminalis at this level (***e***). A few AVP-ir cells in the medial division of the central amygdala (framed area in the left upper corner of ***a***) are shown at high magnification in ***f***. Distance from Bregma is indicated in millimeters (top right corner). Scale bars in ***a*** and ***d***, 200 μm.

The second main group of neurons immunoreactive for AVP in the cerebral hemispheres observed in our material corresponds to what is usually considered in the literature on AVP distribution as the medial amygdala (in mice, (Rood and de Vries 2011); Rood et al., 2012-13; in rats, (Caffe and van Leeuwen 1983; DeVries et al. 1985). However, a careful observation of the amygdala of our material indicates that AVP-ir cell bodies are located in the intraamygdaloid bed nucleus of the stria terminalis (BSTIA) rather than in the medial amygdaloid nucleus (Fig. 1k-l). This is clearly visible in material in which we combined AVP immunostaining with NADPHd histochemistry (Fig. 2d-e), a technique which is especially useful for delineating the medial amygdala (strongly stained) from adjoining structures (see (Martínez-García et al. 2012). The medial amygdala, especially but not exclusively its ventral part, shows a characteristic densely stained neuropile, as observed in Fig. 2d. In contrast, the main group of AVP-ir cells in the amygdala is located in a region lateral to the MePD, which is crossed by the bundles of the *stria terminalis* (*st*) and shows a comparatively fainter NADPHd staining (Fig. 2d). In fact, AVP-ir cells in this location are intercalated with the bundles of the *st* (Fig. 2e), thus clearly corresponding to the BSTIA according to (Paxinos and Franklin 2001).

Besides the presence of densely immunostained cells in the locations described above (posterior BST, AC/ADP and the BSTIA), colchicine-treated animals also show some AVP-ir cells in the MeA, usually bipolar cells located parallel to the optic tract (arrowheads in the female of Fig. 3c') plus a few additional cells in the medial division of the central amygdala (CeM, see Fig. 2d and 2f).

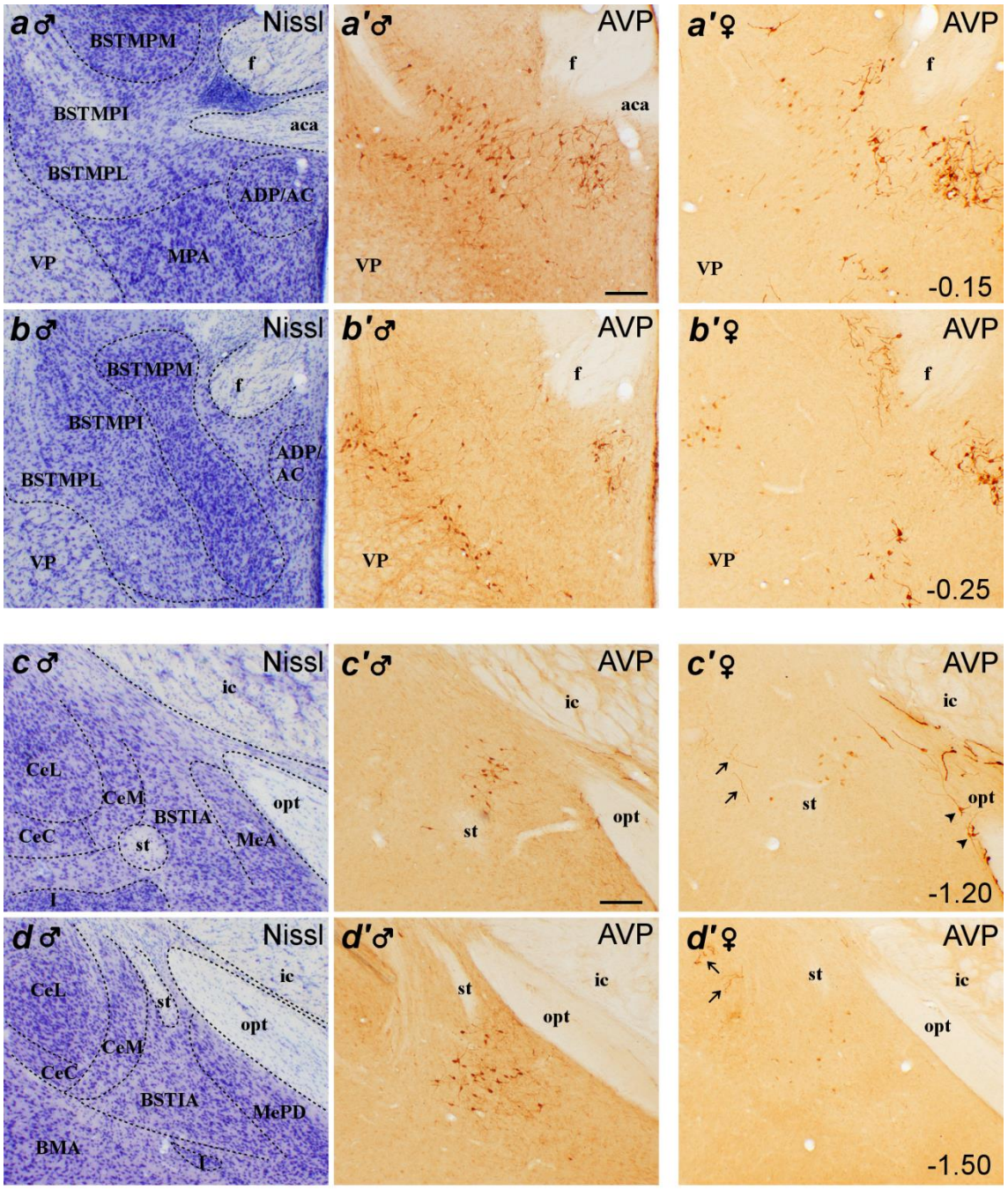


**Fig. 3. AVP-immunoreactive cell bodies in the cerebral hemispheres of male and female mice**. Coronal sections through the posterior bed nucleus of the stria terminalis (***a*** and ***b***) and the amygdala (***c*** and ***d***) of the left cerebral hemisphere, stained with toluidine blue (*a-d)* and immunoreacted for AVP (***a'-d'***). The central column corresponds to a colchicine-treated male, whereas the column on the right shows the immunostaining in a colchicine-treated female. Nissl stained sections in the column on the left are immediately adjacent to those in the central column. Arrowheads in c'female point to AVP-ir cells in the MePD, whose dendrites are oriented parallel to the optic tract. Arrows in the ***c'***♀ and ***d'***♀ indicate some visible large caliber fibers in the central amygdala. In contrast, AVP-ir fibers are barely visible in the male (***c'***♂ and ***d'***♂).♂). Distance from bregma is indicated in milimiters (bottom right of each row). Scale bars, 150 µm.

*1.1.2. Distribution of AVP-ir fibres in the cerebral hemispheres*

Immunohistochemistry for AVP reveals a complex system of AVP-ir fibres in the cerebral hemispheres of CD1 mice, similar to the one described in C57BL mice by Rood and De Vries (2011). In brief, AVP-ir fibres are very scarce in the cerebral cortex (prelimbic and cingular areas, endopiriform nucleus) except for the temporal hippocampus (stratum oriens of the CA1 field), but virtually absent in the dorsal and ventral striatum (see Fig. 1). In contrast they form moderate to dense terminal fields in the lateral septum, medioventral striato-pallidal boundary, bed nucleus of the stria terminalis and amygdala. In the lateral septal complex, fibres are observed septo-hypothalamic nucleus (SHy) and the laterointermediate and lateroventral nuclei (LSI and LSV), where labelling is especially dense at caudal (fimbrial) levels (Fig. 1b-e). In the septum, AVP-ir fibres often form perisomatic nests.

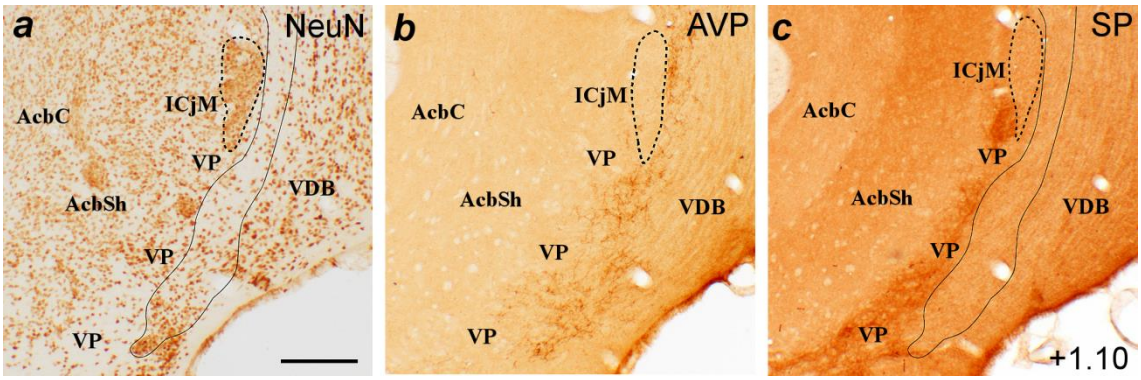


**Fig. 4. Terminal field of AVP-ir fibers in the medioventral striato-pallidum**. Photomicrograph of a section trough the left ventral striato-pallidum immunostained for AVP (***b***), as well as of adjacent sections processed for the immunohistochemistry of NeuN (***a***), and substance P (***c***). The dotted line delineates de major island of Calleja (ICjM) whereas the thin continuous line, was traced around the AVP-ir innervation observed in ***b***, and transposed to figures ***a*** and ***c*** using relevant landmarks (anterior commissure, margin of the tissue, blood vessels) as a reference. This reveals that AVP-ir fibers are concentrated in a sparse-celled zone (see ***a***) which is interposed between the ventral pallidum (characterized by a dense innervation by SP-ir fibers, C) and the diagonal band. Distance from bregma is indicated in each level in millimeters. Scale bar 200 µm.

The ventral striato-pallidal boundary shows a remarkable network of AVP-ir fibres innervating an area with a low cell density, not identified in the atlas of (Paxinos and Franklin 2001), which separates the medial shell of the nucleus accumbens from the nucleus of the diagonal band and the medial edge of the olfactory tubercle (compare Fig. 4a and b). Some AVP-ir fibres in this area are apparently apposed onto the medial aspect of the Callejal complex, which includes the major island of Calleja and the small anteromedial islands which flank medially the rostral olfactory tubercle. Caudally, this terminal field seems to extend into the rostral edge of

the lateral preoptic area (LPO), and into the bed nucleus of the stria terminalis (BST). The immunohistochemical detection of substance P has been used in sections adjacent to the ones processed for AVP immunohistochemistry, as a specific marker of pallidal territories (Napier et al. 1995). The comparison of the immunostaining for AVP and substance P clearly indicates that the AVP-ir fibres innervate a region that does not belong to either the ventral striatum or the ventral pallidum, but constitutes a third territory just medial to the pallidum (Fig. 4).

The presence of AVP-ir fibres is a characteristic feature of the BST that allows delineating its boundary with the nucleus accumbens (devoid of fibres) (Fig. 1a-h). At anterior levels of the BST, AVP-ir fibres are dense in the medial anterior nucleus (BSTMA), where thin and thick fibres are mixed together, but scarce in the medioventral division (BSTMV) where innervation is mainly composed of thin fibres (Fig. 1d-e). In contrast, the different divisions of the lateral BST (laterodorsal, BSTLD; lateroventral, BSTLV; juxtacapsular, BSTLJ) show very light AVP-ir innervation (Fig. 1d-e). At posterior levels, the medial posteromedial (BSTMPM) and posterointermediate (BSTMPI) nuclei show a moderate, non-uniform density of labelled fibres, which in the case of the BSTMPM is composed of thin fibres forming perisomatic nests, as well as some thick immunoreactive fibres, mainly located near the fornix (Fig. 1f-h). In contrast, the laterointermediate (BSTLI) and medial posterolateral (BSTMPL) nuclei show a low density of thin AVP-ir fibres, whereas the lateral posterior BST (BSTPL) is nearly devoid of AVP-ir innervation (Fig. 1f-h). At these caudal levels, the so-called strial part of the preoptic area (StA), shows a characteristic dense innervation by thick AVP-ir fibres. This is in sharp contrast with the relatively poor innervation of the adjacent BSTMV (Fig. 1e).

Regarding the amygdala, AVP-ir fibres are heterogeneously distributed in all of its divisions. In the cortical amygdala, thin labelled fibres are relatively dense in the anterior cortical amygdala (ACo), moderately dense in the cortex-amygdaloid transition zone (CxA), scarce in the posterior cortical amygdala (PLCo and PMCo) and virtually absent in the nucleus of the lateral olfactory tract (LOT) (Fig. 1i). Where they are present, labelled fibres in the cortical amygdala mainly innervate layer 2 (e.g. in the ACo; Fig. 1i-l). The deep pallial amygdala nuclei (basolateral division and amygdalo-hippocampal area) only show some patches of moderate to dense innervation by AVP-ir fibres, located in the anterior basomedial nucleus (BMA) and in the ventral and posterior subdivisions of basolateral (BLP) nucleus, as well as in a specific region of the medial posterior amygdalo-hippocampal area (AHiMP) (Fig. 1j-o).The rest of nuclei are virtually devoid of labelling. In the subpallial amygdala, there is a clear-cut difference between the anterior amygdaloid area (AA), the medial and the central division. The anterior amygdala shows a uniform sparse innervation by thin, varicose AVP-ir fibres, similar to the one

of the adjacent substantia innominata (Fig. 1i). In contrast, the medial amygdala (Me) displays an important but heterogeneous innervation by AVP-ir fibres. The anterodorsal (MeAD) and posterodorsal (MePD) nuclei shows a dense innervation, the latter composed of perisomatic nests that also extend into the BSTIA. The ventral anterior medial amygdala (MeAV) shows very few labelled fibres, whereas in the posteroventral medial amygdala (MePV) there is a moderately dense innervation by thin fibres located in the cell layer (Fig. 1j-m). In addition, both the MeAV and the MePV (especially its rostral part) show a bunch of very thick neurites that run just below the pial surface, and appear to be dendrites of the immunoreactive cells of the anterior supraoptic nucleus (Fig. 5a-b; see insets). Finally, the central amygdala (Ce) shows no AVP-ir fibres except for a few thick, sparsely distributed ones (Fig. 5c-d). These fibres show a large inter-subject variability concerning both, density and location.

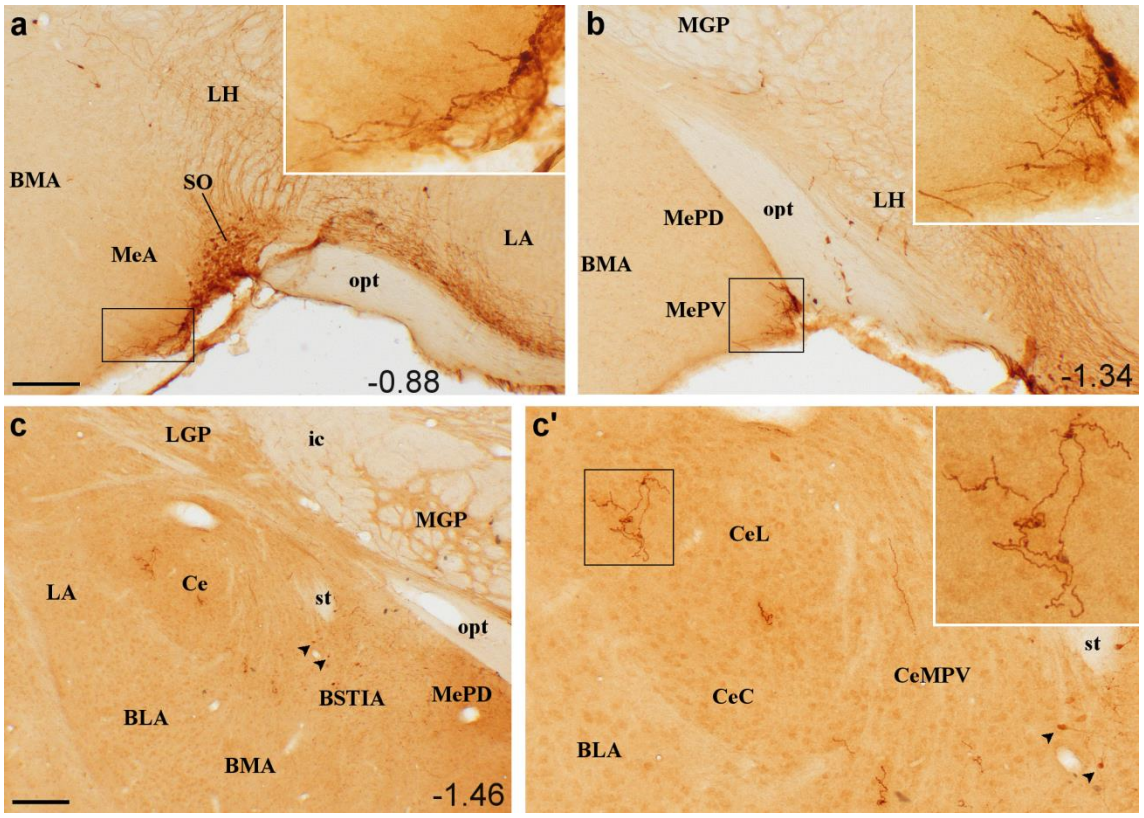


**Fig. 5. Details of the AVP immunoreactivity in the medial and central amygdaloid divisions**. Coronal sections through the medial (***a*** and ***b***) and central (***c*** and ***d***) amygdaloid nuclei immunoreacted for AVP. Dendritic processes from the AVP-ir cell bodies of the supraoptic nucleus (SO) extend into the subpial anterior (***a***, inset) and posteroventral (***b***, inset) medial nuclei of the amygdala. In the central amygdala (***c***), large caliber axon-like processes are seen in the medial (CeM) and lateral divisions (CeL). Details in ***c'*** and inset, allow appreciating its peculiar appearance. AVP-ir cell bodies are also observed in the BSTIA (arrowheads in ***c*** and ***c'***). Distance from bregma is indicated in millimeters in the bottom right corner of each level. Scale bars correspond to 200 µm in ***a*** (valid also for ***b***) and ***c***, and to 100 µm in ***c'***.

Out of the telencephalon, many AVP-ir terminal fields are visible, matching the results by Rood and deVries (2011) for C57BL mice. The hypothalamus shows a complex pattern of fibre labelling (including the thick-calibre fibres connecting the magnocellular neurosecretory cells with the median eminence), with an especially dense innervation of the periventricular and lateral compartments (especially at preoptic and anterior levels), but relatively scarce innervation of most of the medial nuclei, the main exception being the dorsomedial hypothalamic nucleus. At mammillary levels the perifornical, medial tuberal, tuberomammillary, premammillary (especially the dorsal) and supramammillary (especially the medial) nuclei also show low density of AVP-ir fibres. Labelled fibres are also abundant in the paramedian cell groups of the thalamus (central median and interanterior nuclei, most of the paraventricular thalamus, nucleus reuniens, rhomboid, xyphoid and mediodorsal nuclei), in the lateral habenula and in the zona incerta. Finally, in the midbrain and tegmentum, patches of labelled fibres are found in the substantia nigra pars compacta and adjoining midbrain reticular formation. A relatively dense innervation is also seen in the ventral tegmental area and interfascicular nucleus. The dorsolateral and dorsomedial columns of the anterior periaqueductal gray also display AVP-ir fibres, whereas a prominent terminal field is observed in the caudal aspect of its ventrolateral column. In addition, the caudal linear and dorsal raphe nuclei and the nucleus O (also called nucleus incertus, see (Olucha-Bordonau et al. 2003) display a relatively dense innervation. Finally, the lateral parabrachial nucleus shows a low density of AVP-ir fibres, whereas the locus coeruleus the nucleus of Barrington and the adjoining central gray show a denser AVP-ir innervation.

### *1.2. Sexual dimorphism in the AVP-ir innervation the medioventral striato-pallidal boundary (mvStP)*

The number of AVP-ir cell bodies was recorded in three locations of the cerebral hemispheres in each animal of the three groups (intact males, castrated males, females). At the level of the BST two antero-posterior levels were selected, at approximately -0.3 mm and -0.1 mm relative to Bregma. There, two populations of AVP-ir cell bodies were recorded independently: on the one hand the AVP-ir neurons in the lateral aspect of the posterior BST (BSTMPI, BSTMPL, BSTLP) and on the other hand the neurons located in the anterior edge of the dorsomedial preoptic region, where cells are distributed in the AC and ADP. In addition, the cells in the BSTIA were also recorded in both hemispheres at four antero-posterior levels (approximately at -1.46, -1.58, -1.70 and -1.82 mm relative to Bregma). For each structure (posterior BST, AC/ADP and BSTIA) data of all levels and of both hemispheres were pooled to render a single figure for each structure and animal.

The data from the animals of all three groups were analysed independently for each structure using a simple ANOVA. The results indicate that there is a significant effect of the GROUP (intact males, castrated males, females) on the number of AVP-ir cells in the posterior BST ($F_{2,15}$= 6.545, p=0.009) and BSTIA ($F_{2,15}$= 8.027, p=0.004), but not for the AC/ADP ($F_{2,15}$=2.158, p=0.15). In the BSTP and BSTIA, Bonferroni pair-wise comparisons reveal that males have more AVP-ir cell bodies than females and castrated males (p<0.05), whereas females and castrated males have similar numbers of AVP-ir somata (p>0.5) (Fig. 6a).

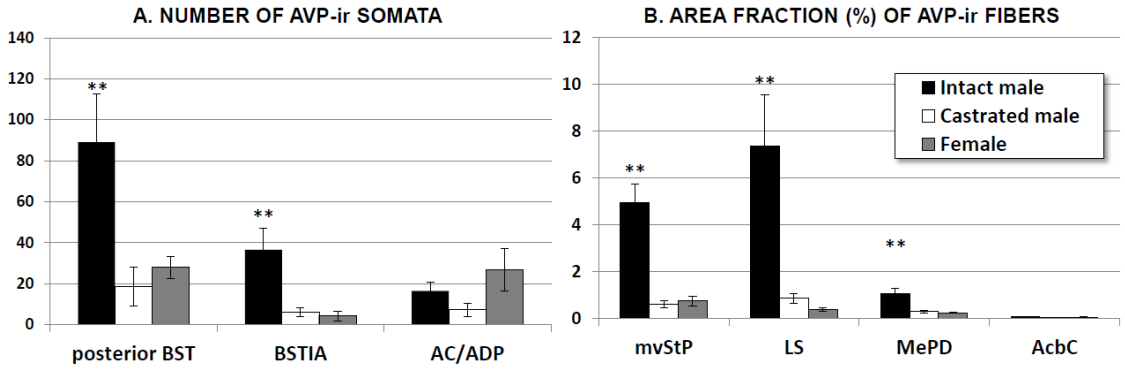


**Fig. 6. Sexual dimorphism in the AVP-ir systems of the cerebral hemispheres of mice**. Bar histogram showing the mean (±SEM) number of AVP-ir cell bodies (***a***) and the area fraction occupied by AVP-ir fibers (***b***) in different areas of the telencephalon of intact males, castrated males and intact female mice of the strain CD1. Statistical analysis (ANOVA) applied independently to each center reveal significant differences (** p<0.01) among groups in some of the nuclei. In these cases, post-hoc tests indicate that intact males show higher number of cells or higher density of AVP-ir innervation than castrated males or females.

Concerning the terminal fields, an inspection of the material from females and castrated males reveals apparent differences with males in several regions of interest, including the lateral septum (LS) and mvStP, but also in the BST and the amygdala. In addition, most of the extra-telencephalic terminal fields showing characteristically thin AVP-ir fibres also display apparent differences among intact males and castrated males or females (e.g. lateral habenula and thalamus; perifornical, tuberal, premammillary and supramammillary hypothalamus; midbrain tegmentum; periaqueductal gray; raphe nucleus and parabrachial-coerulear area). In general, the density of fibres appears higher for intact males than for the rest of animals.

Two notable exceptions should be noticed, relative to the amygdala. First, the AVP-ir neurites of the MeAV and MePV, apparently connected with the cells in the supraoptic nucleus (SO) (Fig. 5a-b), appear as dense and abundant in females and castrated males as in intact males. Second, the thick AVP-ir fibres in the central amygdala show a large variability in our material

concerning both their density and distribution within the nucleus. However, this seems to be independent of the group, as animals with high and low density of AVP-ir fibres are found in all three groups, intact males, castrated males and females. Figure 3c'-d' illustrates a female with a relatively high density of AVP-ir fibres in the Ce (arrows) and a male with scarce AVP-ir innervation. In contrast, figure 5 c-c' shows a male in which the density of AVP-ir fibres in the Ce is comparatively higher.

To further demonstrate the presence of sexual dimorphism in the AVP system of the cerebral hemispheres and its dependence on testosterone in males, the area fraction covered by the AVP-ir fibres was measured for the main terminal fields of the telencephalon, e.g. the mvStP, LS and the posterodorsal medial amygdala (MePD; see Fig. 6b). In addition, the core of the Acb (AcbC) was analysed as a negative control. In all centres, data from both hemispheres of each animal were pooled. Possible differences among groups in the density of these terminal fields were analysed independently for each structure with a simple ANOVA. The ANOVA revealed a significant effect of the GROUP on the density of AVP-ir fibres for the mvStP ($F_{2,15}$=25.149; $p<0.001$), the LS ($F_{2,15}$=9.381; $p=0.002$ ) and the MePD ($F_{2,15}$=8.903, $p=0.003$), but no significant differences were found for the AcbC ($F_{2,15}$=2.355, $p=0.129$). The post-hoc analysis reveals that, where groups differ in their AVP-ir innervation, fibre density is higher in males than in females or castrated males ($p<0.05$), which do not differ from each other ($p>0.1$).

We used Pearson's correlation to explore the relationship between the area fraction covered by AVP-fibres in the terminal fields mentioned above (mvStP, LS, AcbC, MePD) and the number of AVP-ir cell bodies in the posterior BST, AC/ADP and intra-amygdaloid BST (BSTIA), using data from all animals (intact and castrated males, and females). The results indicate (Table 4) a strong positive correlation between the number of AVP-ir cell bodies in the posterior BST with the density of AVP-ir fibres in the LS and MePD, and a moderate correlation with those in the mvStP. The number of AVP-ir cells in the BSTIA is also strongly correlated with the fibre density in the LS and MePD, but there is only a tendency ($p=0.057$) to a mild correlation (Pearson's $r=0.456$) with the innervation of the mvStP. In contrast, neither the number of cells in the AC/ADP nor the density of AVP-ir fibres in the AcbC, show correlation with labelling in the remaining analysed structures. It is interesting to note that the number of AVP-ir cell bodies in the posterior BST and BSTIA are strongly cross-correlated, but show no correlation with the ones in the AC/ADP. In a similar way, there are highly significant positive correlations among the density of AVP-ir fibres in the mvStP, LS and MePD, but they are not correlated with the innervation of the AcbC.

Concerning the thick AVP-ir fibres in the central amygdala and the AVP-ir processes in the subpial layer of the rostral Me, we have not performed a quantitative analysis of their density due to their generally low density, which renders an extremely low area fraction. Nevertheless, direct observation of the fibres reveals a low variability in the medial amygdala, where thick AVP-ir fibres are present in every animal irrespective of its sex and hormonal status. In contrast, the density of AVP-ir fibres in the central amygdala shows a huge variability that ranges from virtual absence of fibres to a moderate density. This variability appears similar in males (both intact and castrated) and females.

**Table 4.** Correlation analysis of the AVP-ir elements in the different nuclei of cerebral hemispheres

| | | Cells posterior BST | Cells BSTIA | Cells AC/ADP | Fibers mvStP | Fibers LS | Fibers MePD | Fibers AcbC |
|---|---|---|---|---|---|---|---|---|
| Cells posterior BST | • Pearson's | 1 | **0.777**** | 0.291 | **0.566*** | **0.835**** | **0.712**** | -0.045 |
| | • p value | | **<0.001** | 0.241 | **0.014** | **<0.001** | **0.001** | 0.858 |
| Cells BSTIA | • Pearson's | **0.777**** | 1 | 0.263 | 0.456 | **0.841**** | **0.572*** | -0.092 |
| | • p value | **<0.001** | | 0.292 | 0.057 | **<0.001** | **0.013** | 0.717 |
| Cells AC/ADP | • Pearson's | 0.291 | 0.263 | 1 | 0.035 | 0.159 | 0.051 | -0.198 |
| | • p value | 0.241 | 0.292 | | 0.890 | 0.528 | 0.840 | 0.431 |
| Fibers mvStP | • Pearson's | **0.566*** | 0.456 | 0.035 | 1 | **0.678**** | **0.841**** | 0.382 |
| | • p value | **0.014** | 0.057 | 0.890 | | **0.002** | **<0.001** | 0.117 |
| Fibers LS | • Pearson's | **0.835**** | **0.841**** | 0.159 | **0.678**** | 1 | **0.897**** | 0.129 0.609 |
| | • p value | **<0.001** | **<0.001** | 0.528 | **0.002** | | **<0.001** | |
| Fibers MePD | • Pearson's | **0.712**** | **0.572*** | 0.051 | **0.841**** | **0.897**** | 1 | 0.299 |
| | • p value | **0.001** | **0.013** | 0.840 | **<0.001** | **<0.001** | | 0.228 |
| Fibers AcbC | • Pearson's | -0.045 | -0.092 | -0.198 | 0.382 | 0.129 0.609 | 0.299 | 1 |
| | • p value | 0.858 | 0.717 | 0.431 | 0.117 | | 0.228 | |

## 2. Origin of the AVP-ir innervation of the medioventral striato-pallidum

To elucidate the site of origin of the AVP-ir innervation of the mvStP we followed two complementary strategies. First, we performed injections of a fluorescent retrograde tracer in the mvStP, followed by AVP immunofluorescence, to identify doubly-labelled neuronal somata in the putative sites of origin of the AVP-ir innervation. Once localized, we lesioned the site of origin of the AVP-ir fibres and analysed the subsequent depletion of AVP-ir innervation of various forebrain areas.

### *2.1. Neuroanatomical tract-tracing*

In order to identify the source of the AVP-ir innervation of the mvStP, fluorogold injections where aimed at the mvStP of male mice (n=5). Injections involved the region of the antero-ventral islands of Calleja (Fig. 7a) where the innervation of AVP-ir fibres is especially dense,

whereas the lateral septum was spared by the injection. In all the injections retrogradely labelled somata were found in the lateral aspect of the BSTMP (BSTMPL and BSTMPI; Fig. 7b), among other regions. The BSTIA showed few, if at all present, retrogradely labelled cells. Series of those animals showing labelling in the BSTMP where revealed for AVP immunofluorescence and we looked for retrogradely labelled AVP-ir cells. Double labelled somata where found in the BSTMPL in very few instances (Fig. 7c-d), the number of doubly labelled cells being always extremely low (one or two per animal). However, singly labelled cells (either with fluorogold or AVP immunoreactivity) were common in the BST (Fig. 7e) and other areas of the brain. The low frequency of double labelling in the BST can be attributed, in part, to the low signal provided by the AVP immunofluorescence, a technical problem that we were not able to overcome. As a consequence, in experiment 4 we tried a different approach to check the origin of the AVP-ir innervation of the mvStP.

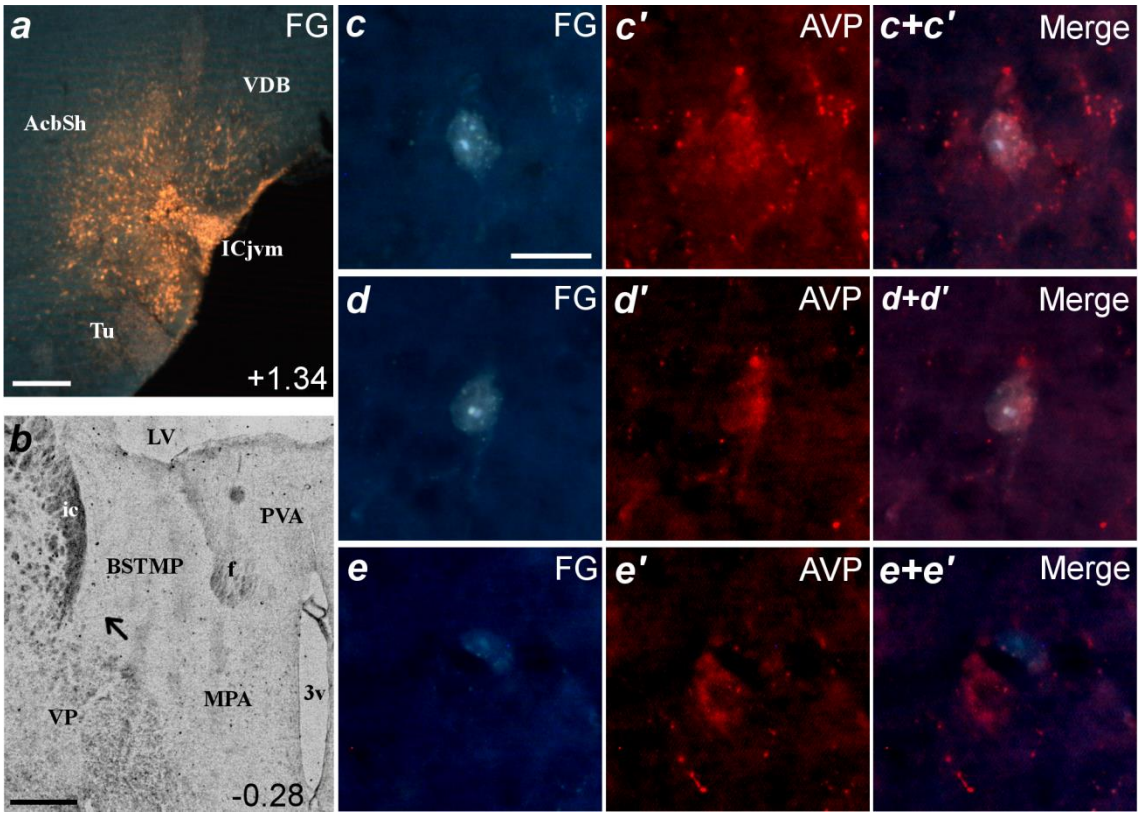


**Fig. 7. Injection of fluorogold (FG) in the medio-ventral striato-pallidum (mvStP)** renders retrograde labeling in AVP-ir cells of the BST. The injection site is centered in the ventromedial island of Calleja (ICjvm, ***a***) but also involves adjacent territories in the shell of the accumbens, ventral pallidum and diagonal band nucleus. Examples of retrogradely labeled AVP-ir cells (***c*** and ***d***) in the BSTMPL, the approximate location of which is indicated with an arrow in a bright field photomicrograph of the same section, in ***b***. Singly labeled cells are shown in ***e***, to prove the specificity of the labeling. Distance from bregma is indicated in millimeters in the bottom right corner (***a*** and ***b***). Scale bars represent 200 µm in ***a***, 400 µm in ***b***, and 20 µm in ***c*** (valid also for ***d*** and ***e***).

### *2.2. Excitotoxic lesions of the BST*

Unilateral injections of ibotenic acid were performed in the BSTMP of seven male mice. The resulting lesions were confined to the BST and preoptic area of one side, the other side appearing intact (no apparent neuronal loss) in NeuN preparations (Fig. 8a). In adjacent sections processed for AVP immunohistochemistry (Fig. 8b), the injection site contains a few AVP-ir cells with picnotic appearance (arrows in Fig. 8$c_{ipsi}$). The number of AVP-ir neurons in the BSTMPL/BSTMPI was assessed in both sides (Fig. 8$c_{ipsi}$-$c_{contra}$) by a person blind to the experimental conditions. A Student's t test for related samples comparing the injected and the contralateral sides of the brain revealed a significant reduction of AVP-ir neurons caused by the injection of ibotenic acid (28.7±4.2 cells in the lesion side, vs 60.0±7.7 cells in the contralateral hemisphere, mean±SEM; $t=3.917$, $p<0.01$).

A similar comparison of the area fraction covered by the AVP-ir innervation revealed a decrease in the density AVP-ir fibres in the lateral septum ($t=2.609$, $p=0.04$; Fig. 8d), mvStP ($t=2.649$, $p= 0.038$; Fig. 8e) and MePD ($t=3.605$, $p=0.01$; Fig. 8f). In this experiment the AVP-ir innervation of the mvStP of both hemispheres was sampled and averaged from four different regions of the striato-pallidum: the area immediately lateral to the anteromedial island of Calleja (framed in Fig. 1b), the area medially adjacent to the major island of Calleja (framed in Fig. 1c), the area just dorsal to the caudal olfactory tubercle and adjacent to the caudomedial island of Calleja (framed in Fig. 1d) and the region named as lateral preoptic area in (Paxinos and Franklin 2001) (LPO, framed in Fig. 1e). Although lesions were not complete, the reduction of cells in the BSTMPL/BSTMPI (AVP-ir cells in the contralateral minus cells in the lesion side) showed a marginally significant correlation with the reduction in area fraction covered by AVP-ir fibres in the whole mvStP ($r=0.723$, $p=0.066$).

Taken together, these data indicate that the BSTMPL/BSTMPI innervates the main regions of the cerebral hemispheres showing AVP-ir innervations, including the lateral septum, the posterior medial amygdala and the medioventral striato-pallidal boundary. Concerning the thick AVP-ir fibres in the central amygdala and the AVP-ir processes in the subpial layer of the anterior medial amygdala, no apparent difference is observed between the ipsilateral and contralateral hemispheres although, for the reasons explained in experiment 2, no fibre quantification was performed.

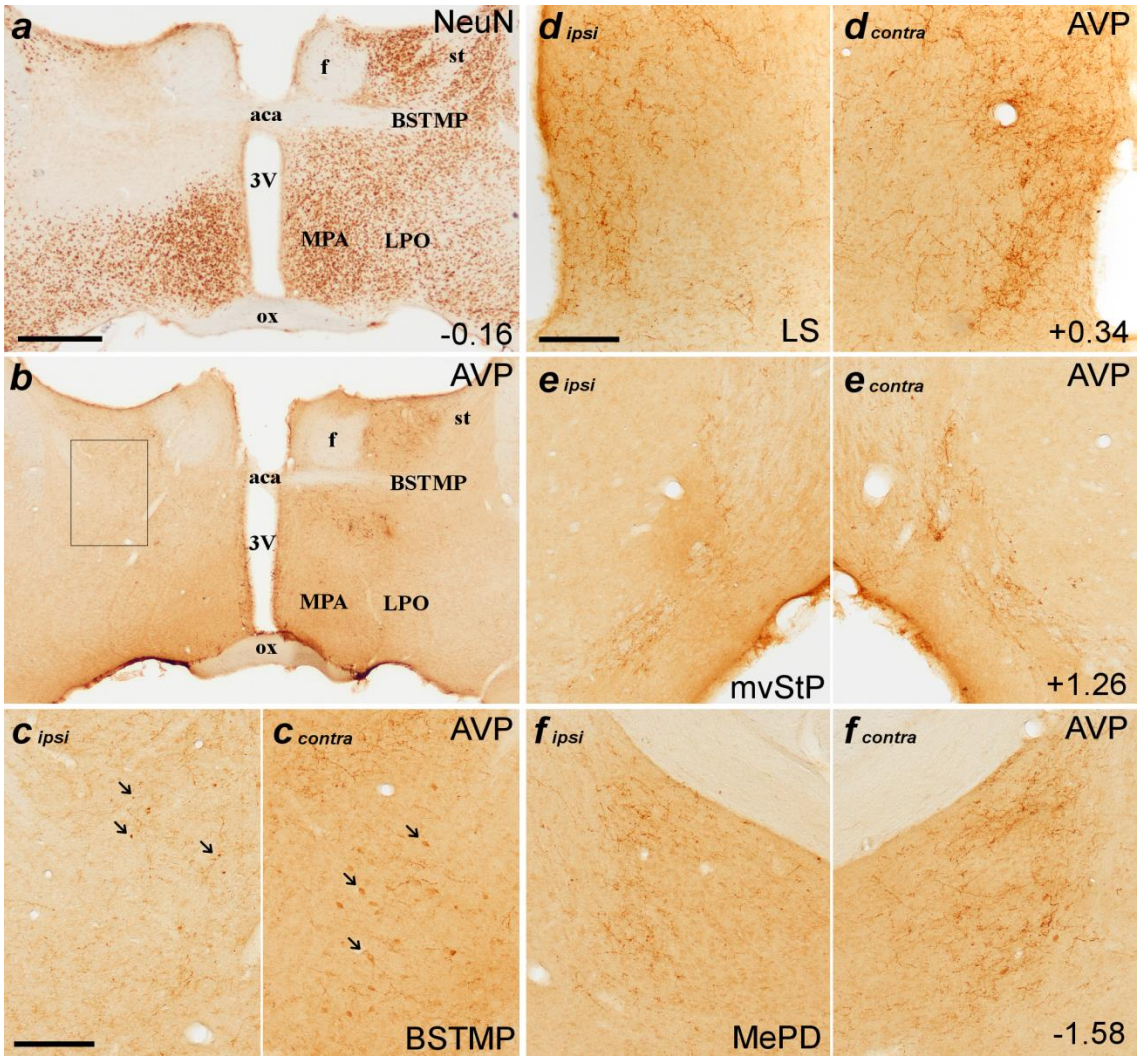


**Fig. 8. Effects of fiber-sparing excitotoxic lesions of the BSTMP on AVP immunoreactivity in male mice**. ***a***. Neu-N immunoreactivity reveals the loss of neurons in the left BST after a unilateral injection of ibotenic acid in case M1152. ***b***. An adjacent section processed for AVP immunohistochemistry shows a loss of AVP-ir cells within the BSTMPL ipsilateral to the injection (detail in $c_{ipsi}$) as compared to the contralateral side (detail in $c_{contra}$). The arrows in $c_{ipsi}$ point to AVP-ir somata with picnotic appearance, whereas those in $c_{contra}$ indicate apparently normal AVP-ir somata. On the other hand, lower density of AVP-ir innervation can be noted in the ipsilateral LS ($d_{ipsi}$), mvStP ($e_{ipsi}$) and MePD ($f_{ipsi}$) as compared to their contralateral counterparts. Distance from bregma is indicated in millimeters in the bottom right corner. Scale bars correspond to 500 µm in ***a*** (valid also for ***b***) and to 150 µm in ***c*** and in ***d*** (valid also for ***e***-***f***).

## 3. Distribution of OT immunoreactivity in the cerebral hemispheres of mice

Our results fit and extend previous anatomical findings on the distribution of OT-related neurophysin in the brain of mice (Castel & Morris, 1988). The antibodies against OT and OT-specific neurophysin (NP-OT) employed in the present work (see Table 1) revealed an identical distribution of cells and fibres, thus confirming previous studies of antibody specificity (Ben-

Barak, Russell, Whitnall, Ozato, & Gainer, 1985; Whitnall, Key, Ben-Barak, Ozato, & Gainer, 1985). OT and NP-OT are colocalized at subcellular level (Belenky, Castel, Young, Gainer, & Cohen, 1992) and immunostaining of both peptides is undistinguishable (Butovsky et al., 2006). We will therefore refer jointly to these immunolabellings as OT-like immunoreactivity (OT-ir). In addition, removing the primary antibody resulted in a complete lack of labelling.

Distribution of OT immunoreactivity was apparently indistinguishable between the males and the females analysed, thus suggesting that, in basal physiological conditions, there is no apparent sexual dimorphism in the distribution of OT. Likewise, and in spite of the sexually dimorphic distribution of AVP (Rood et al., 2014; Otero-Garcia et al., 2014) the distribution of cells and fibres in which AVP+OT are co-localized was similar in the two males and two females analysed.

For the description of the results we will follow the atlas by (Paxinos & Franklin, 2001). We will first describe the location of OT-ir cell bodies followed by the distribution of OT-ir neural processes, based on our material of indirect (ABC) immunoperoxidase.

### *3.1. Distribution of OT immunoreactive cells*

Most OT-ir somata are grouped in four locations: a) a cell group located next to the anterior commissure; b) the paraventricular hypothalamic nucleus; c) the supraoptic nucleus; and d) the medial amygdala. In addition, scattered cells appear in different hypothalamic locations, most of which in the proximity to these cell groups and surrounding the walls of the third ventricle (3V).

The most rostral group of OT-ir cells is located at the boundary between the extended amygdala and the preoptic area, next to the anterior commissure. This cell group was named as the anterior commissural nucleus by (Rhodes, Morrell, & Pfaff, 1981), or the rostral paraventricular nucleus by (Hou-Yu et al., 1986) in their descriptions of the OT-ir cells in the rat. However, using the atlas of the mouse brain by (Paxinos & Franklin, 2001), this OT-ir cell group seems located neither in the bed nucleus of the anterior commissure (BAC) nor in the paraventricular nucleus but in an ill-defined, unnamed region located ventral to the BAC, medial to the bed nucleus of the stria terminalis, medial division (BSTM) and lateral the anterodorsal preoptic nucleus (ADP) (Fig. 9e) (Fig. 11a,b). Following our previous description of the distribution of AVP (Otero-Garcia et al., 2014) we name this cell group as the ADP/AC. The OT-ir cells of the ADP/AC form a compact group, which occasionally is in close apposition to large-calibre blood vessels (Fig. 10a, a'). A close look into the OT-ir cell group, combined with

DAPI counterstaining (not shown), allows to perceive that some immunoreactive cells extend into the posterointermediate part of the medial BST (BSTMPI), notably at rostral levels (Fig. 11a). Outside the main group, a few cells also extend dorsally within the space between the fornix (f) and the posteromedial BSTM (BSTMPM). Also ventrally, scant OT-ir cell bodies spread into the caudal medial preoptic area (MPA) and lateral preoptic area (LPO) (Fig. 9f; Fig. 11a-b). Slightly more rostrally, a few OT-ir cell bodies can also be seen around the anterior edge of the third ventricle, next to the ventricular wall, in the organum vasculosum of the lamina terminalis (VOLT) or ventromedial preoptic area (VMPO) (Fig. 9c).

In the anterior hypothalamus, dense populations of OT-ir cells are located in all the subdivisions of the Pa, with the exception of the lateral Pa (PaL; see Fig. 9 and 4), where there are very few OT-ir cells (Fig. 9g, h). Thus, abundant immunoreactive cells are observed in the anterior parvicellular (PaAP) and ventral (PaV) subdivisions, while more disperse cells appear in the medial (PaM) and posterior (PaPo) subdivisions (Fig. 9i, j). The OT-ir cell group of the Pa appears to extend into the periventricular nucleus (Pe), where OT-ir cells usually display processes oriented parallel to the ventricular wall (Fig. 9d-h). ). In fact, at those antero-posterior levels where few cells are present in the Pa, OT-ir cells are lacking in the adjacent Pe (e.g. at the level of the PaPo; Fig. 9i-j).

In the SON, there is a cluster of OT-ir cells that shows a fainter staining than those in the Pa. Within the SON, OT-ir cells are heterogeneously distributed. Most of the OT-ir neurons are located in the anterior part of the SON where they occupy the dorsal and medial aspects of the nucleus (Fig. 9g, h). Whereas few OT-ir, small cell bodies surpass the rostral border of the SON (ventral part of Fig. 11 a, b). The retrochiasmatic division of the supraoptic nucleus (SOR) also contains relatively few moderately stained cell bodies (Fig. 9j). Here also, OT-ir cells are mainly located in the dorsal (deep) portion of the nucleus (Fig. 13e, e').

At the rostral-most levels of the SON, some OT-ir cells seem to have migrated caudolaterally, surpassing the boundaries of the nucleus, to enter the medial region of the rostral aspect of the medial amygdala (Me) (Fig. 9h-j). Within the Me there is a population of OT-ir cells especially dense in its anterior division (MeA) but a few immunoreactive neurons are also seen in the posterodorsal one (MePD). There, most of the cells are oriented parallel to the optic tract (opt). Between the Pa and the SON, immunoreactive somata are scattered in the lateral hypothalamic area (LH) and anterior hypothalamic area (AH) (Fig. 9g-j), being more abundant in the strip between the LH and the zona incerta (ZI), near the PaPo (Fig. 9i). A scattered population of OT-ir somata is also observed ventral to the anterior Pa and dorsolateral to the

SCh, between the medial preoptic nucleus (MPO) and the ventromedial preoptic nucleus (VMPO) (Fig. 9f). This cell group may correspond to the "mouse accessory nuclei (mAC)" described by (Castel & Morris, 1988). Finally, scarce OT-ir cells appear in the ventral portion of the dorsomedial hypothalamic nucleus (DMH) (Fig. 9k). All these scattered cells conform the so-called accessory cells or nuclei (Castel & Morris, 1988; Krisch, 1976; Benjamin D. Rood & De Vries, 2011).

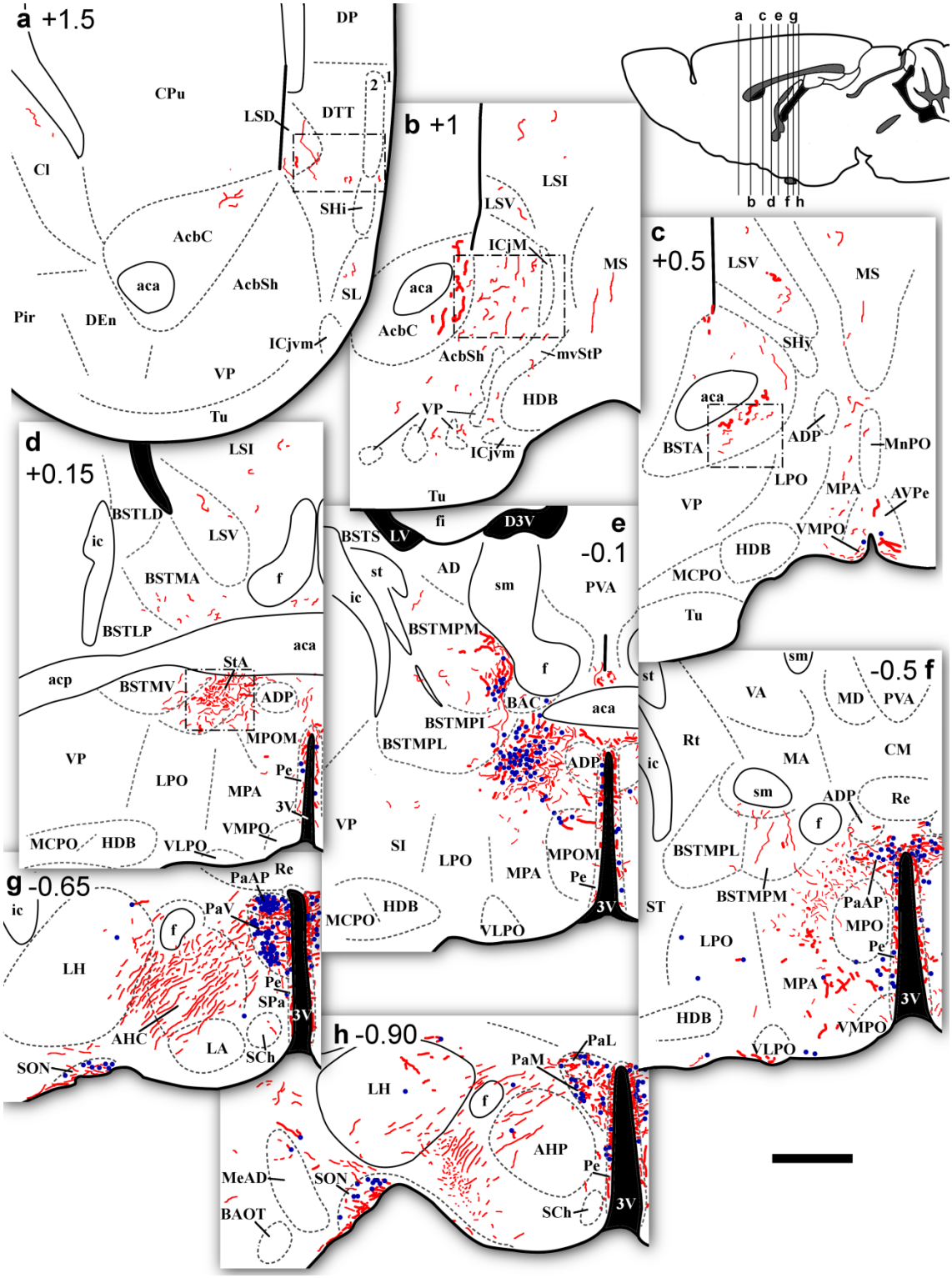

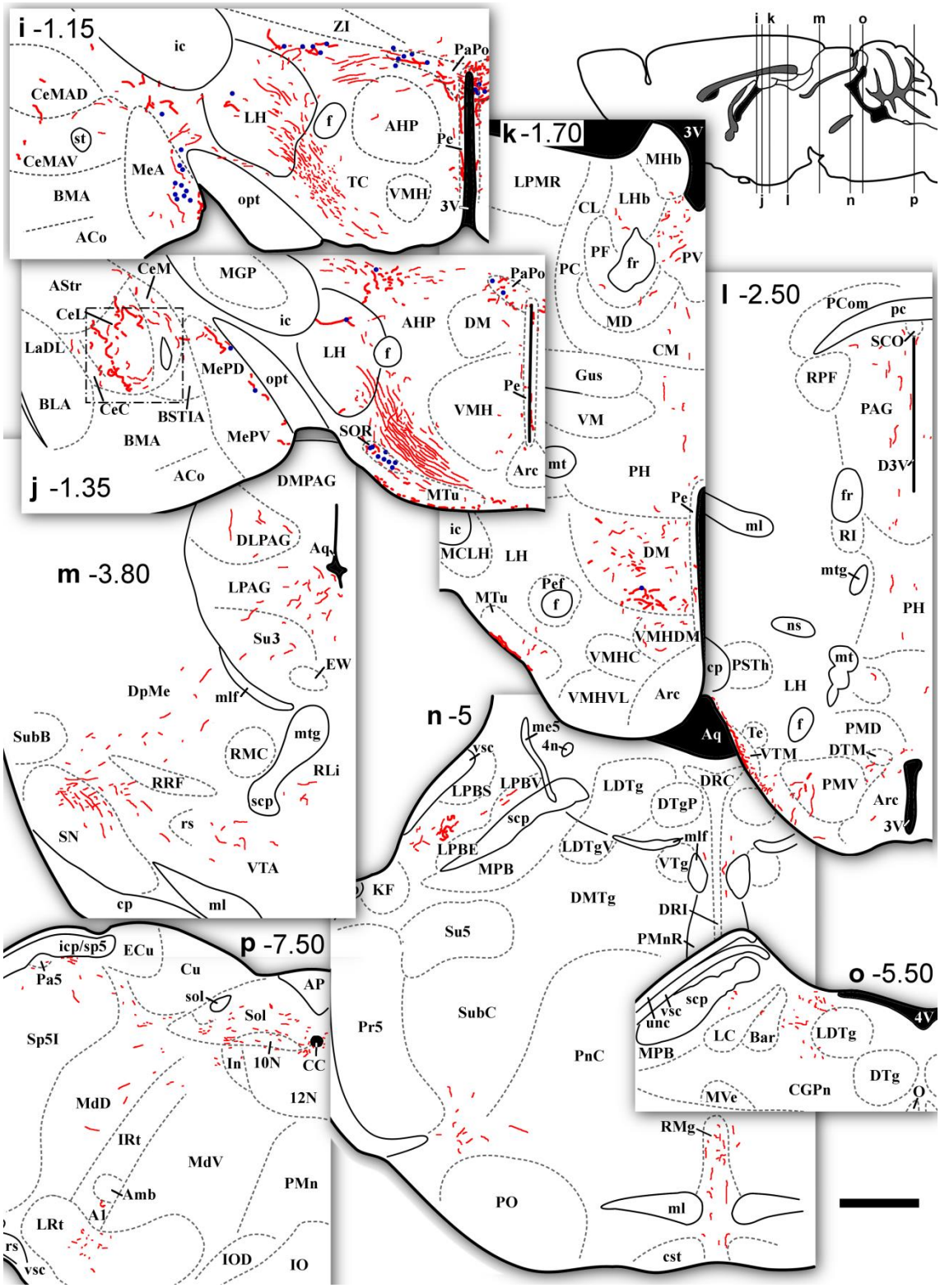


**Fig. 9. Distribution of oxytocin immunoreactivity in the brain of female mice.** Semi-schematic camera lucida drawings of specific regions of selected coronal sections through the left hemisphere of a representative case. The approximate rostro-caudal level of each section is indicated on a schematic sagittal-view of the mouse brain and the distance to bregma in mm is indicated in each section. Immunostained somata are shown as solid blue circles and thick and OT-ir fibres are represented as thick and thin red lines to reflect their actual appearance. Details of framed areas are shown in Fig. 14. Scale bars 500 µm.

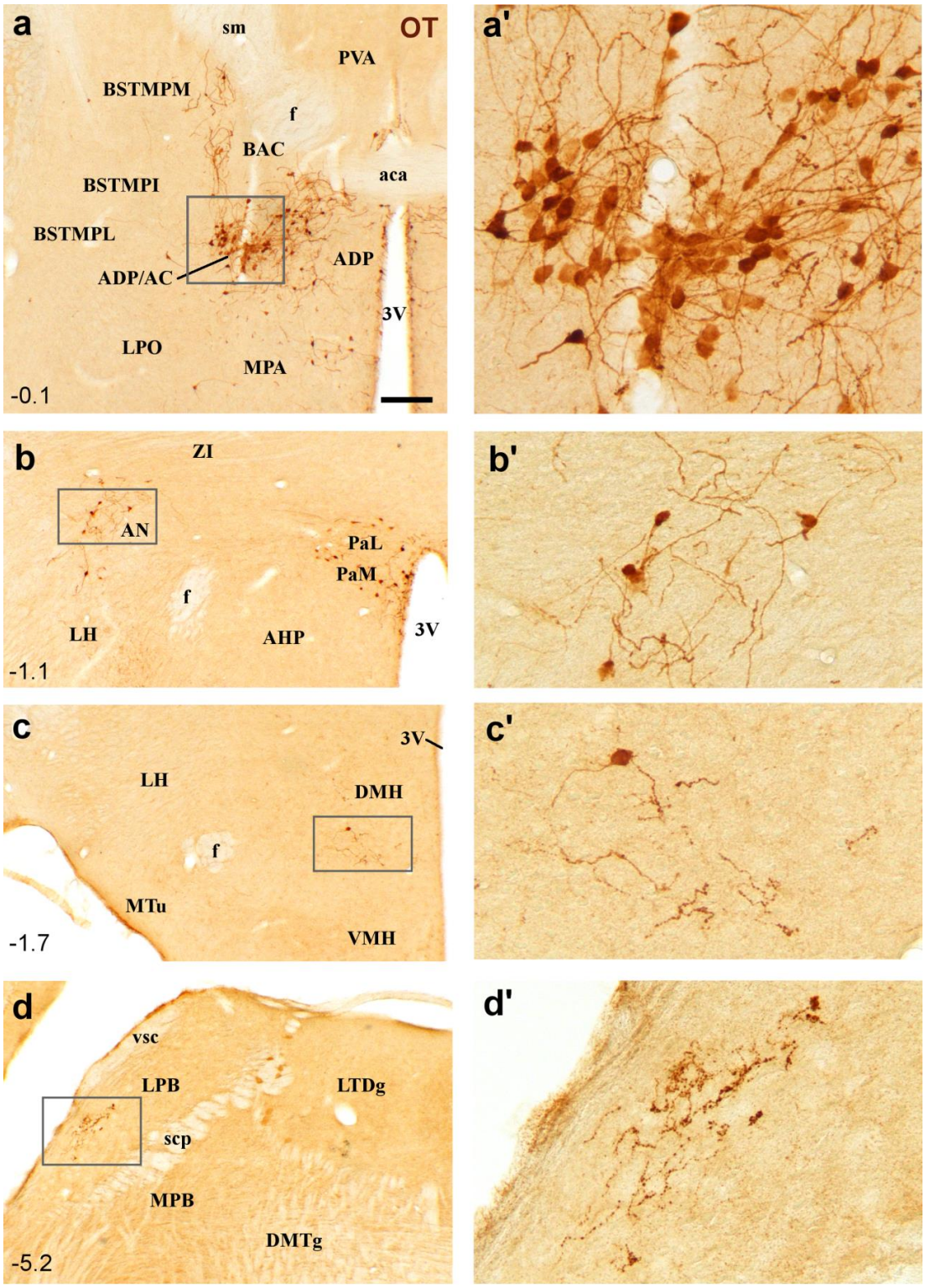


**Fig. 10. Details of OT elements in immunoreacted coronal sections of the brain of female mice** (antero-posterior level is indicated as distance from bregma in mm)**.** Picture **a** corresponds to an antero-posterior level similar to Fig. 9 e. In the framed area, shown in **a'**, AC/ADP immunoreactive cells appear closely associated to a blood vessel crossing vertically. **b** A caudal level of the Pa and lateral hypothalamic OT-ir accessory group. The framed area containing the AN somata is illustrated in **b'**. **c** Section of the medial hypothalamus showing the AN of the DMH. **c'** corresponds to the framed area of the DMH containing OT-ir cells. **d** The LPB contains highly OT-ir fibres in its ventrolateral portion. The beaded and twisted aspect of these OT-ir fibres is shown in **d'**. Scale bar in **a** 200 µm.

### *3.2. Distribution of OT-ir fibres*

Immunoreactive OT fibres are largely restricted to the cerebral hemispheres and hypothalamus with fewer and sparser terminal fields in the midbrain and pons.

In the cerebral hemispheres, sparse OT-ir fibres are observed in very few cortical structures: the dorsal taenia tecta (DTT), the claustrum (Cl) and dorsal endopiriform cortex (DEn) (Fig.1a, semi-schematic). There, immunoreactive processes are very thick and show a characteristic twisted morphology. In addition, the OT-ir innervation of these structures shows a high inter-individual variability and, in some cases, an apparent asymmetrical distribution, with fibres nearly or completely restricted to a single hemisphere.

From the DTT, OT-ir fibres extend into the rostral tip of the septum. In relation with this, sparse linear fibres are observed in the septohippocampal (SHi) and semilunar nuclei (SL), as well as in the lateral (ventral and lateral divisions; LSV and LSI) and medial (MS) septal nuclei. Also in the subcortex, OT-ir processes are seen in the ventral striatum. Thick, intensely immunoreactive fibres appear in the medial half of the core of nucleus accumbens (AcbC) (Fig.1a, b), whereas thin, branched, beaded fibres cross the medial accumbens shell (AcbSh) (Fig. 9b). Beyond the AcbSh, a few OT-ir fibres enter the medioventral striaptopallidum (mvStP) and the cell bridges of the ventral striatum, but no immunoreactivity is observed in the olfactory tubercle (Fig. 9b).

The terminal field in the ventral striatum extends caudally into the bed nucleus of the stria terminalis (BST) and innervates many elements of the so-called extended amygdala (see (Martínez-García et al., 2012; Olucha-Bordonau, Fortes-Marco, Otero-García, Lanuza, & Martínez-García, 2014). Within the BST, OT-ir innervation is noteworthy in the medial aspect of the anterior BST (BSTA and BSTMA; Fig. 9c,d). An especially dense field of OT-ir processes is present in the so-called strial part of the preoptic area (StA; Fig. 9d) where thick, dendrite-like processes are intermingled with thinner, beaded fibres (Fig. 11a'; Fig. 14d, d'). In the posteromedial BSTM (BSTMPM), there is a network of thin fibres intermingled with thick processes that might be dendrites of the OT-ir cells of the nucleus. This network is restricted to the medial half of the BTMPM and concentrates in the cell-poor area located next to the fornix and the BAC (Fig. 9e; Fig. 10a). Caudally, few long passing-fibres appear in the posterior edge of the BSTMPM (Fig. 9f).

The amygdala contains, as expected, notable OT immunoreactivity confined to the central (Ce) and medial (Me) nuclei. In the Me OT-ir fibres are concentrated in the anterior subnucleus

(MeA) where there is a mixture of thick-calibre, dendrite-like processes, probably associated to the cell bodies of the MeA and/or the adjacent SON, and thin, axon-like fibres. These fibres and processes are mainly oriented parallel to the optic tract (opt) (Fig. 9i,j). The central amygdala shows a remarkable OT-ir fibre network composed of thick and thin, beaded fibres located in all three divisions of the nucleus (medial, CeM; lateral, CeL; capsular CeC; Fig. 9i-j). This innervation shows a high degree of inter-individual variability concerning its distribution and density. Consequently, in some individuals there is a dense field of fibres in the Ce of both hemispheres, in some others there is an asymmetrical distribution of OT-ir fibres and they are only visible in one of the hemispheres, and in others no immunoreactive fibres are virtually observed in the Ce.

In the preoptic region, most OT-ir processes are located in the medial preoptic area (MPA). Neural processes originating from the group of OT-ir cells in the ADP/AC (described above) spread rostrally through the strial part of the medial preoptic region (StA) (Fig. 9d). Some thick OT-ir processes appear in the ventral half of the caudal MPA, while thinner ones are located in the dorsal half, bordering the anterior hypothalamus (Fig. 9e,f). The rest of the preoptic region, including the lateral preoptic area (LPO) and medial preoptic nucleus (MPO), is virtually devoid of OT-ir fibres, except for the processes derived from the scattered somata of the accessory nuclei (AN) (Fig. 9f)

At rostral levels of the anterior hypothalamus, abundant OT-ir fibres cross the anterior hypothalamic nucleus on their way to the median eminence (Fig. 9g). At the level between the anterior and medial hypothalamus, the neurosecretory axons go through the lateral hypothalamic nucleus (LH) and the retrochiasmatic area (Fig. 9h-j). Dendrite-like processes arise from the OT-ir somata of the Pa, SON and AN (Fig. 9g-j). In the medial hypothalamus, only the dorsomedial hypothalamic nucleus (DMH) contains OT-ir innervation (Fig. 9k). Some fibres run through the ventral surface of the media tuberal (MTu) and ventral tuberomamillary (VTM) nuclei (Fig. 9k,l). In the premammillary area, few fibres appear in the lateral half of the ventral premammillary nucleus (PMV) and around the arcuate (Arc) (Fig. 9l).

From the hypothalamus, a few OT-ir fibres are seen to cross the boundaries with the thalamus. Thus, in the posterior hypothalamic area, thin OT-ir fibres oriented in the dorsoventral direction enter the central medial thalamic nucleus and provide a sparse innervation of the mediodorsal thalamic nucleus (MD), parafascicular nucleus (around the fasciculus retroflexus), lateral habenula and the lateral aspect of the caudal paraventricular thalamic nucleus (Fig. 9 k)

In the mesencephalon, the density of OT-ir fibres is significantly lower than in the forebrain. The periaqueductal gray (PAG) shows the most noticeable OT-ir innervation. In the rostral PAG, thin OT-ir processes gather in its dorsolateral portion and around the aqueduct (Fig. 9l). In more caudal sections of the PAG, OT-ir innervation appears in the dorsolateral column and in the ventral half of the PAG, again being denser near the aqueduct (Fig. 9m). The innervation of the ventrolateral PAG extends ventrolaterally, with long fibres crossing the deep mesencephalic nucleus (DpMe) and branching into a denser terminal field in the dorsomedial region of the substantia nigra (SN). Scattered fibres appear also in the ventral tegmental area (VTA) and dorsal linear nucleus of the raphe (RLi) (Fig. 9m). Caudally, few OT-ir fibres appear in the dorsal raphe and in two unnamed areas, one between the periolivary region (PO) and the subcoeruleus nucleus (SubC) (Fig. 9n) and also between the Barrington nucleus (Bar) and laterodorsal tegmental area (LDTg) (Fig. 9o).Interestingly, the raphe magnus (RMg) shows considerably denser innervation (Fig. 9n). The lateral parabrachial (LPB) nucleus contains a small cluster of OT-ir fibres in its ventrolateral half. These OT-ir processes in the LPB display two different morphologies: typical thin fibres with axonal buttons accompany highly immunoreactive wrenched thick fibres (Fig. 9n).

Finally, thin OT-ir fibres innervate various areas at the level of the medulla (Fig. 9p). The nucleus of the solitary tract (Sol) shows OT-ir processes, apparently running rostro-caudally, that extend into the dorsal reticular nucleus (MdD). The dorsal tip of the spinal trigeminal nucleus (Sp5) also contains few immunoreactive fibres, but this innervation does not enter the adjacent cuneate nucleus (Cu). Ventrally, the lateral reticular nucleus (LRt) shows a cluster of OT-ir fibres, near the putative location of the noradrenergic cell group A1.

### 4. Distribution of OT+AVP co-localization in the brain of mice

Using double immunofluorescent labelling, we simultaneously stained OT and AVP in male and female CD1 mice. The distribution of AVP and OT immunoreactivity was indistinguishable from that observed in Experiment 1 and Experiment 3, respectively. Removing the primary antibody for either OT or AVP in the primary antibody solutions resulted in lack of labelling for the corresponding peptide, discarding cross-reactivity between AVP and OT detection methods. Sequential acquisition of the confocal images and posterior examination of labelled elements discarded crossed AVP and OT signals, which were confirmed by the presence of singly (either OT- or AVP-ir) and doubly labelled structures in the samples.

### *4.1. Coexpression of AVP and OT: double labelling of cell bodies*

We have mapped cell bodies co-expressing both nonapeptides in the brain of male and female CD1 mice, employing double immunofluorescence for AVP and OT. Although in the present study we have not performed a quantitative analysis, our results strongly suggest that females and males show a similar pattern of double immunoreactive cells, with no noticeable differences between sexes or between individuals. In fact, most of the somata were immunoreactive for either OT or AVP exclusively, with just a minority of cells showing double labelling in preoptic and hypothalamic locations. Remarkably, vasopressinergic cells of the sexually dimorphic cell group in the BSTMPI (Rood and deVries, 2011; Otero-Garcia et al., 2014), where no OT-ir somata have been described before (Cassel and Morris, 1989), displayed only AVP immunolabelling, especially visible in male specimens (not shown).

By contrast, in the dorsal preoptic area, the group labelled as the AC/ADP (Otero-Garcia et al., 2014) contains the higher rate of double-stained cells. In most cases, peptidergic cells in the AC/ADP show high oxytocin immunoreactivity (OT-ir) together with low and variable arginine-vasopressin immunoreactivity (AVP-ir) (Fig. 11a, b, a', b'), a trait that is also found in the anterior Pa (Fig. 12a, a'). In these two peptidergic cell groups (AC/ADP and anterior Pa) OT-immunoreactivity seems equally intense in all the cells, whereas AVP immunofluorescence shows a low, but remarkably heterogeneous intensity within OT-ir cells (Fig. 11a', b'). In addition, some intensely stained AVP-ir cells, negative for OT, are located in the proximities of the anterior Pa (Fig. 11b'''). In the medial area of the BSTMPM, bipolar cells singly stained for OT-ir or AVP-ir appear oriented parallel to the border between the BSTMPM and the stria medullaris (Fig. 11c).

With the exception of the anterior edge of the paraventricular nucleus, where we found many double-labelled cells, in the rest of the Pa OT-ir and AVP-ir cells are partially segregated in different subnuclei (as described in rats by (Hou-Yu et al., 1986) and double labelled somata are scarce. In the anterior Pa, there are abundant singly labelled cells for OT with few intermingled cells displaying intense AVP-immunoreactivity, negative for OT (Fig. 12a, a'). In the intermediate portion of the Pa, OT-ir cells occupy its medial subdivision (PaM) and the juxtaventricular compartment (periventricular nucleus, Pe), with few OT-ir somata entering the lateral nucleus (PaL). Here, most AVP-ir cells gather in the dorso-lateral portion of the PaL, but few singly AVP-ir cells and processes appear intermingled with OT-ir ones in the PaM (Fig. 12 b, b'). Similarly to anterior levels, at these intermediate ones there are few doubly labelled cells, usually located in the ventromedial portion of the PaM, which show equal intensity for AVP-

and OT-immunoreactivity (Figs. 3a'' and b''). In the posterior nucleus of the Pa (PaPo), only OT-ir cell bodies remain, intermingled with some AVP-ir thick processes (Fig. 12c).

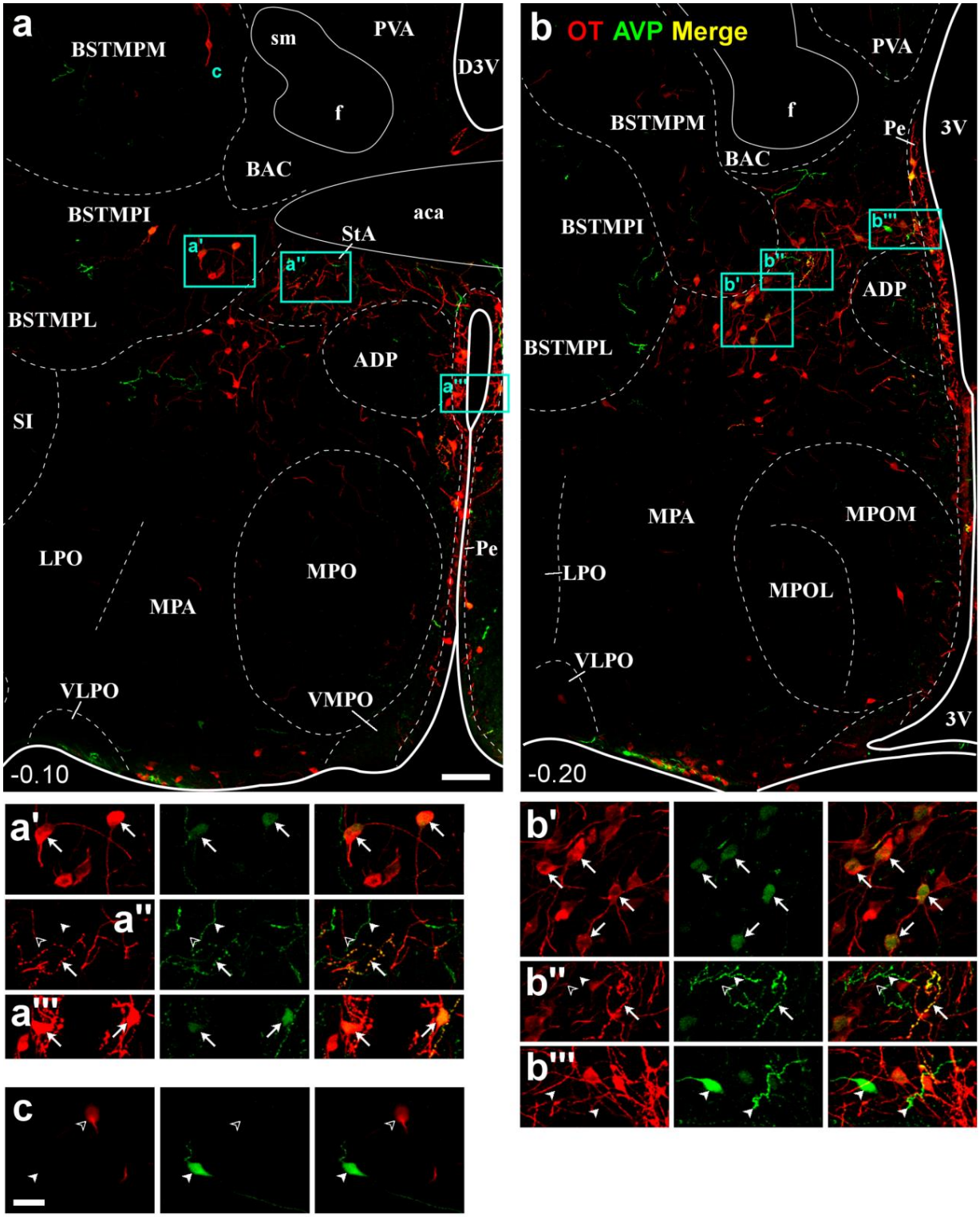

**Fig. 11. Simultaneous immunofluoresce for oxytocin (red) and vasopressin (green) in two coronal sections** (**a** and **b**) **through the left preoptic area of a female mouse** (distance from bregma is indicated in mm). In picture **a,** the rostral-most part nonapeptidergic cells of the AC/ADP appear between the ventral BSTM and the dorsal MPA. In **b,** a slightly more caudal section shows the rest of AC/ADP immunoreactive somata occupying the dorsal MPA, confined between the ventral BSTM, the BAC and the ADP. **a', b'** Confocal sections through the AC/ADP group show a majority of double-stained cells (white arrows) displaying intense OT labelling plus mild AVP labelling. OT immunoreactivity of similar intensity appears in the soma periphery and processes, whereas AVP immunoreactivity concentrates in the soma centre and shows variably intensity among cells. **a'', b''** Singly OT-ir (black arrowheads), single AVP-ir (white arrowheads) and doubly labelled fibres (white arrows) appear in the strial part of the preoptic area. **a'''** In the periventricular nucleus (Pe) somata show a pattern of double staining, similar to that of AC/ADP (intensely stained for OT, variably stained for AVP). **b'''** illustrates the transition between the AC/ADP and the nonapeptidergic cells of the rostral Pa . At this level of the Pe, there are singly labelled AVP-ir cells plus a variety of doubly labelled neurons. In addition to the AC/ADP somata, single OT- or AVP-immunoreactive bipolar cells are clearly visible in the medial border of the BSTMPM (**a**). Picture **c** shows a high magnification view of the medial BSTMPM (location indicated within picture **a**) to illustrate singly AVP-ir (white arrowhead) and singly OT-ir (black arrowhead) labelled neurons. The two low-power images (**a** and **b**) are the sum of two confocal slices, separated 4 um in the z-axis, acquired sequentially with a 10x objective. The cytoarchitecture is inferred from DAPI staining of the same sections (not shown). Scale bar in **a** 100 μm (valid also for **b**). Scale bar in **c** 30 μm (valid also for **a/b' '' '''**)

In the periventricular area (Pe), immunoreactive somata gather near the ventricular walls. Relative OT and AVP immunoreactivity in Pe somata depends on the rostro-caudal level and parallels the pattern found in the adjoining AC/ADP or Pa. Thus, double labelled cells are frequent in the Pe next to the AC/ADP (Fig. 11a''') and anterior edge of the Pa, but scarcer at more caudal levels. As a rule, however, doubly labelled cells highly immunoreactive for both OT and AVP appear frequently within and nearby the Pe.

Apparently, the supraoptic nucleus (SON) contains more AVP-ir than OT-ir cells. Oxytocinergic somata are located in the dorso-medial aspect of the SON and are more abundant at rostral levels (Fig. 13a,b). By contrast, the caudal tip of the nucleus contains mostly AVP-ir cells (Fig. 13c). In the retrochiasmatic division of the supraoptic nucleus (SOR), OT-ir cells also appear dorsally to the AVP-ir, and are more abundant in rostral levels (not shown). Throughout the SON, almost all cells were immunoreactive exclusively for either AVP or OT. Occasionally, scattered somata show double labelling of similar intensity (Inset in Fig. 13 b').

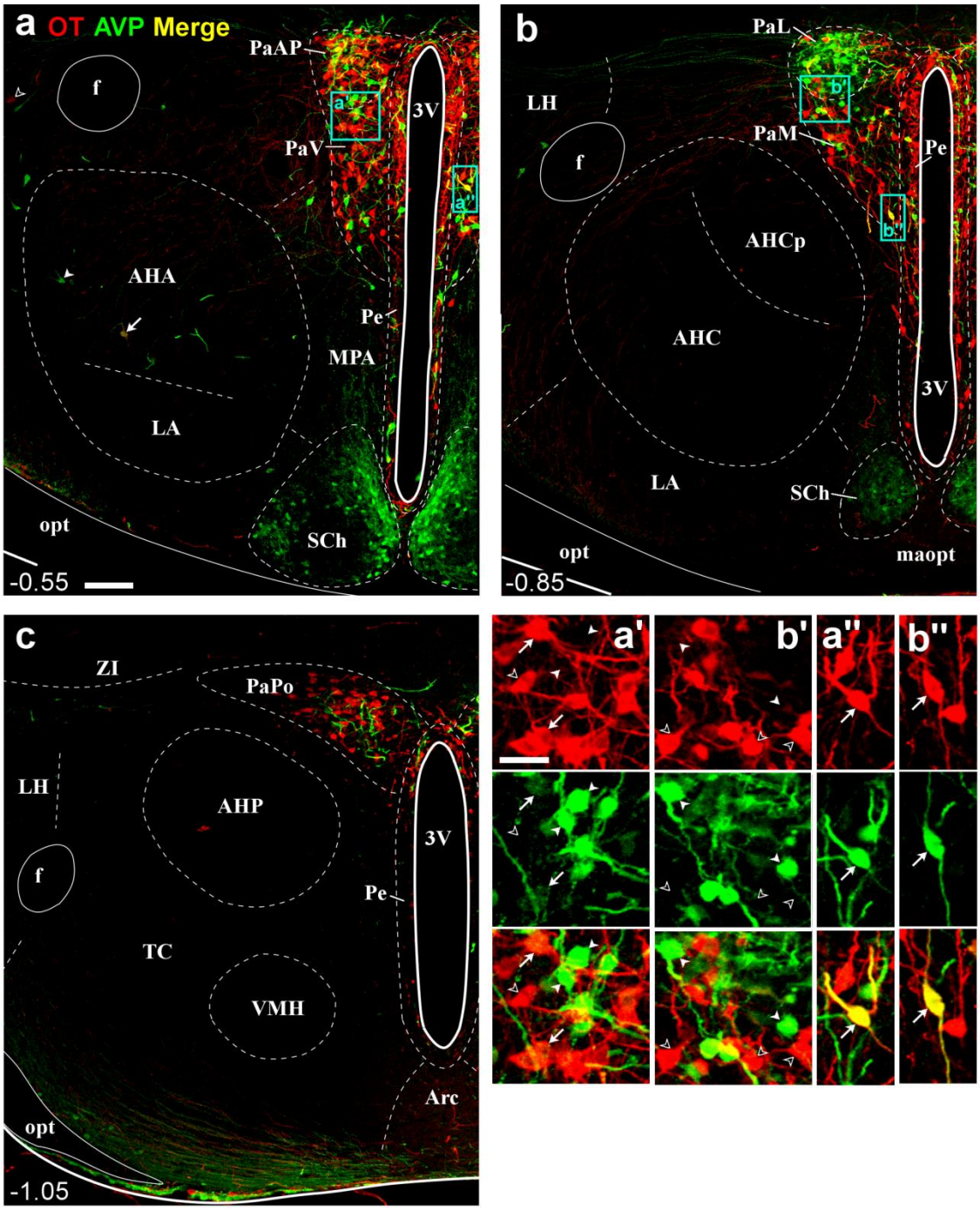


**Fig. 12 Simultaneous immunolabelling of oxytocin (red) and vasopressin (green) in three coronal sections of the left paraventricular nucleus (Pa) of a female mouse** (antero-posterior level is indicated as distance from bregma in mm). **a, a'** The rostral Pa contains double labelled cells similar to the ones in AC/ADP (white arrows), as well as single OT-ir cells (black arrowheads) and single AVP-ir cells (white arrowheads). The anterior and lateral hypothalamus show also OT-ir, AVP-ir and double stained somata at this level. **b, b'** In the middle area of the Pa, double-labelled somata are infrequent. AVP-ir cells gather in the lateral subnucleus of the Pa (PaL), while OT-ir somata predominate in the medial subdivision of the Pa (PaM). **a'' b''** Intensely double-stained cells appear in the ventro-medial portion of the Pa and adjacent periventricular region (Pe). **c** The caudal Pa (PaPo) contains only OT-ir somata and some AVP-ir processes. Low-magnification images (**a, b, c**) are the sum of two confocal slides, separated 4µm in the z-axis, acquired sequentially with a 10x objective. The cytoarchitecture is inferred from DAPI staining of the same sections (not shown). Scale bar in **a** 100 µm (also valid for **b** and **c)**. Scale bar in **a** 30 µm (also valid for **a/b' ''**).

As described for OT-immunoperoxidase material, some OT-ir, but also some AVP-ir cells with monopolar or bipolar morphology trespass the SON boundaries to enter the medial region of the anterior medial amygdala (MeA) (Fig. 13c,d). There, doubly labelled cells are also present but infrequent (Fig. 12d').

### *4.2. Coexpression of AVP and OT: distribution of doubly labelled fibres*

In the examined specimens, double-labelled fibres only appear in some forebrain regions. All thalamic, hypothalamic and mesencephalic areas analysed only display single AVP-ir or OT-ir processes. Therefore, in this section we focus on the areas where we observe co-localization of OT and AVP immunoreactivity.

As we have described above, in the cortical areas of the frontal lobe OT-ir fibres are restricted to a few cortical structures in the anterior cerebral hemispheres, namely the DTT, claustrum and dorsal endopiriform cortex. Some of these structures also show AVP-ir fibres and, in some instances, fibres are doubly labelled. Figure 5a'' shows a representative case in the boundary between the DTT and SHi, where winding varicose fibres are found to be intensely immunoreactive for AVP and faintly stained for OT (white arrows). Singly labelled fibres for either peptide are also seen (black arrowheads point to a OT+/AVP- fibre).

Within the subcortex, the dorsal lateral septal nucleus (LSD) shows some lineal processes that appear intensely OT-ir but negative for AVP (white arrow), whereas others are weakly AVP-ir and negative for OT (white arrowhead, Fig. 14a'). In the so-called medioventral striato-pallidum (mvStP, the region located between the Acb and the VDB, Otero-Garcia et al., 2014) there is a relatively dense, AVP-ir-only terminal field in. In addition, the Acb itself shows a remarkable population of nonapeptide-immunoreactive fibres. There, many fibres observed are intensely immunoreactive for both OT and AVP (white arrows, Fig. 14 b''), although there are also abundant fibres showing strong OT-immunoreactivity but weak AVP signal (white arrows, Fig. 14 b'''). Less frequently, highly AVP-ir processes show weak OT-immunoreactivity (white arrow, Fig. 14 b'). Immediately caudal to the Acb, the anterior portion of the medial bed nucleus of the stria terminalis (BSTMA) and strial part of the medial preoptic area (StA) also contain OT-ir processes of different diameters (Fig. 14 c, d). Similarly to the adjacent Acb, the BSTMA and StA display some singly OT-labelled fibres (black arrowheads; Fig. 14c', d'), some fibres singly labelled for AVP (white arrowheads), but also doubly labelled fibres. Most of the latter show strong OT immunolabelling with variable, but reduced AVP labelling (white arrows, Fig. 14c', d').

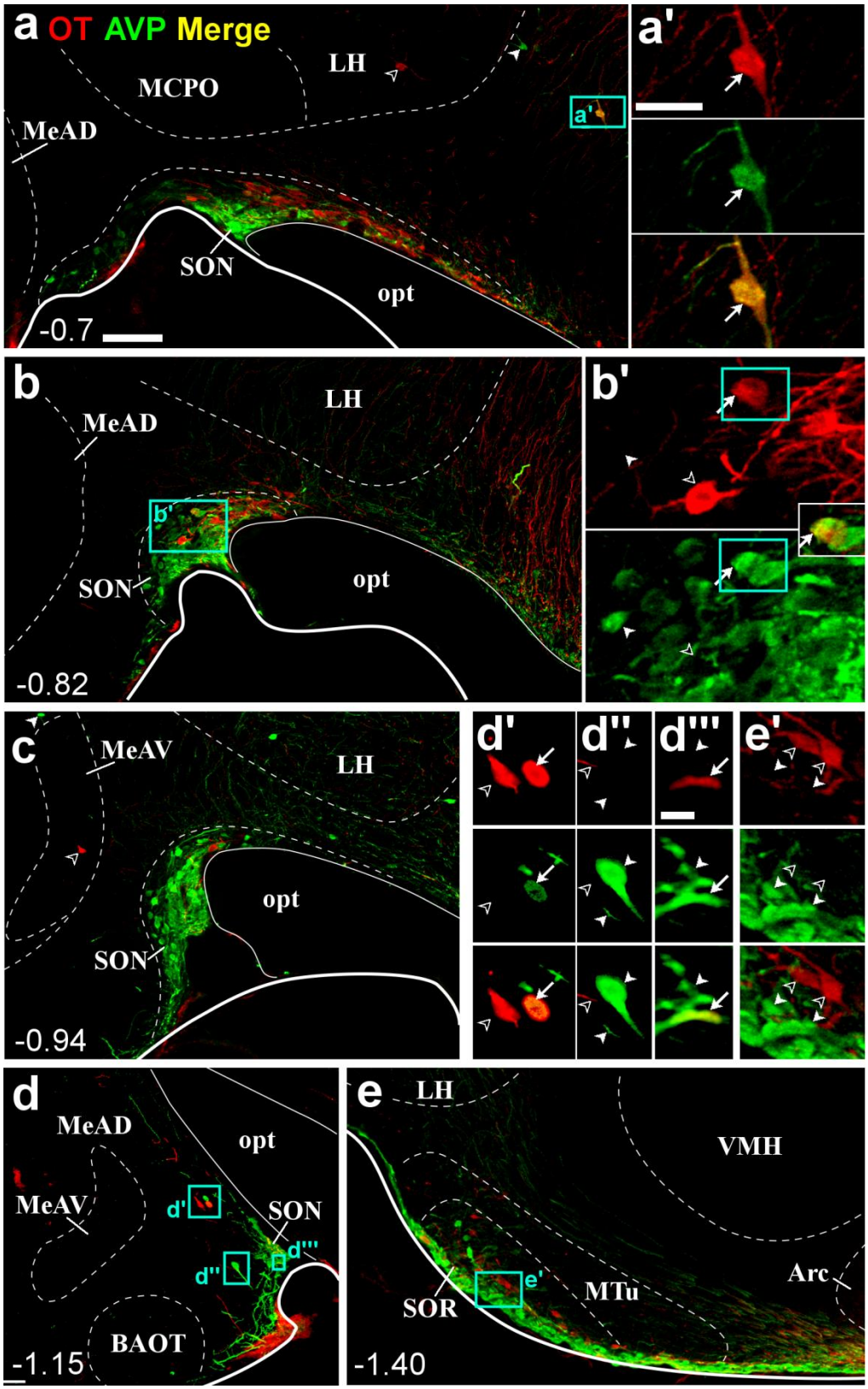
a OT AVP Merge
LH
MCPO
MeAD
a'
SON
opt
-0.7
a'
b
LH
MeAD
b'
SON
opt
-0.82
b'
c
MeAV
LH
opt
SON
-0.94
d'
d''
d'''
e'
d
MeAD
opt
MeAV
d'
SON
d'''
d''
BAOT
-1.15
e
LH
VMH
SOR
e'
MTu
Arc
-1.40

**Fig. 13 Simultaneous immunolabelling of oxytocin (red) and vasopressin (green) in three coronal sections of the left supraoptic nucleus (SON) of a female mouse** (antero-posterior level is indicated as distance from bregma in mm). **a** The rostral SON contains mostly OT-ir cells, situated in the dorso-medial region of the nucleus, whereas AVP-ir somata are located in the ventrolateral portion of the SON. OT-ir (black arrowhead), AVP-ir (white arrowhead) as well as double-stained somata (**a**', white arrow) appear in the lateral hypothalamic region at this rostro-caudal level. **b** AVP-ir cells arrange in the ventrolateral and caudal regions of the SON. **b'** Scarce double-labelled somata appear at medio-dorsal locations. **c** The caudal SON contains almost exclusively AVP-ir cells, alike the adjacent hypothalamic area. Scattered OT-ir (black arrowhead) and AVP-ir (white arrowhead) cells appear in the medial border of the nearby anterior medial amygdala (MeA). **d** At caudal levels of the SON, abundant AVP-ir and few OT-ir processes enter the medial amygdala edge. **d', d''** Some single OT-ir (black arrowhead), AVP-ir (white arrowhead) and double immunoreactive somata (white arrow) appear in the medial portion of the anterior medial amygdala. **e, e'** In the retrochiasmatic supraoptic nucleus (SOR), abundant AVP-ir cells (white arrowheads) and processes extend along the ventral surface, next to the optic tract, while few OT-ir somata (black arrowheads) and fibers are located immediately dorsal to the AVP-ir elements. Low-magnification images are the sum of two confocal slides, separated 4µm in the z-axis, acquired sequentially with a 10x objective. The cytoarchitecture is inferred from DAPI staining of the same sections (not shown). Scale bar in **a** 100 µm (also valid for **b**, **c, d** and **e)**. Scale bar in **a'** 30 µm (also valid for **b/d/e**' and **d''**). Scale bar in **d'''** 5 µm.

In the amygdala, the central nucleus (Ce) contains long immunoreactive processes of different calibres (Fig. 14 e). Although some singly labelled fibres for OT (black arrowheads in Fig. 14e') or for AVP are found (white arrowhead in Fig. 14e'), most of the fibres in the Ce are immunoreactive for both OT and AVP (white arrows, Fig. 14 e', e''). Most (but not all) of the doubly labelled fibres were intensely immunostained for OT and faintly labelled for AVP, although the reverse situation is also occasionally observed.

In the medial amygdala (Me), immunoreactive processes enter its ventromedial edge apparently arising from the rostral SON. Most of the labelled processes in the Me are singly immunoreactive for AVP (white arrowheads in Fig. 13 d'', d'''), few are only immunoreactive for OT (Fig. 13 d'', black arrowhead), and only scattered fibres display both signals (Fig. 13 d''', white arrow). These observations are consistent with the pattern of labelling of the nearby SON immunoreactive somata, which probably originate the mentioned processes.

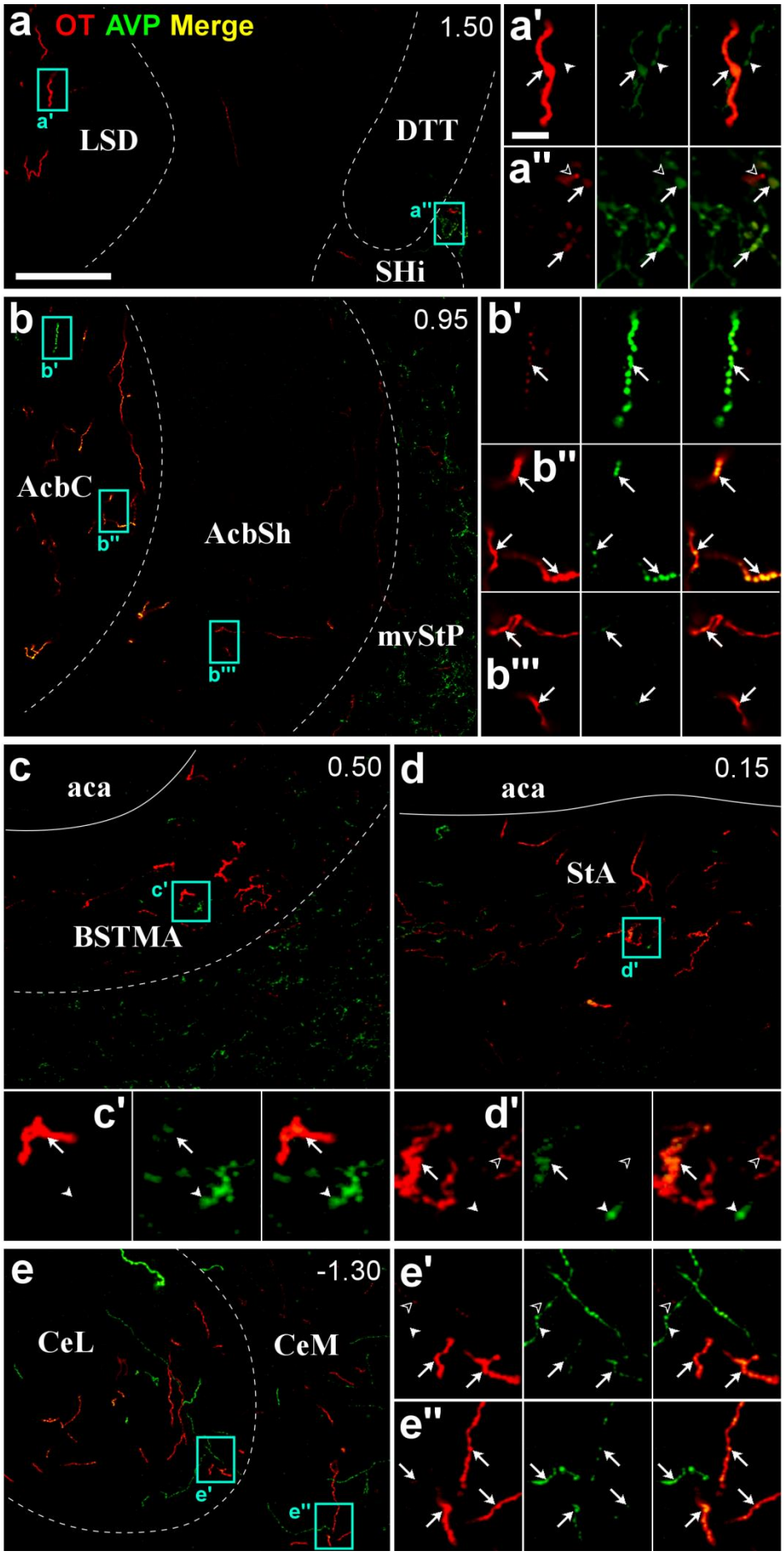
a
OT AVP Merge
1.50
a'
LSD
DTT
a''
SHi
a'
a''
b
0.95
b'
AcbC
b''
AcbSh
mvStP
b'''
b'
b''
b'''
c
aca
0.50
c'
BSTMA
d
aca
0.15
StA
d'
c'
d'
e
-1.30
CeL
CeM
e'
e''
e'
e''

**Fig. 14 Simultaneous immunolabelling of oxytocin (red) and vasopressin (green) in coronal sections of five selected areas displaying doubly stained processes in the left hemisphere of a female mouse** (antero-posterior level is indicated as distance from bregma in mm). Approximate location of the selected areas is framed in Fig. 9 a, b, c, and j. Antero-posterior level is indicated in each area as distance from bregma in mm. **a** In the rostral-most septal area, straight and thick OT-ir processes display also very weak AVP-immunoreactivity (white arrow in **a'**). Occasional AVP-ir fibre tangles show low OT-immunoreactivity near the dorsal taenia tecta (DTT) and septohippocampal neucleus (Shi) (white arrows in **a''**). Some fibers show only OT (black arrowhead, **a''**) or only AVP (white arrowhead, **a'**) immunoreactivity. **b** In the nucleus accumbens (Acb), doubly-labelled long processes display different levels of immunoreactivity for OT and AVP (**b', b'''**, white arrows), being most of the fibers highly immunoreactive for both peptides (**b''**, white arrows). The medially adjacent ventral diagonal band (VDB) shows an AVP-ir terminal field which continues dorsally into the medial septum (**b**). **c, d** Ventrally to the anterior commissure, at its caudal edge, OT-ir processes of different diameters appear in the anterior medial bed nucleus of the stria terminalis (BSTMA) and strial part of the medial preoptic area (StA). Most of these OT-ir processes also show mild AVP immunoreactivity (**c', d'**, white arrows). Some highly AVP-ir elements appear intermingled and show no OT-immunoreactivity (**c', d'**, white arrowheads). **e** In the central amygdala (Ce), long immunoreactive processes of different calibers display AVP and OT immunoreactivity. Most of the fibers are immunoreactive for both OT and AVP (white arrows, **e' e''**). Intensity of OT and AVP immunoreactivity is variable, with some processes labelled only for OT (black arrowhead) or AVP (white arrowhead) (**e'**). The cytoarchitecture is inferred from DAPI staining of the same sections (not shown). Scale bar in a 100 µm (also valid for **b, c, d** and **e**). Scale bar in a' 10 µm (also valid for **a/b/c/d/e' '' '''**).

# DISCUSSION

The present work constitutes the first comprehensive description of the nonapeptidergic systems of the brain of the mouse. Besides the well-known neurosecretory nuclei in the hypothalamus, our experiments have unveiled a series of cell groups located mainly in the cerebral hemispheres of the telencephalon and the telencephalon-diencephalic junction, which express AVP, OT or both nonapeptides simultaneously. In addition, we have observed several terminal fields that reveal the existence of important nonapeptidergic central pathways in the brain of mice, whose modulatory roles on social behaviours are discussed below.

We will first discuss our findings relative to AVPergic systems. As we will see, the mouse brain contains sexually dimorphic groups of AVP-ir cells that give rise to a complex axonal system innervating most of the nodes of the SBN. In addition, AVP-ir fibres and processes displaying no apparent dimorphism are found in several key centres of the subpallial amygdala. Therefore, the medial amygdala contains both, sexually dimorphic and non-dimorphic AVP-ir processes, likely involved in the modulation of different components of social behaviour. Finally, our data allow us identifying a novel case for a sexually dimorphic centre in the medial ventral striato-pallidum (mvStP), on the basis of its AVP immunoreactive dimorphic innervation. We discuss therefore whether it should be included as a node of the SBN system, in which it would likely play a role in the control of motivational aspects of social interactions.

We devote the second part of the discussion to our results on the distribution of OT in the brain of mice. Our findings can be discussed from a neurodevelopmental perspective as indicative of a double origin of the OT cell groups in the brain from two distinct regions of the embryonic hypothalamic neuroepithelium from where cells would follow two main migratory streams. From a functional viewpoint, our data reveal different neural mechanisms that would mediate synchronous neuroendocrine (bloodstream) and central (synaptic) OT release. This would explain a correlation between circulating OT levels and several behaviours in spite of the low permeability of the blood-brain-barrier to nonapeptides. We will also discuss the possible significance of the apparently asymmetric distribution of OT-ir innervation in several regions of the telencephalon, as suggestive of a functional specialization of the cerebral hemispheres that would be present in the ancestral mammals and would explain the origin of some functional asymmetries in the human brain.

Finally, our experiments have revealed the existence of a set of cells expressing both OT and AVP at immunohistochemical detectable levels. This is associated to the presence of doubly labelled (OT+AVP-ir) fibres in several regions of the subcortical telencephalon. This is strongly

suggestive of the existence of a specific OT+AVP central nonapeptidergic system in the cerebral hemisphere, whose possible role in the control of the expression of maternal behaviours is then fully discussed on the basis of previous literature on that issue in rats.

## 1. Vasopressinergic circuits in the cerebral hemispheres: sexually dimorphic and non-dimorphic

Our results from males and females of the outbred mouse strain CD1 generally fit previous reports by different authors (Ho, Murray, Demas, & Goodson, 2010; Plumari et al., 2002; B D Rood & de Vries, 2011) in the commonly used inbred strain C57BL. However, our material reveals some interesting findings relative to AVPergic systems in the brain of mice and other mammals.

As discussed above, most of the AVP-ir cells are found in the hypothalamic magnocellular nuclei, where AVP-ir cells appear in close association with their OT-ir equivalents in the Pa and SON. However, there are at least four main AVPergic populations in the brain that are not found in the classical neurosecretory nuclei. One belongs to the suprachiasmatic nucleus, where a dense population of AVP-ir cells is found which is not sexually dimorphic (see Fig. 1 and Fig. 12). Two-three additional AVP-ir cell populations are found in the amygdala and BST/preoptic junction. Two of these populations are sexually dimorphic (in favour of males) and testosterone-dependent: they are located in both poles of the extended amygdala, one in the intraamygdaloid BST (BSTIA; Fig. 1 k, l and Fig. 2 d) and the other one in the posterointermediate medial BST (BSTMPI; Fig. 1 f, g and Fig. 2 a). Finally, a third cell group, showing no clear sexual dimorphism but a non-significant dominance in our female samples, is found in the dorsal anterior preoptic area, just medial to the posterior BST and ventral to the nucleus of the anterior commissure, the so-called ADP/AC. The latter cell population is characterised by co-expressing NADPH-diaphorase (Fig. 1 f, g and Fig. 2 a, c). As we will later discuss, many cells in this group are co-expressing oxytocin.

### *1.1. Sexually dimorphic AVPergic cells in the brain of rodents*

#### *1.1.1. Sexually dimorphic AVP-ir cells lie in the intra- and extra-amygdaloid bed nucleus of the stria terminalis*

The first works describing the distribution of AVP immunoreactivity in the rat brain defined two main populations of AVP-ir cells in the extended amygdala, one in the posterior BST (Caffe and van Leeuwen 1983) (see below) and another group that was assigned to the medial

amygdala (Caffe and van Leeuwen 1983; DeVries et al. 1985). This finding has been apparently replicated in subsequent studies in rats (Szot and Dorsa 1993) and mice (Rood et al. 2008; Ho et al. 2010; Rood and de Vries 2011b). A close observation of the illustrations in DeVries et al. (1985; see their figure 3C and 4A) and in Rood and de Vries (2011b; see their figure 1E-H), the only reports that show low-power photographs or drawings allowing such an analysis, indicate that most of the AVP-ir cells in the amygdala are located out of the Me, just lateral to the posterodorsal medial amygdala and next to the *stria terminalis* (see also figure 3A in Ferris et al. 1995). Using a chemoarchitectonic approach (NADPHd histochemistry) and considering current cartography not available in the times when these cells were first described, our results lead us to conclude that the AVP-ir cells in the amygdala of rats and mice should be better considered as belonging to the intra-amygdaloid bed nucleus of the *stria terminalis* (BSTIA). Our colchicine injections reveal few additional AVP-ir neurons in the MePD (bipolar cells parallel to the optic tract, Fig. 3c') and also in part of the central amygdala (Fig. 2d and 2f).

Our results (see experiment 1) confirm previous observations in mice (Rood et al. 2011) and rats (DeVries et al. 1985) indicating that this population of AVP-ir neurons is sexually dimorphic, being more abundant in males, where AVP expression seems dependent on testosterone. This dependence on testosterone probably underlies the activational effects of androgens on AVP-mediated behaviours in males. Whether these effects depend on androgen (through the testosterone metabolite dihydrotestosterone) or oestrogen receptors (through its aromatized metabolite estradiol), or on both, remains unclear (see discussion in de Vries, 2008). In this respect, it has been shown that aromatase knockout male mice show an apparent reduction in the population of AVP-ir cells in the BST and in the density of AVP-ir terminal fields in different centres (Plumari et al., 2002). Although this is compatible with a role of oestrogen (from aromatized testosterone) in AVP expression in adult life, it can also be due to organizational effects of testosterone through oestrogen receptors during development. In fact, it has been shown that masculinization of the BST in mice involves the actions of oestrogen mostly binding to alpha oestrogen receptors during the postnatal critical period (Tsukahara et al., 2011). Furthermore, female and male gonadectomised adult rats treated with equal amounts of testosterone still show a marked differences in the levels of AVP mRNA expression in the BST (G J De Vries, Wang, Bullock, & Numan, 1994), thus suggesting that organizational effects underlie the activational effects in adult life. Apparently, during postnatal life, testosterone (acting on androgen and/or oestrogen receptors) directs galanin-expressing cells to co-express AVP, using stable epigenetic mechanisms. However,

intersexual differences in the cerebral AVP neural circuits are not exclusively due to circulating hormones, but to sex chromosomal complement (see full discussion in De Vries 2008).

Concerning the AVP-ir cell groups in the BST proper, our results and those by others (Ho et al. 2010; Rood and De Vries 2011a) in C57BL mice, reveal at least three populations in the BST/preoptic area of mice, clearly visible in colchicine treated animals (see Figs. 2a-c; Fig. 3a-b). First, immunoreactive cells are abundant in the lateral aspect of the posterior BST, distributed between the BSTMPL and BSTMPI. Cells here are faintly immunostained except after colchicine treatment. A second AVP-ir cell group is located in the medial aspect of the BSTMPM, next to the fornix and *stria terminalis*, which shows darkly stained cells in both males and females even without colchicine treatment. Finally, a population of AVP-ir/NADPHd-positive neurons is seen in the ADP/AC. In our quantitative analysis we have recorded the number of AVP-ir somata in two regions of the BST/preoptic area. The lateral one comprised cells in the BSTMPI/BSTMPL, whereas the medial one was restricted to cells in the ADP/AC. While the number of AVP-ir cells in the lateral aspect of the BSTMP is larger in males than in females or castrated males, the number of cells in the ADP/AC is similar in intact and castrated males and in females. This fact indicates a distinct functional significance for these two vasopressinergic cell groups, thus fitting previous reports of cell activation during mating and male-male interactions in mice (Ho et al. 2010).

It is not clear whether the sexually dimorphic and non-dimorphic AVP-ir cell groups in the BST-preoptic junction have the same or different embryonic origin. Thus ADP/AC might be generated in the Otp-expressing supraopto-paraventricular domain like other hypothalamic nonapeptidergic cell populations (Bupesh et al. 2011; Garcia-Moreno et al. 2010). This is supported by the apparent continuity between the AVP-ir cells in the ADP/AC group and those in the anterior paraventricular nucleus, as proposed by the cytoarchitectonic classification of the BST in the rat according to Dong and Swanson (2004). However, as discussed in more detail bellow (see section 3.1.1.), the commissural-preoptic neurogenetic domain of the embryonic neuroepithelium might also contribute to the origin of these cell populations located in the BST-preoptic junction.

*1.1.2. Vasopressinergic neurons and the medial extended amygdala: comparative analysis in mammals*

The dimorphic, testosterone-dependent expression of AVP in cells of the posteromedial BST and BSTIA gives support to the concept of extended amygdala originally proposed by Alheid and Heimer (1988). The medial extended amygdala, which is composed of the medial

amygdala (in the amygdala proper) plus the posteromedial BST, contains the sexually dimorphic population of AVP-ir cells of the cerebral hemispheres. Vasopressin would therefore constitute a reliable marker of a specific cell population of the medial extended amygdala, to which the BSTIA would belong. In addition, a portion of the medial extended amygdala also shows a rich AVP-ir innervation but no AVP-ir cell bodies. This includes the medial portion of the supracapsular BST and portions of the sublenticular *substantia innominata,* which are interposed between the two poles of the medial extended amygdala (see Martínez-García et al. 2012).

The study of AVP immunohistochemistry or in situ hybridization for AVP mRNA in the cerebral hemispheres of other rodents, such as voles (Wang et al. 1994; Wang 1995) or hamsters (Ferris et al. 1995; Bolborea et al. 2010a), indicate that in these species AVP expressing cells are present in the posterior BST but not in the amygdala proper (in spite of some quantitative reports using immunohistochemistry, as Wang 1995). A similar situation is found in marmoset monkeys, where cells positive for AVP mRNA and for AVP immunoreactivity (Wang et al. 1997a; Wang et al. 1997b) are described in the bed nucleus of the *stria terminalis* but not in the medial amygdala. These findings suggest that the posterior BST is the main (or only) population of AVP-expressing cells in the cerebral hemispheres of mammals, but some rodents, namely rats and mice, have an additional population of AVPergic cells that, according to our interpretation, are mostly confined to the BSTIA (instead of the medial amygdala).

### *1.1.3. Vasopressin innervation of the medial amygdala: a case for nonapeptide-receptor mismatch*

According to our results, within the amygdala the main field of AVP-ir innervation is found in the MePD and BSTIA. Assessment of the density of AVP-ir innervation in the MePD reveals that: a) it is sexually dimorphic in favour of males, where it is dependent on testosterone (Experiment 1); b) it becomes partially depleted after unilateral lesions of the posterior BST (Experiment 2). These data demonstrate that the innervation of the MePD (and maybe BSTIA) arises in part from the dimorphic cell group of the posterior BST. It is likely that the AVP-ir cells in the BSTIA, immediately adjacent to the MePD, also contribute to the AVP-ir innervation of the medial amygdala, as there is a correlation between the number of AVP-ir cell bodies in the BSTIA and the area fraction occupied by the AVP-ir fibres in the MePD (Experiment 2, Table 2).

These fibres probably play a role in both, sexually dimorphic and non-dimorphic social behaviours modulated by AVP release in the Me. For instance, it has been shown in rats that AVP in the Me mediates the aversion to disease signals from conspecifics, a behaviour which is

shown by males (Arakawa et al. 2010) and in females, at least in mice (see Kavaliers et al. 2005). Since the AVP innervation of the MePD is sexually dimorphic, it is expected that AVP in the medial amygdala also modulates sexually dimorphic behaviours such as aggression in males (Koolhaas et al. 1990), or maternal memory in females (Nephew and Bridges 2008). Although, in male mice social interaction correlates with V1aR gene expression in Me (Murakami et al. 2011), it is not clear if this constitutes a sexually dimorphic role of AVP or it also occurs in females.

Our results, together with binding studies in the literature (mouse, Dubois-Dauphin et al. 1996; rat, Veinante and Freund-Mercier 1997a; 1997b; singing mice of the genus *Scotinomy*s, Campbell et al. 2009), reveal a noteworthy mismatch between the distribution of AVP-ir fibres and its receptors in the extended amygdala, which is especially evident in the medial (and central, see below) amygdaloid nuclei. Thus, AVP-ir innervation is quite dense in the MePD and BSTIA but it is scarce and variable in the central amygdala (as discussed below). In contrast, dense V1aR vasopressin binding sites are observed in a large portion of the central amygdala (especially the medial and capsular divisions) whereas no AVP binding is apparently observed in the medial amygdala. This is further discussed below (see section 4).

### *1.2. Non-dimorphic AVP-ir processes in the amygdala of mice*

Our results confirm previous reports in the mouse by Rood and de Vries (2011a) on the presence of medium-to-thick AVP-ir fibres in the central amygdala, and indicate the existence of an additional group of dendrite-like AVP-ir processes in the medial amygdala. In both cases, females and males, irrespective of they being gonadally intact or castrated, show a similar distribution of AVP-ir processes thus suggesting that these are non-dimorphic neural elements.

#### *1.2.1. Vasopressin immmunoreactive fibres in the central amygdala*

These fibres apparently show a high inter-individual variability as some animals apparently lack fibres in the Ce whereas others show a moderate innervation, which is always composed of sparse beaded axon-like processes. This occurs equally in male (both intact and castrated) and female mice. This fact and the relatively thick diameter of the fibres in the Ce suggest that they do not derive from the sexually dimorphic BST and BSTIA cell populations, but likely arise in hypothalamic populations (Buijs 1978) as suggested by the tracking of the fibres in our preparations. In fact, ibotenic acid lesions of the posterior BST have no apparent effect on the innervation of the Ce (experiment 2). Using viral tracers, Knobloch et al. (2012) have shown a

similarly sparse innervation of the Ce by oxytocin-expressing hypothalamic cells (see section 4).

Oxytocin and AVP released from these fibres might act on top of the AVP diffusing from the terminal field of the MePD/BSTIA (see above). In this respect, the highly variable density and distribution of the AVP-ir innervation of the Ce (compare Figs. 2c'-d' and 3c') constitutes a possible anatomical substrate for individual differences in stress coping in relation to aggression. A detailed analysis of the innervation of the medial, lateral and capsular portions of the central amygdala in animals showing different degrees of aggressiveness might shed light on the role of AVP in the central amygdala in relation to stress coping and aggression.

*1.2.2. Non-dimorphic AVP-ir processes in the ventral medial amygdala*

Another remarkable finding of our work is the presence of a group of AVP-ir thick neural processes in the ventral aspect of the Me (MeAV and the anterior portion of the MePV), apparently connected with the AVP cells in the supraoptic nucleus (Fig. 5a-b), which we interpret as dendrites of magnocellular neurosecretory AVP cells in the anterior SO. This interpretation is in agreement with the presence of AVP-ir processes in males (intact and castrated) and females, and the fact that they are not affected by lesions of the posterior BST (not shown).

Data from rats fit our interpretation. Smithson et al. (1989; 1992) found similar dendritic processes originating in the SON and described anatomically direct inputs from the main and accessory olfactory bulbs on SON cells. Electrophysiological recordings confirmed monosynaptic olfactory inputs to the SON after stimulation of the lateral olfactory tract (Hatton & Yang, 1989). This olfactory input was found to increase dendritic coupling in the SON of lactating rats and also in rats induced to show maternal behaviour (Modney, Yang, & Hatton, 1990), suggesting a role of the SON in maternal behaviour, independent from its role in milk ejection reflex.

The presence of these AVP-ir dendritic processes in the ventral medial amygdala has important consequences. On the one hand, as the Me receives projections from the main (anterior Me and parts of the MePD) and accessory olfactory bulb (the whole nucleus) that terminate in the subpial layers (see Gutierrez-Castellanos et al. 2010), these AVP-ir processes might receive direct olfactory and vomeronasal inputs from the bulbs. Although, to the best of our knowledge, this has never been studied in the mouse, there are anatomical observations supporting a direct olfactory input to the magnocellular neurosecretory neurons of the SON in

the rat (Smithson et al. 1989; Smithson et al. 1992). Also in the rat, Hatton and Yang (1989) demonstrated that electrical stimulation of the lateral olfactory tract monosynaptically activates vasopressinergic and oxytocinergic cells in the SON. This should, nevertheless, be checked in mice, where the presence of this AVP-ir processes into the ventral Me make synaptic contacts with olfactory and vomeronasal fibres even more likely.

If these contacts were present, they would be able to promote activation of the magnocellular neurosecretory system, resulting in an increase in circulating AVP, by olfactory and/or vomeronasal stimuli. Although, to the best of our knowledge, this putative neuroendocrine response has never been reported, more subtle effects are possible. For instance, stimulation of the lateral olfactory tract leads to an increase in electrotonic coupling within the supraoptic nucleus (Hatton and Yang 1989), probably due to establishment of gap junctions between SON cells or reinforcing pre-existing ones (Yang and Hatton 1988). Electrotonic coupling may boost the neuroendocrine responses induced by other physiological factors, such as (in the case of AVP) hydrosaline stress. This may be a mechanism to cope with physiologically demanding situations, such as lactation in females. In fact, Hatton and collaborators reported a higher incidence of olfactory-induced coupling in the SON cells of lactating or maternally behaving rats as compared to virgin females or males (Hatton and Yang 1990; Modney et al. 1990). However, the apparent lack of sexual dimorphism in the AVP-ir processes of SON origin in the ventral Me, suggests additional, non-dimorphic functions for a possible olfactory/vomeronasal input to the AVP-ir cells of the anterior SON, an issue that obviously requires further investigation.

The dendrite-like processes in the ventral Me is also relevant due to the well-documented dendritic release of AVP at the level of the SON, which leads to very high local concentrations of neuropeptide (some 100-1000 fold higher than in blood; Ludwig and Leng 2006). Vasopressin released from AVP-ir processes in the Me would be able to modulate the activity of Me cells and/or olfactory vomeronasal fibres, by binding oxytocin and/or vasopressin receptors, thus modulating responses to chemical cues (Ludwig and Leng 2006). One such behaviour might be aggression. Aggression is strictly dependent on vomeronasal inputs (Leypold et al. 2002; Chamero et al. 2011) and the ventral Me seems a likely candidate for this vomeronasal control of aggression, in both males and females. First, the ventral Me receives direct inputs from the accessory olfactory (Gutierrez-Castellanos et al. 2010). Second, the MeAV and MePV are involved in the expression of defensive behaviours (Newman 1999a; Canteras 2002) and project to the hypothalamic aggression area in both rats (Toth et al. 2010) and mice (Pardo-Bellver et al. 2012).

Dendritic release of AVP (and other peptides) is regulated independently of axonal release, and apparently involves nitric-oxide and glutamate signalling (Gillard et al. 2007). The ventral aspect of the Me (especially its anterior portion) is extremely rich in nitric oxide synthase (Guirado et al. 2008; Martínez-García et al. 2012). In addition, nitric oxide is known to be involved in the control of maternal (Popeski and Woodside 2004; Ankarali et al. 2009) and inter-male aggression (Demas et al. 1997). All these data lead us to speculate that SO dendritic release of nonapeptides (AVP and/or oxytocin) at the level of the ventral Me, mediated by nitric oxide and glutamate (maybe released from the vomeronasal input related to conspecific chemical cues), might facilitate or trigger aggression. These hypotheses obviously require experimental checking.

## 2. Extending the socio-sexual brain: functional significance of the AVP-ir innervation of the mvStP

As discussed above, the sexually dimorphic cell groups in the BSTMPI and BSTIA very likely give rise to sexually dimorphic, testosterone-dependent terminal fields in the dorsal medial amygdala. This is, however, not the only target for the projections of the dimorphic AVPergic cells of the medial extended amygdala. As recently described in details by Rood and collaborators (2013), AVP-ir terminal fields sensitivity to gonadectomy in C57 male mice are found in many locations of the brain. These include the lateral septum and basal forebrain, other portions of the amygdala (e.g. BMA, BLP, PLCo, AHi) and extended amygdala, posterior hippocampus, lateral habenula and portions of the midline thalamus, posterior lateral, perifornical and tuberomammillary hypothalamus, tegmental and interpeduncular areas, portions of the paraqueductal grey and large portions of the raphe complex. Since most, if not all, of these brain centres belong to the SBN system, the AVPergic sexually dimorphic system in the medial extended amygdala has a potentially extraordinary impact on the expression of social behaviours. This nicely fits the devastating effects of mutations of the genes encoding for AVP receptors (V1aR, Wersinger et al. 2007a; V1bR, Wersinger et al. 2004; 2007b; Caldwell et al. 2010) or the use of specific antagonists (Bayerl, Klampfl, & Bosch, 2014) on social interactions, including aggression, female-to-male attraction through odours (socio-sexual motivation) or maternal care.

In the present study we focus on one of these areas, the medioventral striato-pallidum (mvStP) and demonstrate that the AVP innervation of the mvStP is sexually dimorphic and depends on testosterone, being denser in males than in females or castrated males (Experiment 1). The neuroanatomical tract-tracing and the study of the effects of excitotoxic lesions in the BST

(experiment 2) indicate that the AVP-ir innervation of the mvStP originates, at least in part, in the sexually dimorphic AVP-ir cell population of the BSTM, as it was shown in the rat (DeVries and Buijs 1983). Our data also suggest that the innervation field of the lateral septum, medial amygdala and mvStP have a common origin in the sexually dimorphic AVP cell group of the posterior BST. First, terminal fields in all three structures are depleted after lesions of BSTMP AVP-ir neurons. Second, there is a correlation between the number of AVP-ir cells in the BSTMP and the area fractions occupied by AVP-ir fibres in all three structures, which are in turn cross-correlated (see Table 4). However, from our results it is not clear whether the cells in the BSTIA contribute to the AVP-ir innervation of the mvStP.

The presence of a relatively dense AVP innervation in the medio-ventral forebrain has been shown in (male) rats, mice (DeVries et al. 1985; Rood and de Vries 2011a) and spotted hyenas (Rosen et al. 2006). In contrast, innervation is much scarcer in monkeys (Wang et al. 1997b; Wang et al. 1997a) and naked mole rats (Rosen et al. 2007), very scarce in voles (Wang et al. 1996; Lim et al. 2004) and apparently absent in hamsters (Ferris et al. 1995; Bolborea et al. 2010b). This comparative analysis also reveals that the number of cells immunoreactive for AVP in the BST is generally correlated with the density of AVP-ir fibres in the medio-ventral forebrain. The specific location of these AVP-ir fibres is not clear, however. Some studies suggest they innervate the diagonal band of Broca or the ventral pallidum (Lim and Young 2004; Rosen et al. 2006). In contrast, a recent study of the AVP innervation in the mouse brain by Rood and de Vries (2011a) describe fibres in this region as distributed in the so-called ventral septal area, not to be confused with the lateroventral septum. In agreement with their description, we observe this innervation field restricted to a sparse-celled region not named in the mouse brain atlas (Paxinos and Franklin 2001), lateral to the diagonal band and medial to the nucleus accumbens. Using substance P as a marker of the ventral pallidum (Napier et al. 1995; Riedel et al. 2002) in sections adjacent to those processed for AVP-immunohistochemistry, and using topographic landmarks to align the sections, we have observed the AVP-ir terminal field does not correspond to either the nucleus accumbens, the ventral pallidum or the diagonal band (Fig. 4), but belongs to an additional territory the nature of which is not clear. Being located next to the striatal and pallidal territories, in many cases in close proximity to the most anteroventral islands of Calleja (including the major island), we have decided to name this region as the medioventral striato-pallidum.

In relation with this, it is striking that even in those species in which this specific AVPergic terminal field seems quite reduced or absent, this area is extraordinarily rich in V1a vasopressin receptors. For instance, male hamsters show a dense field of receptor binding

(Johnson et al. 1995) that apparently covers the caudal aspect of the mvStP (more rostral levels have not been analysed). Voles show a V1aR binding field (Wang et al. 1996; Lim et al. 2004) that matches the distribution of AVP-ir fibres in mice and rats. In the marmoset monkey (Schorscher-Petcu et al. 2009) a dense field of V1aR receptors is also observed in a region of the basal forebrain in a region adjacent (and including) the islands of Calleja. This suggests that, in spite of the scarcity of AVP-ir fibres, the mvStP of hamsters, voles or monkeys is targeted by vasopressinergic pathway, like it has been shown in rats and mice.

Data on the role of AVP in this centre derive from functional, neurochemical and anatomical studies in different rodents. For instance, in monogamous voles V1aR receptors in the mvStP seem critical for pair bond formation (Lim and Young 2004). In fact, infusion of V1aR antagonists in the mvStP of male prairie voles, but not in the medial amygdala or mediodorsal thalamus (where a high density of these receptors is observed) prevented pair bond formation after mating with receptive females. In addition, mating resulted in c-fos expression in the mvStP, which is mediated by V1aR. This fits the fact that, as compared to promiscuous, monogamous species show higher levels of V1aR in the mvStP in voles (Young et al. 1997), rodents of the genus *Peromyscus* (Bester-Meredith et al. 1999) and primates (Young et al. 1999b; Schorscher-Petcu et al. 2009).

This is, nevertheless, a specific case. Monogamous and promiscuous species usually differ in other aspects of social behaviour, such as paternal care and aggression, as discussed in detail by Bester-Meredith et al. (1999). In this respect, a negative correlation is seen between aggressiveness and the density of AVP-ir innervation in the lateral septum in rats and mice (Everts et al. 1997; Veenema and Neumann 2007), thus suggesting a role for AVP innervation in the septum in the negative control of aggression. As we have observed, there is a strong, significant correlation between the fraction area covered by AVP-ir fibres in the lateral septum and those in the mvStP (see Table 2). As a consequence, it is likely that this innervation is also negatively correlated with aggressive behaviour. Indeed, there are neuroanatomical data suggesting a role the mvStP in the control of aggression. For instance, the hypothalamic aggression area, located just lateral to the ventromedial hypothalamus (Lin et al. 2011), receives descending projections from the mvStP (Toth et al. 2010).

The mvStP might also be involved in other aspects of social behaviour for which a role of AVPergic transmission in the lateral septum has been proposed, such as social recognition (Bielsky et al. 2005). The mvStP occupies a strategic position to mediate motivated behaviours in relation to social interactions. In most rodents, chemical signals detected by the olfactory

and vomeronasal epithelia are crucial for intraspecific communication. Olfactory and vomeronasal pathways, relaying in the main and accessory olfactory bulbs respectively, project in an overlapping manner to the different nuclei of the medial amygdala and the cortical amygdala (Gutierrez-Castellanos et al. 2010; Martínez-García et al. 2012). In turn, the cortical amygdala (Ubeda-Banon et al. 2007; Novejarque et al. 2011) and the medial amygdala (Pardo-Bellver et al. 2012) have important projections to the ventral striato-pallidum. The posteromedial cortical amygdala, which constitutes the vomeronasal cortex (Gutiérrez-Castellanos et al., 2014), and the anterior and posterodorsal medial amygdala, project specifically to the medial aspect of the ventral striato-pallidum (Ubeda-Banon et al. 2008; Novejarque et al. 2011), whereas the posterolateral cortical amygdala which is targeted by a direct input from the main olfactory bulb, projects to more lateral portions of the ventral striato-pallidum (Ubeda-Banon et al. 2007). The afferents from the vomeronasal amygdala to the mvStP terminate in close association to the anteromedial and major islands of Calleja and anteromedial olfactory tubercle (Ubeda-Banon et al. 2008; Novejarque et al. 2011). The close proximity of the AVP innervation with these structures suggests a role for them in the modulation by AVP of the behavioural responses to chemical cues in the context of social interaction. In agreement with this idea, in those mammalian species in which the size of the brain allows a relatively higher resolution (e.g. marmoset monkeys), the islands of Calleja display a remarkable binding to V1aR drugs (see Schorscher-Petcu et al. 2009). Moreover, immunohistochemical detection of AVP receptors of the V1bR type in the rat brain reveals receptor expression in the cells of the anteromedial olfactory tubercle and islands of Calleja (Hernando et al. 2001). Although the neural center(s) where this effect might occur is unknown yet, V1bR receptors are involved in regulation social motivation including chemoinvestigation of social odours (Wersinger et al. 2004) and aggressive behaviour involving the attacks of conspecifics (Wersinger et al. 2007a). Moreover, independently replicated lesion studies indicate that the mvStP is necessary for the hedonic value of sexual chemosignals (Agustin-Pavon et al., 2014; DiBenedictis et al., 2014), and broad evidence from experiments in monogamous voles indicates that this region is crucial for pair-bond formation (Larry J Young & Wang, 2004).

As a conclusion, the dimorphic distribution of AVP in the mvStP is an indication of its belonging to the brain network for socio-sexual behaviour. Besides its sexual dimorphic AVP-ir innervation, this region fulfils all the defining features of a node of the socio-sexual brain (Newman 1999b). First, the mvStP area seems involved in the expression of other social conducts in mice like paternal behaviour (Akther, Fakhrul, & Higashida, 2014). Second, it is

interconnected with other nodes of the socio-sexual circuitry including the posterior BST (our results), the lateral septum (at least in rats, Risold and Swanson 1997) or, as discussed above, the hypothalamic aggression area (Toth et al. 2010) and the medial amygdala (Pardo-Bellver et al. 2012). Finally, like the remaining centres of the socio-sexual network, the mvStP displays a remarkable expression of oestrogen receptors (Mitra et al., 2003; Shughrue & Merchenthaler, 2001).

Although in rodents, afferents to the mvStP are apparently dominated by input from the olfactory and vomeronasal amygdala (see references above), studies in relatively microsmatic mammals (e.g. primates) might reveal additional inputs from other regions of the amygdala conveying social stimuli of other sensory modalities. The presence of AVP (Caffé, Van Ryen, Van der Woude, & Van Leeuwen, 1989) and its receptors (Young et al. 1999) in a region of the basal forebrain anterior to the diagonal band in the brain of monkeys, suggests a similar role of the medioventral striato-pallidum in rodents and primates. In this context, social stimuli reaching this area from the amygdala would mediate motivational changes leading to the expression of appropriate social interactions as a function of the emitter of the stimuli. In addition, data from rats show that the islands of Calleja located within the mvStP, are highly interconnected with the mesolimbic reward system (J H Fallon, Loughlin, & Ribak, 1983; J H Fallon, Riley, Sipe, & Moore, 1978; J. H. Fallon, 1983), as does also the adjacent ventral pallidal area (Kalivas, Churchill, & Klitenick, 1993; Zahm, Williams, & Wohltmann, 1996). This places the mvStP at the interface between the motivational mesolimbic reward system and the SBN, as proposed for the lateral septum and medial extended amygdala by O'Connell & Hofmann (2011) on the basis of a thorough comparative analysis of both systems in different vertebrates (see Fig. 15).

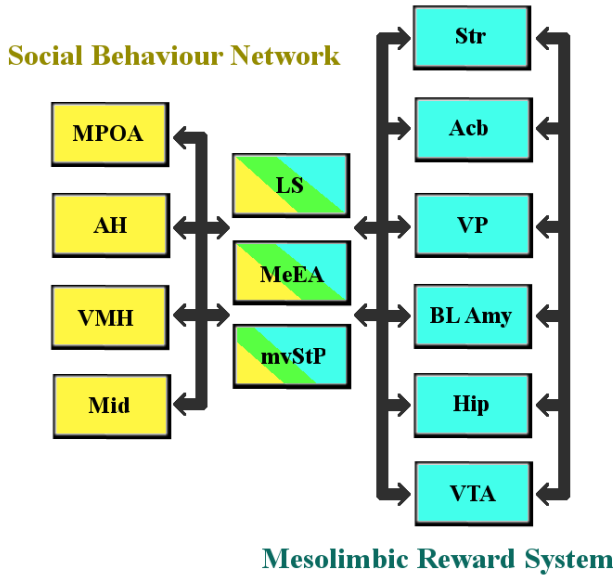


**Fig. 15. The social decision-making network** as proposed by O'Connell & Hofmann (2012). The nodes are highly interconnected (arrows). On the left (yellow), the nodes of the social behaviour network (MPOA, AH, VMH and Mid). On the right, the nodes of the mesolimbic reward system –striatum (St), nucleus accumbens (Acb), ventral pallidum (VP), basolateral amygdala (BL Amy), hippocampus (Hip) and ventral tegmental area (VTA). In the middle, the lateral septum and medial extended amygdala, plus the mvStP make up the interface between both networks.

## 3. Distribution of OT immunoreactivity

Our cartography of OT expressing cells is based on the use of two different primary antibodies. On the one hand, we employed a commercial antibody raised against synthetic OT conjugated to thyroglobulin (see Table 2). On the other hand, a second primary antibody, a generous gift of Dr. Harold Gainer, was directed against the OT-specific neurophysin. Oxytocin and its neurophysin are co-localised at subcellular level (Belenky et al., 1992) and immunostaining for both peptides are undistinguishable in the brain of rats (Butovsky et al., 2006). Our results indicate an expected, similar situation in the brain of mice, as both antibodies rendered undistinguishable patterns of immunostaining, which we will name jointly as oxytocin-like immunoreactivity (OT-ir). Therefore, we are absolutely confident that our results reveal the actual distribution of OT in the brain of the mouse.

### *3.1. Oxytocin immunoreactivity reveals neuroendocrine and centrally projecting neurons*

The distribution of OT-ir cells that we have found in mice looks, in general, similar to that reported in other mammals, including macaques (Caffé et al., 1989), tree shrews (Ni et al., 2014), naked mole rats (Rosen, de Vries, Goldman, Goldman, & Forger, 2008; Valesky, Burda, Kaufmann, & Oelschläger, 2012), voles (Z. Wang, Zhou, Hulihan, & Insel, 1996), Brandt's voles and long-tailed hamsters (L. Xu, Pan, Young, Wang, & Zhang, 2010), rats (Buijs, Swaab, Dogtermon, & van Leeuwen, 1978) and different species of mice (Castel & Morris, 1988; Hermes, Buijs, Masson-Pévet, & Pévet, 1988). Our work provides a detailed description of the distribution and location of OT- immunolabelled cell populations, previously lacking for the laboratory mouse, which has become the species-of-choice for research in neurobiology of social behaviours.

#### *3.1.1. On the developmental origin of OT-ir cell populations*

The distribution of OT-ir cells we have observed supports and refines previous neurodevelopmental studies suggesting a common origin of the OT-ir cells in the embryonic neuroepithelium of the so-called supraopto-paraventricular hypothalamus. As discussed below, there is evidence suggesting the existence of at least two distinct zones in this hypothalamic neuroepithelium. From them, cells would follow two apparently distinct migratory streams (Garcia-Moreno et al., 2010) to five main locations in the adult forebrain. A portion of the supraopto-paraventricular embryonic neuroepithelium would give rise to neurons in: 1) the Pa and adjacent periventricular hypothalamus; and 2) cell groups in the preoptic hypothalamus, rostral to the Pa, including the periventricular (Pe), medial (MPO) and

ventromedial (VMPO) preoptic nuclei, as well as the so-called ADP/AC (located among the preoptic area, the posterior BST and the nucleus of the anterior commissure; see Fig. 10a). A second portion of the embryonic supraopto-paraventricular neuroepithelium would originate the cells in: 3) the SON, including its retrochiasmatic portion; and, 4) the anterior Me adjacent to the anterior SON, from where some cells apparently migrate caudally into the posterior medial amygdala. Finally, 5) cells probably arising in both neuroepithelial regions or in their interface would give rise to the accessory OT-ir nuclei (AN). The AN neurons do not conform a single cell group but are distributed between the main groups of neuroendocrine cells in the Pa and SON/SOR, scattered through the preoptic (see above, point 2), perifornical and lateral hypothalamus, with a denser cell group at the level of the PaPo, just ventral to the zona incerta (Figs. 9i and 10b-b').

This common embryonic origin of all the OT-expressing cells from two adjacent regions of the embryonic hypothalamic neuroepithelium is supported by the migration of cells expressing *otp* (which characterises the supraopto-paraventricular neuroepithelial region; Wang & Lufkin 2000) and by the use of cell-migration tracing techniques in mouse embryos (Garcia-Moreno et al., 2010). Specifically, our view that the OT cells in the Me have a common embryonic origin with those in the anterior SON is supported by the relatively mild effects of null mutations for *otp* onto these two cell groups (W. Wang & Lufkin, 2000). Whereas *Otp-lacZ* null mutants lack labelled cells in the Pa and adjacent hypothalamic regions, the supraoptic region shows plenty of Lac-Z positive cells, which do not conform a well-defined SON however, but extend into the Me where a neat cell group is found (at least at postnatal day 1; see Fig. 1B-J in Wang & Lufkin 2000). By contrast, the lack of LacZ-expressing cells in the BST of these mutant mice suggests that nonapeptidergic cells in the BST-preoptic interface derive from the paraventricular rather than the supraoptic neuroepithelial niche. As discussed above (see section 1.1.1), there is an additional neurogenetic domain that might contribute to cells in this region, namely the commissural preoptic neuroeptihelium (see Bupesh et al. 2011; Garcia-Moreno et al. 2010).

Comparative studies also support the developmental relationship between SON and Me OT-ir cells. Thus, in other mammals such as the mole rat (Rosen et al., 2008), Brandt's voles and long-tailed hamsters (L. Xu et al., 2010), tree shrews (Ni et al., 2014), like in the mouse (Castel & Morris 1988; this work), there seems to be a continuity between the OT-ir cells in the Me and the anterior SON.

In our material, immunoreactive cells in the SON and SOR showed an apparently weaker immunostaining than those in the Pa. This finding could reflect lower rates of synthesis or

higher transport rate of the peptide from supraoptic magnocellular somata. Although most of the OT-ir cells in the SON are likely to be neurosecretory, Hawthorn et al. (1985) performed lesions restricted to the SON in rats and reported a depletion of OT in several central structures such as the striatum (the authors mention the caudate putamen but likely also analyse at least portions of the ventral striatum), the substantia nigra, the parabrachial nucleus and the hippocampus. Although some of these nuclei do not show OT-ir fibres in our material, those findings strongly suggest the existence of SON OT-ir cells displaying central projections. By contrast, the use of viral vectors for tracing specifically the projection of OT-expressing cells in the SON of rats (Knobloch et al., 2012), suggest that central projections of these cells are restricted to the horizontal limb of the diagonal band nucleus, portions of the Acb shell (and maybe of the Ce and hippocampus, see their supplementary figure S2). In any case, there is evidence that OTergic SON cells do show central projections.

In the Pa, OT-ir cells are abundant in all subdivisions except for the lateral subnucleus (PaL) and their distribution is very similar to that found in the rat (Condés-Lara, Martínez-Lorenzana, Rojas-Piloni, & Rodríguez-Jiménez, 2007). Immunostained somata are particularly abundant in the anterior Pa, which mostly contains neurosecretory cells. However, some of the OT-ir cells in the anterior Pa project centrally, as indicated by tracing studies in voles (Ross et al., 2009) and the presence of branching OT-ir axons in the vicinity of the anterior Pa of the rat (Hatton, Cobbett, & Salm, 1985). This suggests that some OT-ir neurosecretory cells in the anterior Pa may originate axon collaterals to central targets such as the Acb. In fact, recent experiments in rats using viral tracers under the control of the OT promoter have demonstrated that neurosecretory cells (e.g. projecting to the posterior pituitary) in the Pa and AN send collaterals to the Ce and Acb (Knobloch et al., 2012). This would allow the coordination of neurosecretion with modulation of behaviour through central release (Veenema & Neumann, 2008). Such coupling of OT neurosecretion with synaptic OT release in central targets is a feasible mechanism that would explain the increase of OT blood levels associated to specific behaviours in humans, such as maternal and paternal care, (Feldman, Gordon, Schneiderman, Weisman, & Zagoory-Sharon, 2010), and non-human mammals (social interactions in cattle youngsters, Yayou et al. 2015). Thus, at least some central effects of OT would not need the transport of OT through the blood-brain barrier, a mechanism that has not been demonstrated (Neumann & Landgraf, 2012). Rather, the same neurons would release OT both peripherally and centrally through axon collaterals. By contrast, data in voles indicate that OT-ir cells in the dorso-caudal portion of the Pa (PaPo) are not neurosecretory, as they do not uptake systemically injected fluorogold (Ross et al., 2009). This is supported by viral tracing

experiments in rats, where OT-expressing cells in the PaPo innervate the nucleus of the solitary tract but do not project to the posterior pituitary (Knobloch et al., 2012).

In addition to the described hypothalamic OT-ir cells, which have also been studied in detail in other species, we have characterized an additional OT-ir cell group in the so-called ADP/AC. As already discussed, in mice this is a cytoarchitectonically ill-defined cell group, located between the ventral BSTMP and the dorsal MPOA (see Paxinos & Franklin 2001). Some authors studying the rat brain consider it as a particular nucleus of the AN or simply name it as the anterior commissural nucleus (ACN, Rhodes et al. 1981). Others envisage these cells as belonging to the anterior division of the Pa (Hou-Yu et al., 1986; Swanson & Kuypers, 1980; Xiao et al., 2005). Wang et al. (1996) described a very similar group of OT-ir cells in the BST of voles, ventral to the anterior commissure. According to our results in the mouse, the ADP/AC constitutes a distinct population of OT-ir cells, separated from the anterior Pa, as shown in horizontal sections in the Brattleboro strain rat by Rhodes et al. (1981; see ACN in their figure 3) and sagittal sections through the hypothalamus of Sprague-Dawley rats (Hou-Yu et al. 1986; rPVN in their figure 6).

Interestingly, some of the OT-ir cells in this region appear densely packed in close association to large blood vessels (Fig. 10a-b). Similar association between OT-ir cells and blood vessels appears in a region somewhere between the Pa and the *stria medullaris* in rats, which might correspond to the mouse ADP/AC (figure 4B in Buijs, 1978) and in other regions of the brain (Hou-Yu et al., 1986). In addition, associations between OT-immunoreactive cells and the capillary endothelium have been observed in the preoptic and paraventricular regions of the hypothalamus in the golden-mantled ground squirrel, *Spermophilus lateralis*, using transmission electron microscopy (Muchlinski, Johnson, & Anderson, 1988). Altogether, these data suggest that cells of the ADP/AC could contribute to neurosecretion through somato-dentritic release of OT to the perivascular space, even if OT-ir neurons of this region apparently do not project to the pituitary, at least in voles (Ross et al., 2009). This is another neuroendocrine mechanism that could explain the correlation between central OT-mediated behaviours and circulating levels of the neurohormone (see above).

### *3.2. Central oxytocinergic terminal fields in the brain of mice*

The distribution of OT-ir fibres depicted in this work is consistent with the previously reported distribution in rats (Buijs, 1978) and mice (Castel & Morris, 1988), and does not differ substantially from less detailed descriptions in other mammals like the naked mole rat (Rosen et al., 2008) and the tree shrew (Ni et al., 2014). In all cases, the majority of OT-ir fibres is

located in the hypothalamus and corresponds to the neurosecretory axons travelling from the paraventricular and supraoptic nuclei to the pituitary. These OT-ir neurosecretory axons show a characteristic straight, varicose morphology. However, other regions of the brain contain remarkable OT-ir terminal fields with fibres of different morphologies, which strongly suggest the existence of many central OTergic circuits arising from some of the populations of OT-ir cells.

*3.2.1. Oxytocinergic innervation of the cerebral hemispheres: variability and asymmetry*

In the rostral telencephalon OT-ir innervation is scarce and displays a high inter-individual variability in terms of abundance. Thus, OT-ir fibres in the dorsal tenia tecta (DTT) and in nearby nucleus semilunaris (SL), like AVP-ir fibres in the pre- and infralimbic cortices (Otero-Garcia et al. 2014; this work), appear with high frequency in some specimens, while they are nearly absent in others. It is tempting to speculate that variability in nonapeptidergic innervation of prefrontal structures might be related to inter-individual variation in sociability (see below).

Terminal fields of OT-ir fibres in other locations of the cerebral hemispheres are likely related to a role of OTergic systems in motivated, emotional, socio-sexual behaviours. A good example is the ventral striatum and adjacent structures. Thus the medial Acb core and the Acb shell show a noticeable density of OT-ir fibres. Similar patterns of OT-ir innervation of the Acb are observed in different rodent species such as rats, voles and mice (Ross et al., 2009). By contrast, the OT receptor (OTR) distribution is highly variable between species and is associated to variations in social behaviour (Beery, Lacey, & Francis, 2008; Staes et al., 2014). In rats, OTR binding occurs in the Acb shell (Veinante & Freund-Mercier, 1997) while in voles OTR binding fills the entire striatum, including the Acb shell and core (Miranda M. Lim, Murphy, & Young, 2004). However, only low resolution descriptions of OT receptor (OTR) distribution are available for the mouse brain (E. a D. Hammock & Levitt, 2013; T. R. Insel et al., 1993). Precise descriptions of OTR binding and presynaptic OT elements in the mouse striatum would be useful, since OT transmission in the Acb is the focus of multiple studies on the neural basis of pair bonding (Larry J Young & Wang, 2004), social reward mechanisms (Dölen et al., 2013) and addiction to drugs of abuse (Sarnyai & Kovács, 1994).

More caudally within the ventral cerebral hemispheres, the BSTA and StA show axon-like OT-ir fibres, similar to those in the adjacent Acb core, intermingled with thick processes. The thick processes could be swollen axons or dendrites from the caudally adjacent ADP/AC immunoreactive cell group. Ross et al. (2009) point to the anterior Pa as the origin of the OT

innervation of these basal telencephalic structures in rodents, as in horizontal sections they observed OT-ir fibres linking the PaAP with the Acb, which cross the intervening StA and BSTA.

Another centre showing OT innervation, which is involved in emotional aspects of social behaviour, is the central amygdala (Ce). There, OT-ir fibres show also quite a variable distribution pattern among individuals, abundant in some specimens while almost absent in others. This recalls the distribution of AVP-ir fibres in the same nucleus, an issue that will be discussed below. Our results in mice do not fit those by Knobloch et al. (2012) in rats, as we did not notice differences in the morphology and density of OT-ir fibres in the CeM, CeL and CeC of mice. This likely reflects inter-specific differences, which might be related to the important differences between rats and mice concerning maternal behaviour (see below).

As discussed above, the nonapeptidergic innervation of the Ce shows a high inter-individual variability. In addition, these terminal fields display an apparent lateralised (asymmetric) distribution, at least in some individuals. Interhemispheric asymmetry in the nonapeptidergic innervation is also observed in other regions of the fronto-temporal lobe that are connected with the amygdala, such as the OT-ir fibres in the DTT and the AVP-ir ones in the infralimbic and prelimbic cortices. This asymmetry may have functional significance. In fact there is evidence of functional left-right asymmetries in the amygdala and prefrontal cortex of rodents (Sanchez & Dominguez 1995; Banczerowski et al. 2003) and humans (Breiter et al., 1996; Evans et al., 2014; Markowitsch, 1998). Therefore, asymmetric, highly variable nonapeptide-containing fibre distribution in the central amygdala, frontal (pre- and infra-limbic) cortex of mice, and other structures, can reveal a hidden functional lateralization in relation to social interaction, which might represent an ancient evolutionary trait inherited by rodents and primates from their common ancestors.

*3.2.2. Oxytocin immunoreactive fibres outside the telencephalon: hints on their function*

In the hypothalamus, our results reveal OT-ir axon-like processes in the dorsomedial hypothalamus (Figs 9k and 10c), a key centre for suckling stimuli to elicit OT-release inducing milk ejection (Takano, Negoro, Honda, & Higuchi, 1992). These fibres suggest backward projections from the Pa and/or SON neurosecretory cells to the dorsomedial hypothalamus, which could modulate the OT-mediated milk ejection reflex (Honda & Higuchi 2010a; 2010b) through feedback mechanisms.

The role of nonapeptidergic transmission in the midbrain and hindbrain has been less studied, in comparison with the forebrain. Nonetheless, our results indicate that OT-ir fibres are quite

dense in several centres of the midbrain and hindbrain. For instance, a relatively dense OT-ir innervation in the PAG may be involved in OT regulation of opiate-mediated nociception (Yang et al., 2011). Considerable OT-ir innervation is also seen in the substantia nigra and ventral tegmental area. In the mouse, OT can directly activate specific neurons in the VTA (Tang et al., 2014), where OT activity appears to regulate various behaviours in rats, including maternal behaviour (C A Pedersen, Caldwell, Walker, Ayers, & Mason, 1994; Cort A. Pedersen, 1997), food intake (Mullis, Kay, & Williams, 2013) and penile erection (Melis et al., 2007; Succu et al., 2008). In women, OT increases the VTA activation to salient sexual and infant stimuli (Gregory, Cheng, Rupp, Sengelaub, & Heiman, 2015) in nulliparous and postpartum women respectively. Finally, the raphe magnus shows a specific OT-ir innervation, from which released OT can act directly on serotoninergic neurons (Eaton et al., 2012; Mottolese, Redouté, Costes, Le Bars, & Sirigu, 2014) modulating anxiety (Yoshida et al., 2009) and aggression (Pagani et al., 2015).

## 4. Comparison of the distribution of AVP and OT and nonapeptide co-expression

### *4.1. Neuronal populations co-expressing OT and AVP*

Early studies using IHC and ISH techniques suggested that AVP and OT were produced in mutually exclusive sets of neurons (Mohr, Bahnsen, Kiessling, & Richter, 1988). However, analyses of the expression of the genes encoding OT and AVP using quantitative RT-PCR suggest that all magnocellular neurosecretory cells in the hypothalamus express both peptides, in some cases at dramatically different levels (Glasgow et al., 1999; Kiyama & Emson, 1990). Thus, mRNA ratios in the range of 1:500 for the minor peptide versus the major one are found in neurons that would probably appear as expressing only one of the peptides, using immunohistochemical or in situ hybridization procedures. By contrast, a ratio of about 1:2 is found in those neurons usually considered to co-express both peptides (which in the rat SON represent 1-3% of the neurosecretory population, Xi et al. 1999). This reflects a limitation of immunohistochemical or *in situ* hybridization techniques.

Taking these limitations into account, in most of the Pa and in the SON, OT-ir and AVP-ir cells constitute distinct, partially intermingled subnuclei. In this respect, our findings roughly fit the results of the studies by Rhodes et al. (1981) and Hou-Yu et al. (1986) comparing the distribution of OT-ir and AVP-ir cells in the rat Pa. Thus, in the Pa, OT-ir cells concentrate in the PaV, PaM and PaPo, as well as in the adjacent periventricular nucleus. In contrast, AVP-ir cells are mainly found in the PaL, with few cell bodies in the antero-ventral aspect of the nucleus, where they are intermingled with the dense population of OT-ir cells (see Fig. 12). However, concerning the SON our findings (fig. 13) differ from those in the rat (Hou-Yu et al., 1986;

Rhodes et al., 1981). Thus, in the mouse AVP-ir cells constitute the large majority of the nonapeptidergic cells of the nucleus, whereas OT-ir somata are restricted to the dorsomedial SON, especially at rostral levels, and to a few scattered cells in the dorsal portion of the SOR (see Fig. 13). By contrast, the rat SON shows a more balanced proportion of OT- and AVP-ir cells, which are intermingled instead of segregated, especially at anterior levels of the nucleus (Hou-Yu et al., 1986; Rhodes et al., 1981).

Interestingly, the use of double immunofluorescence has allowed us to identify and locate various cell populations that show immunoreactivity for both, OT and AVP. Doubly-labelled neurons are relatively frequent at rostral levels of the Pa and in the ADP/AC. In fact, a majority of the OT-ir somata in the rostral edge of the PaAP and in the ADP/AC show also weak-to-moderate AVP immunoreactivity. In the ADP/AC, Rood et al. (2013) reported the same AVP-ir cell group we describe here, different from the sexually dimorphic AVP-ir population of the BST. Our present results indicate that the OT-ir and AVP-ir groups next to the anterior commissure correspond in fact to a single ADP/AC population of cells that are immunolabelled for both peptides. The characteristic immunolabelling of the rostral PaAP and ADP/AC oxytocinergic cells (high OT-ir plus low AVP-ir) reinforces the classification of the ADP/AC as a distinct cell group in the mouse brain.

Other co-localization studies in neuropeptidergic cells of the rat and mouse hypothalamus fit our observations in mice relative to the presence of a distinct population of OT+AVP immunoreactive cells in the ADP/AC. Xiao et al. (2005) described a cell group expressing both OT and nitric oxide synthase in the region corresponding to the ADP/AC of the rat brain (which they call the anterior levels of the anterior magnocellular Pa, see their figure 6A-C). This fits the pattern of co-expression of NADPH diaphorase in the non-dimorphic AVP-ir cell population of the ADP/AC shown here (see Fig. 2c). Note also that, like the OT-ir cells (Fig. 10a), some of these diaphorase/AVP positive cells are associated to blood vessels (Fig. 2a).

Besides these populations of cells expressing high levels of OT and relatively lower levels of AVP, some cells showed comparable levels of immunoreactivity for both OT and AVP. These equally co-labelled cells were mainly located in the Pa near the ventricle and in the Pe. Equally co-labelled cells also occur in the AN and, less frequently, in the SON. Thus, the accessory nonapeptidergic nuclei apparently show a relatively large proportion of somata immunostained for both nonapeptides.

Our qualitative observations fit co-localization studies in the rat using double in situ hybridisation for mRNA of the peptides or their accompanying neurophysins that revealed a

low proportion of OT+AVP-ir cells, about 2-3% in the SON neurons (Mezey & Kiss, 1991). As discussed above, a few OT-ir cells surpass the borders of the SON and enter the medial amygdala. Some of these OT-ir cells in the Me show a co-expression phenotype similar to the ADP/AC and PaAP OT-ir cells (see Fig. 13 d'), namely intense OT immunostaining and weaker AVP immunolabelling. This is relevant because the Me contains high amounts AVP and OT receptors (Dubois-Dauphin et al., 1996; E. a D. Hammock & Levitt, 2013; Veinante & Freund-Mercier, 1997) but lacks important nonapeptidergic innervation (Rood et al. 2013; present work). Thus, these cells could be a source of both nonapeptides via somato-dendritic release (Ludwig & Leng, 2006). Noteworthy, these cells are located in the main area of convergence of olfactory and vomeronasal projections from the main and accessory olfactory bulbs (Cádiz-Moretti, Martínez-García, & Lanuza, 2013; Kang, Baum, & Cherry, 2009). Therefore it is possible that chemosensory information, which in mice is critically involved in socio-sexual behaviours, influences the nonapeptidergic systems at this level of the medial amygdala, a key node of the sociosexual brain network (Newman, 1999).

### *4.2. Fibres showing AVP and OT co-labelling*

In general, OT-ir processes show a more restricted distribution and lower density than AVP-ir ones (compare Fig. 1 and Fig. 9). Interestingly, our results of double immunolabelling indicate that double OT+AVP fibres are restricted to forebrain areas involved in motivational and emotional functions, such as the ventral striato-pallidum, the central amygdala and the intervening BST.

#### *4.2.1. Nonapeptides in the ventral striato-pallidum and amygdala: cases of receptor mismatch*

In the ventral striato-pallidum, the most remarkable nonapeptidergic terminal field is the distinct terminal field of singly AVP-ir fibres in the mvStP, a fibre system that is sexually dimorphic and testosterone dependent. In this region, almost no OT-ir fibres are present. This fits the occurrence of a high density of vasopressin V1a receptor reported in this region in another mice strain (Dubois-Dauphin et al., 1996).

By contrast, the nucleus accumbens (Acb), both its shell and core, contain sparse, thick-calibre fibres intensely immunoreactive for OT many of which are also moderately AVP-ir (Fig. 14). In fact, most of the nonapeptidergic fibres in the Acb are co-labelled, especially in the medial Acb core. Thus, the OT-ir and AVP-ir processes previously described in the Acb core may actually correspond to the same fibres. To our knowledge, the distribution of OT receptors in the ventral striato-pallidum is not properly described in house mice (*Mus musculus*; see Insel et al.

1993). However, it has been studied in other rodents, such as the singing mice of the species *Scotinomys teguina* and *S. xerampelinus* (Campbell, Ophir, & Phelps, 2009) and the rat (Veinante & Freund-Mercier, 1997). Both studies coincide in showing relatively low density of OT binding in the Acb core, but higher density of OTR in the Acb shell. By contrast, AVP binding appears scarce in both Acb shell and core. Thus, if data in these rodents were valid for mice, there would be a clear mismatch among the nonapeptides and their receptors at the level of the Acb. Nonapeptidergic fibres (doubly labelled) would release relatively large amounts of OT and smaller amounts of AVP in both the shell and core. By contrast, receptors, mainly OTR, would be largely restricted to the shell and absent in the core. Receptors for AVP (V1aR) would be absent in the Acb but concentrated in the mvStP, where there is an AVP terminal field arising from a different cell population, thus likely involved in a different function.

Nonetheless, AVP and OT receptors are highly promiscuous (Manning et al., 2012) such that OT could be acting through V1a receptors. Conversely, AVP could bind OT receptors near the site of release (e.g. in the Acb shell). Ross et al. (2009) analysed the ultrastructure of the OT-ir fibres in the Acb of voles and described large calibre unmyelinated axons filled with dense core OT-ir vesicles, which did not form synaptic contacts but were apposed to dendrites of striatal neurons. This is strongly suggestive of an important role of volume transmission of nonapeptides in the Acb (Landgraf & Neumann, 2004). Taken together, receptor promiscuity and volume transmission of OT and AVP suggest a cross talk between both nonapeptidergic systems (the doubly labelled one in the Acb and the AVP-specific one in the mvStP) at the level of the ventral striato-pallidum.

A similar situation is found in the central and medial amygdaloid nuclei. Co-labelled fibres appear in all subdivisions of the Ce (Fig. 14), whereas the adjoining MePD shows a sexually dimorphic, testosterone dependent, AVP-specific terminal field. As discussed above, binding experiments in mice are scarce and restricted to low-resolution description of the distribution of binding to AVP V1a receptors (Dubois-Dauphin et al., 1996). Therefore, we have to rely on data in the rat. Veinante & Freund-Mercier (1997) provided a detailed description of OTR and V1aR binding in the in the extended amygdala of the rat. If their results could be extrapolated to mice (as suggested by comparison with Dubois-Dauphin et al. (1996), they would again show a partial mismatch between nonapertidergic fibres and their receptors. Thus OTR density is high in the CeL and moderate in the MePD (see their fig. 10-12), whereas V1aR binding is low-to-moderate in the CeM and AStr but virtually absent in the CeL and MePD. This partially segregated distribution of receptors contrasts with the nonapeptidergic innervation of these structures. Thus, the MePD shows a relatively dense terminal field of only AVP-ir and no OT-ir

fibres, but expresses high levels of OTR, that can bind AVP with affinity similar to that for OT (Manning et al. 2012). Similarly, doubly labelled AVP+OT fibres (more labelled for OT- than for AVP-ir) are scattered throughout the Ce (CeL and CeM), whereas V1aR are confined to the CeM (and AStr) and OTR is present in the CeL.

Huber et al. (2005) described the cells and local circuits upon which OT acts in the CeL and AVP acts in the CeM, to regulate fear responses in the rat. The likely co-release of OT and AVP at different proportions from the same axons in both divisions of the Ce, suggested by our findings in mice, should be taken into consideration for refining the model of regulation of fear by nonapeptides, based in physiological studies in the rat by Knobloch et al. (2012) and Stoop (2012).

A similar mismatch in the distribution of nonapeptidergic fibres and their receptors is likely occurring in other portions of the cerebral hemispheres within the extended amygdala. Thus, in the BSTMA/StA (Figs. 11a and 14c-d) and in the MPOA, OT-ir fibres are scarcer than AVP-ir ones and show a partially segregated distribution. However, like in the rostrally adjacent nucleus accumbens, many of the nonapeptidergic fibres of the BSTA and StA are double-labelled. The importance of OT and AVP transmission in the BST and MPOA for regulating socio-sexual functions such as maternal behaviour is discussed below, together with the possible origin of central OT+AVP-ir projections.

*4.2.2. Separate but overlapping OT and AVP innervations*

By contrast, other regions of the cerebral hemispheres show innervation by OT- and AVP-ir with no evidence of co-localisation. Thus, in the septal region, especially in its ventrolateral portion, OT-ir and AVP-ir fibres are present with no evidence of double labelling. The septum shows a prominent AVP-ir innervation (Fig. 1d) and few, scattered OT-ir fibres (Fig. 9c). In mice and rats, the septum contains receptors for AVP (Dubois-Dauphin et al., 1996) and OT (E. a D. Hammock & Levitt, 2013; Veinante & Freund-Mercier, 1997). Given that OT and AVP transmission in the septal area play a key role in social behaviour (Bychowski, Mena, & Auger, 2013; Lukas, Toth, Veenema, & Neumann, 2013; Veenema & Neumann, 2008), the interplay between both nonapeptidergic systems may be an important factor in regulating this behaviour.

Nonapeptidergic fibres in other parts of the forebrain, midbrain and brainstem are immunoreactive for either OT or AVP. In most places, like in the PAG, OT- and AVP-ir innervations partially overlap, although AVP-ir fibres are more abundant and cover wider

areas. In other areas both peptides show a complementary distribution. Thus, in the thalamus OT-ir fibres innervate the paraventricular thalamic nucleus (PV) whereas AVP-ir innervation is located in the contiguous habenula (Hb) (not shown). Again, this is a strong case for receptor mismatch. In the male mouse, the Hb is enriched in OTR (T. R. Insel et al., 1993), whereas the paraventricular and latero-dorsal nuclei displays a remarkable density of receptors for AVP (Dubois-Dauphin et al., 1996). As in other parts of the brain, however, volume transmission and receptor promiscuity may allow a cross talk between both nonapeptidergic systems also at these levels (Dubois-Dauphin et al., 1996; L J Young, Nilsen, et al., 1999).

### *4.3. On the origin of the doubly immunoreactive nonapeptidergic fibres in the cerebral hemispheres*

Some similarities are apparent between the distinct nonapeptidergic cell groups showing OT+AVP-ir double-labelled cells and the innervation of particular areas in the forebrain, such as the Acb and Ce. Most co-labelled fibres in the Acb and Ce are highly OT-ir plus moderately AVP-ir. This pattern reminds the labelling of cell bodies in the ADP/AC and anterior Pa, also highly OT-ir and slightly AVP-ir. Thus, it is tempting to speculate that the immunoreactive cells in the ADP/AC and anterior Pa are the origin of the innervation of the Acb and Ce, plus the intervening portions of the BSTMA/StA. This is supported by previous studies using different experimental approaches. For example, Hawthorn et al. (1985) reported that lesions restricted to the Pa or involving large portions of the hypothalamus including the Pa, SON and AN resulted in OT depletion in the caudate-putamen (striatum) and septum, whereas lesions restricted to the SON had no effect. This suggests an origin of OTergic innervation of the cerebral subcortex in Pa cells and maybe the adjoining AN. More recent neural tracing experiments in rats have shown that tracer injections in a region of the BST (dorsomedial BST; Dong & Swanson 2006) apparently equivalent to the ADP/AC of mice, results in anterograde labelling compatible with the view that it projects to the Acb and most of the central amygdala. In addition, using fluorogold injections in the Acb, Ross et al. (2009) reported retrogradely labelled cells in the Pa, some of which were immunoreactive for OT. Finally, anterograde tracing in rats using viral vectors which label specifically OT-expressing cells Knobloch et al. (2012) have shown that OTergic cells in the rostral Pa and AN originate fibres in the Acb and Ce.

As a conclusion, our data fit previous findings in the literature suggesting that nonapeptidergic cells in the ADP/AC, rostral Pa and AN might give rise to important central projections, among other structures to the Ce and Acb. At least some of them are neurosecretory cells projecting

to the pituitary and to these forebrain centres through axonic collaterals (in the rat, Knobloch et al. 2012). Our data strongly suggests that many of these cells projecting to central targets are co-expressing both nonapeptides at immunohistochemically detectable levels.

### *4.4. Nonapeptides and maternal behaviour*

The precise location of co-labelled cells and processes bring about some interesting functional considerations. In our preparations, co-expressing phenotypes are found in the ADP/AC and anterior Pa. The ADP/AC is located in between the MPOA and the ventral BSTM, an anatomical region that is crucial for the expression of maternal behaviour in the rat. Initially, lesions of the MPO performed in rats demonstrated an important role of the preoptic hypothalamus in nest building, pup retrieval and nursing (M Numan, Corodimas, Numan, Factor, & Piers, 1988; Olazabal, Kalinichev, Morrell, & Rosenblatt, 2002). However, using knife cuts Numan & Callahan (1980) demonstrated that dorsolateral isolation of the MPO had also important effects on maternal behaviour. This suggested a role of more dorsal structures, e.g. the BST, in maternal care. Numan & Numan (1996) performed lesions of the dorsal (above the anterior commissure) or the ventral BST and observed that the latter, but not the former, abolished pup retrieval and care. In addition, the authors studied the anatomical projections of this region of the ventral BST and proved that it projects to several structures relevant for maternal behaviour, and also to the Acb core and shell, Ce and ventral tegmental area (VTA).

The adjacent anterior paraventricular hypothalamus, but not more caudal portions of the Pa, also seems critical for these responses. Insel & Harbaugh (1989) reported a specific effect of lesions in this anterior hypothalamic region on day 15 of gestation on the initiation of maternal behaviour. These authors discussed their findings in the context of the role of OT in maternal behaviour. Since our results indicate the presence of abundant double-labelled OT-AVP neurons in both, the ADP/AC (apparently in the so-called BSTv region) and anterior Pa, it is tempting to suggest that these particular nonapeptidergic cell groups and their projections to the Acb and Ce, might play a key role for the expression of maternal behaviours in rodents.

In the model of maternal behaviour proposed by Numan & Woodside (2010), the MPOA and BSTv (M Numan & Numan, 1996) regulate the response to pups through their projections to two different functional systems. On the one hand, projections to the ventral tegmental area (VTA) would facilitate proactive and voluntary maternal responses, which would constitute pup-directed appetitive behaviours. On the other hand, other projections of the MPOA-BSTv would reduce anxiety responses to pups, thus decreasing pup avoidance. These authors also propose a role of OT in facilitating the change from the non-maternal (pup avoidance, no pup-

directed behaviours) to the maternal state (pup approach and pup-directed proactive responses).

Our results suggest that nonapeptidergic cells in the ADP/AC and anterior Pa could be responsible for these effects. Proactive, pup-directed maternal responses might be facilitated not only by preoptic/BSTv OTergic projections to the VTA (M Numan & Numan, 1996), which increase dopamine neurotransmission in the Acb in response to pup stimuli (Shahrokh, Zhang, Diorio, Gratton, & Meaney, 2010), but maybe also by the release of OT/AVP in the Acb shell and core by the ADP/AC nonapeptidergic neurons. In fact, it has been shown in voles that activation of oxytocin receptors in the Acb facilitates maternal behaviour (Olazábal & Young, 2006).

Furthermore, suppression of pup avoidance by OT might also be facilitated by nonapeptide release in the Ce leading to fear/anxiety inhibition, as revealed by the detailed electrophysiological and optogenetic studies by Knobloch et al. (2012) in the rat. Again, these key nonapeptidergic fibres might arise from the OT+AVP-expressing cells in the ADP/AC and anterior Pa.

In this way, activation of this key nonapeptidergic cell groups in the ADP/AC and anterior Pa would lead to both facilitating effects of OT on maternal behaviour. Thus, the onset of maternal behaviour might be associated to either specific activation of these cell groups or, more likely, a change in the expression pattern of nonapeptides in these cells and/or of their receptors in their target areas (e.g. Acb and Ce). Although variations in the expression of nonapeptide receptors during motherhood are well documented (e.g. Caughey et al. 2011), there is also evidence for an increased expression of the nonapeptides in relation to pregnancy and lactation. For instance, in the rat it has been shown that the basal levels of co-localization in SON magnocellular neurons rise from 2-3% up to 17% in SON somata, and up to 24% at nerve terminals in the posterior lobe (Mezey & Kiss, 1991) at the second day of lactation, due to an increase in the expression of AVP in OT neurons (see also Jirikowski et al. 1991). In addition, OTergic projections from the Pa to the Ce overexpress the neuropeptide during lactation (Knobloch et al., 2012). Further studies are needed to check whether similar up-regulation of the expression of nonapeptides occurs in the central-projecting cell groups in mice during motherhood.

As a conclusion, our results show that in the brain of mice there is a population of cells expressing both OT and AVP at immunohistochemically detectable levels. These cells are located in a preoptic centre just ventromedial to the posterior BST, in the rostral edge of the

Pa and in the AN. The distribution of fibres with a similar immunohistochemical pattern, together with tracing studies in other rodents, suggest that these cells might innervate the Acb, Ce and portions of the intervening BST. A review of previous literature indicates that cells in this location are critical for the expression of maternal behaviour (Numan and Numan, 1996), through their projections onto systems involved in motivation (increased pup-directed responses) and anxiety (decreased pup-elicited avoidance responses). Our data thus suggest that changes in these cells or in their targets in the ventral striatum and central amygdala (e.g. in the expression of nonapeptides or their receptors), might result in the onset of maternal behaviour involving decreased pup avoidance and the expression of pup-directed appetitive responses.

# CONCLUSIONS

1. Arginin-vasopressin (AVP) immunoreactive cells are present in the magnocellular neurosecretory hypothalamic nuclei, plus several brain centres in the cerebral hemispheres, including portions of the intra- and extra-amygdaloid bed nucleus of the stria terminalis (BST) and the region between the anterodorsal preoptic area and the nucleus of the anterior commissure (ADP/AC). Our histochemical data suggest that the cells located in the intra-amygdaloid BST were previously misinterpreted as belonging to the medial amygdala.

2. The AVP-ir cell groups in the BST are sexually dimorphic so that they are more abundant in males than in females. Castrated males show a female-like phenotype thus indicating that the expression of AVP is testosterone dependent.

3. Fibres immunoreactive for AVP make up dense terminal fields in many parts of the brain, including all the nodes of the social brain network.

4. A quantitative assessment of the density of AVP-ir fibres in the centres located in the cerebral hemispheres, namely the lateral septum, posterodorsal medial amygdala and the medioventral striatopallidum, indicates that the density of these terminal fields is higher in males then in females. In males the density of these AVP-ir innervations is dependent on testosterone.

5. The AVP-ir terminal field in the medioventral striato-pallidum covers a citoarchitectonically ill-defined region located between the nucleus accumbens and the ventral diagonal band, which does not correspond to the ventral pallidum.

6. Using tract-tracing techniques combined with immunohistochemistry and analysing the effects of unilateral lesions of the BST in the density of AVP-ir innervation in the medioventral striatopallidum leads to the conclusion that this innervation arises in the sexually dimorphic cell group in the intermediate and lateral posteromedial BST.

7. The above-mentioned evidence leads to the conclusion that the medioventral striatopallidum is a key node at the interface between the social brain network and the mesolimbic reward system, likely playing an important role in the expression of motivated socio-sexual behaviours.

8. Besides the sexually dimorphic vasopressinergic systems, two nuclei of the amygdala show non-dimorphic highly immunoreactive processes, namely axon-like fibres in the central amygdala and dendrite-like ones in the ventral medial amydaloid nucleus. The

AVP-ir processes in the ventral medial apparently arise from cell bodies in the anterior supraoptic nucleus.

9. Like for AVP, oxytocin immunoreactive (OT-ir) cells are concentrated in the magnocellular neurosecretory nuclei of the hypothalamus, but additional cells are located in the accessory nuclei and in the ADP/AC of the BST-preoptic junction.

10. In contrast to AVP, OT-ir cell groups show no apparent sexual dimorphism. Accordingly, OT-ir terminal fields are similar in males and females.

11. As a general rule, the OT-ir terminal fields are scarcer and less extensive than their vasopressinergic counterparts. With few exceptions, such as the periaqueductal gray, OT- and AVP-ir innervations do not overlap but cover adjacent regions.

12. Double immunofluorescence for OT and AVP reveal cells co-labelled for both nonapeptides, which are very scarce in the neurosecretory hypothalamic nuclei but concentrate in the ADP/ACP group and rostral edge of the hypothalamic paraventricular nucleus. This population is mainly composed of cells showing intense immunofluorescence for OT and relatively fainter immunostaining for AVP.

13. In the same vein, double labelling experiments reveal nonapeptidergic fibres with a similar immunostaining profile in two locations of the brain: the nucleus accumbens (shell and core) and the different divisions of the central amygdala.

14. These findings strongly suggest that nonapeptidergic innervation of the accumbnes and central amygdala arises from the nonapeptidergic cells of the ADP/AC and anterior portion of the paraventricular nucleus.

15. Its location and putative nonapeptidergic projections to the nucleus accumbens and central amygdala, strongly suggest that the ADP/AC corresponds to the region ventral to the BST that, according to Numan and Numan (1996), is critical for the expression of maternal behaviour in rats.

# RESUMEN EN CASTELLANO

# 1. INTRODUCCIÓN

## *1.1. El comportamiento social*

El comportamiento social se define como el conjunto de interacciones que ocurren entre dos o más individuos de una misma especie. Presumiblemente, los comportamientos sociales evolucionaron al suponer una ventaja selectiva para los individuos que los practicaban. Por ejemplo, interacciones cooperativas pueden ayudar en la búsqueda de alimento, incrementar la protección contra depredadores o facilitar los desplazamientos y la cría.

Las especies sociales pueden clasificarse como eusociales o presociales. La eusocialidad corresponde al grado más alto de organización social y se encuentra en numerosas especies de Himenópteros (hormigas, abejas, avispas) e Isópteros (termitas), pero también en dos especies de roedores llamadas "ratas topo" (*Heterocephalus glaber* and *Fukomys damarensis*) (O'Riain & Faulkes, 2008; Wilson & Hölldobler, 2005). Con menor grado de organización social, los animales presociales pueden dividirse en: subsociales, solitarios pero sociales y parasociales (que incluye comunales y semisociales). Esta clasificación fue ideada por Michener (1969) para insectos, pero es ampliamente utilizada en otros taxones animales. De hecho, el comportamiento social aparece en gran variedad de especies animales, incluyendo invertebrados, peces, pájaros y mamíferos. Dentro de una misma especie, los comportamientos sociales pueden tener varios propósitos y generalmente se clasifican como agonísticos (competitivos), afiliativos, sexuales o parentales.

Durante largo tiempo, el comportamiento social ha resultado demasiado complicado para ser estudiado mediante aproximaciones mecanicistas. En la actualidad, los avances técnicos en neurociencia y el uso de modelos animales adecuados están revelando las redes neurales implicadas sus conexiones y su neuroquímica. Estos circuitos están sujetos a regulaciones fisiológicas internas y a la influencia de estímulos sensoriales externos. Si embargo, gran parte de los comportamientoa socio-sexual aparecen de forma innata, lo que indica que la circuitería subyacente está codificada en el genoma, lo que facilitaría su estudio.

Uno de los modelos animales por excelencia para la investigación neurocientífica es el ratón (*Mus musculus*). Igual que muchos otros roedores, tiene una compleja vida social que depende del reconocimiento de otros conespecíficos y la correcta identificación de su género, edad, estado hormonal y estatus. Al igual que otros animales macrosmáticos, los ratones obtienen la mayor parte de esta información a través del uso de señales químicas. De esta forma, su vida social está guiada por el olfato y la vomerolfacción, de igual manera que la interacción social en humanos depende principalmente de información visual y auditiva. En el caso de los ratones, se ha demostrado que algunas señales químicas producidas por un individuo pueden desencadenar respuestas estereotipadas en otros individuos, ajustándose por tanto a la definición clásica de feromona (Karlson & Luscher, 1959).

En trabajos previos, nuestro grupo se ha dedicado a identificar la naturaleza olfativa o vomeronasal de las feromonas que median la atracción sexual en ratones y los circuitos cerebrales que median su efecto. Los primeros estudios indicaron que las excreciones y secreciones de los machos resultan innatamente atractivas para las hembras (Moncho-Bogani

et al. 2002). Estas supuestas feromonas actuan como estímulo reforzante como lo demuestran experimentos de inducción de preferencia de lugar condicionada (Martinez-Ricos et al., 2007). Además, las lesiones del bulbo olfatorio accesorio eliminan tanto la atracción como la preferencia de lugar, demostrando que estas posibles feromonas son detectadas por el sistema vomeronasal (Martinez-Ricos et al., 2008).

Trabajos más recientes han conseguido identificar algunas de estas feromonas. Por ejemplo, se ha identificado un péptido en la secreción lacrimal de los machos que induce receptividad en las hembras (Haga et al., 2010), y una proteína urinaria responsable de la atracción femenina hacia los machos (MUP-20 o darcina, Roberts et al. 2010) que también induce preferencia condicionada de lugar (Roberts et al, 2012).

Nuestro grupo ha demostrado que la darcina promueve la agresión maternal en hembras lactantes (Martín-Sánchez et al, 2015), lo que contrasta con sus propiedades atractivas en las mismas hembras en otros períodos de su ciclo vital (por ejemplo en vírgenes). De forma similar, las proteínas urinarias son responsables de la agresión entre machos (Chamero et al., 2007). En conjunto, estos datos indican que las señales químicas juegan un papel clave en la modulación del comportamiento social en ratón, y sugieren que los núcleos cerebrales que procesan la información olfativa y vomeronasal forman parte de la red neural que controla el comportamiento social, como discutimos a continuación.

### *1.2. El cerebro socio-sexual y la amígdala*

El comportamiento social está dirigido por un sistema cerebral específico, la red cerebral socio-sexual (*socio-sexual brain network*, SBN) compuesta por seis nodos, según lo propuesto originalmente por Newman (1999; Fig. A). Cada nodo de la SBN ha de cumplir tres criterios: estar implicado en el control de más de un comportamiento social, estar recíprocamente interconectado con los demás nodos y contener receptores para esteroides sexuales. Otras áreas cerebrales también son importantes para el control del comportamiento social, y la SBN debería entenderse como el "núcleo" de la red que controla dichos comportamientos. En lugar de tratarse de un circuito lineal, la SBN constituye una red en la que cada nodo responde una gran variedad de estímulos y la respuesta comportamental resultante está asociada con un determinado patrón de actividad de los nodos que componen la red (Fig. A). El modelo tiene sus limitaciones, pero se apoya en gran cantidad de evidencia experimental. Además, de acuerdo con su importancia adaptativa, se encuentra muy conservado, estando presente en todos los vertebrados estudiados (Goodson, 2005).

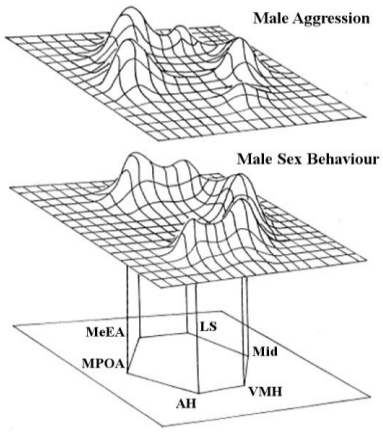


**Fig. A. La red neural socio-sexual (socio-sexual brain network, SBN), según Newman (1999), adaptado del artículo original.** La red está compuesta por seis nodos: la amígdala medial extendida (MeEA), septum lateral (LS), área preóptica medial (MPOA), hipotálamo anterior (AH), hipotálamo ventromedial (VMH) y núcleos mesencefálicos (Mid). Arriba, representaciones esquemáticas de datos de genes de expresión temprana muestran dos patrones de activación diferentes en dos situaciones comportamentales.

En el caso de los roedores, la modulación de comportamiento social por estímulos quimio-sensoriales se produce a través de inputs directos e indirectos a la SBN, principalmente a la amígdala. La amígdala medial extendida (MeEA, Fig. A) contiene gran cantidad de receptores para hormonas esteroideas (Mitra et al., 2003; Simerly et al., 1990), además de los centros vomeronasales secundarios y muchos olfativos secundarios y terciarios (Martínez-García et al., 2012). Junto con otras áreas amigdalinas como la amígdala cortical posteromedial, que constituye la corteza vomeronasal (Gutiérrez-Castellanos et al., 2014), la MeEA envía proyecciones a una región específica de la porción medial del estriado-pálido ventral (mvStP; Ubeda-Banon et al. 2008; Novejarque et al. 2011; Pardo-Bellver et al. 2012). Este hecho resulta muy relevante, ya que el estriado ventral es una región clave para el control de comportamientos motivados. El input directo desde la amígdala quimiosensorial, sugiere que el estriado-pálido ventral puede incluir una región para el control de los comportamientos motivados por feromonas, que sería crucial para el control de interacciones intraespecíficas como decidir entre atacar, expresar comportamientos afiliativos, parentales o sexuales. De hecho, esa región es fundamental para la formación de lazos de pareja en topillos (Larry J Young & Wang, 2004), y trabajos independientes en diversos laboratorios, incluido el nuestro, han mostrado que la lesión del mvStP elimina el valor reforzante de las feromonas sexuales en ratones (Agustin-Pavon et al., 2014; DiBenedictis et al., 2014).

Dado que el comportamiento socio-sexual difiere entre machos y hembras, la red neural que controla dichos comportamientos, el SBN, también muestra diferencias entre sexos. Estas diferencias están gobernadas por esteroides sexuales, también en la edad adulta. No es de extrañar, pues, la abundancia de receptores de hormonas esteroideas en el SNB.

### *1.3. Los nonapéptidos y la regulación del comportamiento social*

Además de la expresión de receptores sexuales y conectividad recíproca, las áreas que componen el SBN poseen otra característica distintiva: una abundante inervación nonapeptidérgica y la expresión de receptores para nonapéptidos. Los roedores y otros mamíferos (incluyendo los humanos) expresan dos nonapéptidos estrechamente emparentados, la arginina-vasopresina (AVP) y la oxitocina (OT). De sus nueve aminoácidos la AVP y OT difieren únicamente en la tercera y octava posición. La evidencia indica que la AVP y la OT proceden de la duplicación génica de un ancestro común, poco antes de la divergencia evolutiva de los vertebrados (H. Caldwell & Young 3rd, 2006). El péptido ancestral puede encontrarse en especies tan distantes como moluscos y anélidos, y su función está altamente conservada, cumpliendo roles similares en las respectivas especies (Choleris et al., 2013).

Ambos nonapéptidos son sintetizados en forma de péptido precursor, que es almacenado en vesículas y procesado dentro de las mismas. Las respectivas prohormonas son cortadas dando lugar a la forma madura de AVP y OT, sus proteínas transportadoras (neurofisina-I y neurofisina-II respectivamente) y péptidos residuales. De esta forma, las neurofisinas I y II son almacenadas y liberadas junto a sus correspondientes nonapéptidos (Burbach et al. 2001).

En roedores y humanos se han identificado cuatro receptores para nonapéptidos: V1aR, V1bR, V2R y OTR). Los más abundantes en el sistema nervioso central son el V1aR y OTR, mientras

que el V1bR se expresa en unas pocas regiones cerebrales y el V2R está prácticamente restringido a tejidos periféricos (Gimpl et al., 2001; Verbalis, 2010). Todos estos receptores pertenecen a la familia de receptores acoplados a proteína G y su activación tiene efectos sobre canales iónicos, movilización de calcio y regulación de la expresión génica entre otros (ver Stoop, 2012). Es importante tener en cuenta la elevada promiscuidad de los receptores para nonapéptidos. A pesar de lo que sus nombres sugieren, la AVP puede unirse al OTR y a los V1Rs con similar afinidad. La OT es más específica, aunque puede unirse a los V1Rs con una afinidad cien veces menor que al OTR (Manning et al., 2012).

En el sistema nervioso central, la activación de V1aR y OTR por AVP y OT parece implicada en el control de comportamientos sociales y no sociales, así como funciones reproductivas, incluyendo olfacción y procesamiento sensorial, miedo y ansiedad, estrés y homeostasis, y aprendizaje y memoria (Carter et al., 2008; Donaldson & Young, 2008; Meyer-Lindenberg et al., 2011; Neumann & Landgraf, 2012; Stoop, 2012). Además la expresión de nonapéptidos y sus receptores en la SNB sugiere un papel importante en el control de las funciones sociales mediadas por estímulos olfativos, como el reconocimiento social (Ferguson et al. 2001; Bielsky et al. 2005) y la agresión y motivación social (S. R. Wersinger et al., 2007; Scott R. Wersinger et al., 2004).

En una excelente revisión, Thomas Insel (2010) explica la relación entre la expresión de receptores para nonapéptidos en el estriado ventral y los lazos afectivos. Un caso muy conocido es el de algunas especies de topillos, en las que los vínculos afectivos de pareja dependen de la expresión del V1aR en el estriado-pálido ventral (M M Lim & Young, 2004). Este hecho pone de manifiesto la relevancia de las proyecciones desde la amígdala vomeronasal al mvStP en las interacciones sociales.

También se ha visto que variaciones genéticas en el locus del receptor V1a (AVP1RA) se relacionan con diferencias en el comportamiento socio-sexual en topillos (E. A. D. Hammock & Young, 2005) y en humanos (Israel et al., 2009; Prichard et al., 2007), llegando a asociarse con la aparición de trastornos autistas (Kim et al., 2002; Wassink et al., 2004). La mayor parte de estudios en humanos utilizan la administración intra-nasal de oxitocina y, en menor medida, de vasopresina. Aunque no se ha demostrado que puedan atravesar la barrera hemato-encefálica, la OT parece tener efectos pro-sociales (Kosfeld et al. 2005; Domes et al. 2007), mientras que la AVP tiene efectos sexualmente dimórficos, pro-sociales en mujeres y agonísticos en hombres (Thompson et al., 2006).

### *1.4. Sistemas nonapeptidérgicos centrales: neuromodulación compleja de funciones complejas*

La oxitocina y vasopresina tienen un papel dual, actuando como neurotransmisores centrales y como neurohormonas periféricas. Sintetizadas en los grupos magnocelulares del hipotálamo, son secretadas a sangre, donde la OT promueve la contracción uterina durante el parto y la eyección de leche durante la lactancia, mientras que la AVP tiene efectos vasopresores y antidiuréticos. En el sistema nervioso central, existen células e inervación nonapeptidérgica fuera del hipotálamo, y tanto AVP como OT pueden ser liberados desde los axones, dendritas y somas neuronales (Ludwig & Leng, 2006; Sabatier et al., 2004; Tobin et al., 2012).

Tras liberarse en sitios sinápticos, la AVP y OT se unen a sus receptores (Liu et al., 1994) pero luego no son recicladas y pueden difundir y actuar sobre neuronas distantes (Zoli & Agnati, 1996). Los nonapéptidos también se liberan extra-sinápticamente actuando sobre amplias regiones. Este tipo de transmisión extra-sináptica se denomina **transmisión de volumen** y parece jugar un papel importante en la modulación nonapeptidérgica (Landgraf & Neumann, 2004; Trueta & De-Miguel, 2012), que podría deber su eficacia a una combinación de transmisión sináptica precisa y extra-sináptica difusa. Un hecho que refuerza la importancia de la transmisión de volumen, es la frecuente disparidad entre la localización de la inervación nonapeptidérgica y el respectivo receptor.

En cualquier caso, los receptores para AVP y OT están localizados en regiones bien definidas, donde los circuitos locales son muy importantes en la modulación nonapeptidérgica. En una revisión reciente, Stoop (2012) discute este hecho, además de la interacción entre AVP y OT en sus acciones neuromoduladoras.

### *1.5. Datos previos y justificación del trabajo*

Los roedores son ampliamente utilizados en la investigación de la neurobiología del comportamiento social (Bosch, 2011; Nephew & Bridges, 2008; Takahashi & Miczek, 2013; Toth & Neumann, 2013). La información anatómica procedente de estudios en ratas muestra que tanto la SBN como el sistema mesolímbico del refuerzo (según las definiciones de Newman 1999 y O'Connell & Hofmann 2012) expresan receptores para AVP y OT (Veinante & Freund-Mercier, 1997), y muestran una importante inervación vasopresinérgica (DeVries et al., 1985). Sin embargo, no hay apenas información sobre la distribución de oxitocina, salvo el mapeo de células oxitocinérgicas en el hipotálamo (Hou-Yu et al., 1986).

Los ratones se están convirtiendo en la especie de elección en los estudios de neurobiología del comportamiento social. Por un lado, se están identificando las feromonas que median las interacciones sociales en el ratón (Chamero et al., 2007; Isogai et al., 2011; Nodari et al., 2008; Roberts et al., 2010). Por otro, porque ya hay disponibles una gran variedad de ratones modificados genéticamente que generan información muy útil sobre las bases del comportamiento social (Bielsky et al., 2005; H K Caldwell et al., 2008; Dölen et al., 2013; Egashira et al., 2007; Jin et al., 2007; Nishimori et al., 2008; Pobbe et al., 2012). Sin embargo, la información neuroanatómica es muy escasa en ratón en comparación con la rata. Respecto a los nonapéptidos, recientemente se han publicado varias descripciones de la distribución de AVP, aunque en la cepa endogámica C57BL/6 (Rood & De Vries 2011). Es interesante comparar esta información la de otras cepas, como por ejemplo la CD1, que presenta niveles de agresividad significativamente mayores y menor ansiedad que muchas cepas endogámicas como la C57BL (Parmigiani et al., 1999). Por lo tanto, se necesita una descripción detallada de los sistemas vasopresinérgicos de varias cepas de ratón, prestando especial atención a las áreas cerebrales que dirigen el comportamiento socio-sexual.

Consecuentemente, el primer objetivo del presente trabajo es proporcionar una descripción anatómica precisa de los elementos vasopresinérgicos en el cerebro de la cepa CD1 de ratón, centrándonos en los nodos de la SBN. También analizaremos la presencia de dimorfismo sexual (descrito en otras especies) y el control esteroideo de la expresión de AVP. Prestaremos

especial atención al mvStP, dada su participación en la expresión de comportamientos sexualmente dimórficos, el input quimiosensorial que recibe y su conectividad (que lo sitúa entre el SBN y el sistema de refuerzo mesolímbico).

En el caso de la oxitocina, solo existe una descripción previa de su distribución en el encéfalo del ratón (Castel & Morris, 1988). Se necesita urgentemente un re-análisis y descripción detalladas. Además, los datos sobre la distribución de receptores para AVP (Dubois-Dauphin, Barberis, & De Bilbao, 1996) y OT (Insel et al. 1993; Hammock & Levitt, 2013) refuerzan la idea de una clara discordancia entre la distribución de fibras nonapeptidérgicas y sus receptores.

En el escenario que acabamos de exponer, se hace evidente la necesidad de identificar los lugares de liberación de AVP y OT y su contenido relativo para entender mejor su funcionalidad (Merighi et al., 1989; Stoop, 2012). Por lo tanto, sería muy interesante comparar la distribución de AVP y OT. Aunque tradicionalmente se considera que la AVP y OT son expresadas de manera excluyente, hay evidencia de que la mayoría de células nonapeptidérgicas sintetizan ambos RNAs (Glasgow et al., 1999; Xi et al., 1999). Esta co-expresión es funcionalmente relevante, dado que se ve alterada en condiciones fisiológicas como la privación de agua (Telleria-Diaz et al., 2001) o la maternidad (Mezey & Kiss, 1991). Sin embargo, no existe ningún trabajo sobre los patrones basales de co-expresión de ambos nonapéptidos.

### *1.6. Objetivos específicos del trabajo*

1. Describir la distribución de vasopresina en el cerebro de ratones CD1 y analizar la presencia de dimorfismo sexual y su control hormonal. Nos centraremos en el estriado-pálido ventral, dado su posible papel modulador del comportamiento social mediado por feromonas.
2. Trazar el origen de la inervación sexualmente dimórfica del estriado-pálido ventral, para entender mejor su relación en el SBN.
3. Realizar de una descripción detallada de la distribución de oxitocina en el cerebro de ratones CD1.
4. Comparar directamente la distribución de AVP y OT en el mismo material, analizando la presencia de elementos en los que se co-expresan ambos nonapéptidos.

## 2. METODOLOGÍA

Para este trabajo, utilizamos 62 ratones adultos de la cepa CD1 (de 9 a 16 semanas de edad; Harlan, Barcelona, España; Janvier-Europe, Le Genest Saint Isle, France). Los animales fueron tratados de acuerdo con la normativa de la comunidad europea del 24 de noviembre, 1986 97 (86/609/EEC) y todos los procedimientos fueron aprobados por el comité de ética y experimentación animal de la *Universitat de València*.

### *2.1. Experimento 1. Distribución de la inmunoreactividad de AVP en los hemisferios cerebrales del ratón y análisis de su dimorfismo sexual*

En este experimento procesamos un total de 24 machos adultos y 15 hembras adultas para la inmunohistoquímica de AVP.

#### *2.1.1. Inyecciones de colchicina*

Antes del procesado para inmunohistoquímica, seis de los animales (3 hembras y 3 machos) recibieron inyecciones intracerebrales de colchicina para inhibir el transporte axónico e incrementar así el marcaje en somas neuronales. Brevemente, cada animal se mantuvo bajo anestesia gaseosa (Isofluorano al 2%) en un marco estereotáxico. Tras realizar una incisión longitudinal en la piel del cráneo, se tomaron las referencias en las suturas craneales y se trepanó un pequeño orificio sobre uno de los ventrículos laterales (según un atlas de referencia). Mediante un capilar de vidrio, inyectamos una solución salina con unos 30 microgramos de colchicina en uno de los ventrículos laterales. Tras día y medio de supervivencia, los animales fueron sacrificados y procesados como se indica en el punto 1.3.

#### *2.1.2. Orquidectomía*

Datos previos en varios vertebrados muestran que la inervación AVP-ir en varios centros cerebrales es sexualmente dimórfica. Para explorar si esto es cierto también para el mvStP, estudiamos la densidad de fibras AVP-ir en tres grupos de hembras, machos y machos castrados (n=9 por grupo). Para la gonadecomía de los machos, los animales fueron anestesiado con pentobarbital según Shipley & Adamek (1984). Administramos atropina (0.4 mg/kg) para prevenir la depresión cardio-respiratoria y 0.02 mg/kg (subcutáneos) de buprenorfina como analgésico y extrajimos las gónadas a través de una sola incisión en el saco escrotal. Tras tres semanas de recuperación (para asegurar el descenso en los niveles de testosterona), tanto los machos castrados como los machos intactos y las hembras fueron sacrificados y procesados como se indica en el punto 1.3.

#### *2.1.3. Perfusión, fijación y corte*

Los animales fueron sacrificados mediante sobredosis de pentobarbital y perfundidos transcardíacamente con de solución salina (5.5 mL) seguida de paraformaldehido al 4% en tampón fosfato 0.1M pH 7.4 a razón de 5.5 mL/min. Los encéfalos fueron extraídos cuidadosamente y sumergidos en sacarosa al 30% en tampón fosfato para su crioprotección, durante cinco días. Acto seguido, los seccionamos en un micrótomo de congelación y

recogimos los cortes en cinco series paralelas. La primera y tercera series se usaron para la detección inmunohistoquímica de AVP, mientras que la segunda serie fue procesada para la tinción de Nissl o inmunohistoquímica del marcador neuronal NeuN. El resto de series fueron congeladas (-18ºC) para su uso posterior. En algunos casos, una cuarta serie fue procesada para la inmunodetección de substancia P o la histoquímica de NADPH diaforasa, para delimitar la arquitectura del mvStP y la amígdala, respectivamente.

*2.1.4. Inmunohistoquímica*

Para la inmunohistoquímica utilizamos el método indirecto estandarizado del complejo Avidina-biotina-peroxidasa (ABC), con sucesivas incubaciones en solución de bloqueo, anticuerpo primario y secundario y ABC (según la metodología y diluciones indicadas en la Tabla 1), lavando cuidadosamente entre cada paso. Finalmente, las preparaciones fueron reveladas con diaminobenzidina, montadas y cubiertas para hacerlas permanentes.

Table 1. Anticuerpos y procedimiento de los experimentos 1 y 2.

| Anticuerpo primario | Dilución | Anticuerpo secundario | Dilución |
|---|---|---|---|
| **Rabbit anti-Vasopressin IgG** (Millipore Cat#AB1565) Antigen: Full-length vasopressin Inmunogen: Synthetic vasopressin conjugated to thyroglobulin | 1:10,000 | Biotinylated goat anti-rabbit IgG (Vector Labs, BA-1000) | 1:200 |
| | 1:2,500 | Alexa Fluor 546-conjugated Goat anti-rabbit IgG (Molecular Probes, A-11071) | 1:300 |
| **Mouse anti-NeuN IgG** (Millipore Cat#MAB377) | 1:5,000 | Biotinylated horse anti-mouse IgG (Vector Labs, BA-2000) | 1:300 |
| **Rabbit anti-Substance P IgG** (Millipore Cat#AB1566) | 1:10,000 | Biotinylated goat anti-rabbit IgG (Vector Labs, BA-1000) | 1:200 |

*2.1.5. Histoquímica para NADPH diaforasa y combinación con inmunohistoquímica para AVP*

Para la detección histoquímica de NADPH diaforasa se siguió el protocolo de Barbaresi, Quaranta, Amoroso, Mensà, & Fabri (2012). Para el doble marcaje, utilizamos dos series de un animal que había recibido inyección de colchicina: realizamos primero la inmunohistoquímica contra AVP, seguida de la histoquímica para NADPH diaforasa.

*2.1.6. Estudio de las preparaciones*

Las preparaciones histológicas se estudiaron con un microscopio Leitz DMRB (Leica AG, Germany) y se fotografiaron con una cámara acoplada (Leica DFC300 FX). Las imágenes se procesaron con ImageJ para optimizar el brillo y contraste sin retoque alguno, y las figuras fueron elaboradas con Gimp (ambos programas de software libre).

*2.1.7. Análisis del dimorfismo sexual*

Para comparar los sistemas vasopresinérgicos entre machos, machos castrados y hembras, realizamos análisis cuantitativos de la inervación AVP-ir en una región con dimorfismo sexual ya descrito (septum lateral, LS), el campo terminal del mvStP y otra región del estriado ventral (núcleo accumbens, Acb).

Tomamos fotografías digitales de las áreas seleccionadas, restamos el fondo y normalizamos el histograma usando ImageJ. Sobre el canal verde, binarizamos la imagen usando la misma regla para todos los casos: los píxeles con un nivel de gris menor del 80% de la moda fueron seleccionados como fibras marcadas. Registramos la fracción de área ocupada por estos píxeles en las regiones seleccionadas en cada animal.

En los mismos animales, tomamos fotografías de secciones de la división posteromedial del núcleo lecho de la stria terminalis (BSTMP). Una persona sin conocimiento del grupo experimental contó el número de células AVP-ir usando ImageJ, en los tres grupos experimentales.

Analizamos estadísticamente la fracción de área ocupada por la inervación AVP-ir y el contaje de somas AVP-ir con el software SPSS. Después de comprobar la normalidad de los datos (Kolmogorov-Smirnov con corrección de Lilliefor) y la homogeinicidad de la varianza (Levene), realizamos una ANOVA de una vía para buscar diferencias inter-grupo en el marcaje de cada área. Cuando ser encontraron diferencias, realizamos comparaciones post-hoc para localizarlas (correcciones de Bonferroni o Games-Howell). Además, buscamos posibles correlaciones entre la densidad de la inervación y el número de somas marcados en las diferentes regiones analizadas, mediante el test de Pearson.

***2.2. Experimento 2. Origen de la inervación AVP-ir en el estriado-pálido ventral.***

La correlación positiva entre la densidad de la inervación del mvStP y el número de somas en el BSTMP sugiere la existencia de una proyección desde el BSTMP al mvStP. El experimento 2 se diseñó para comprobar dicha hipótesis.

*2.2.1. Trazado retrógrado de aferencias al mvStP*

Una primera aproximación consistió en utilizar un trazador retrógrado fluorescente (Fluorogold, FG) en combinación con la detección AVP mediante inmunofluorescencia. Para inyectar el FG utilizamos un método similar al del experimento 1 en la administración de colchicina, usando capilares de vidrio de unos 15µm de diámetro interno en la punta. Administramos el FG mediante iontoforesis (+5 µA durante 5-10min; 7s ON, 7s OFF), a partir de una solución al 2%. Para evitar atravesar estructuras que pudieran dar un falso positivo al recibir trazador durante la trayectoria de la pipeta (como el septum lateral), realizamos las inyecciones con un ángulo lateral de 25 grados (siendo las coordenadas relativas a Bregma, en milímetros: AP-1.42, L0.20, DV-4.00 desde la meninge).

Tras una semana de supervivencia, los animales fueron sacrificados y procesados como en el experimento 1. Dos de las cinco series fueron procesadas para la inmunodetección de AVP usando anticuerpos secundarios fluorescentes, según lo especificado en la Tabla 1 (arriba).

Una vez montadas y cubiertas las preparaciones, analizamos las muestras mediante epifluorescencia (Leica EL-6000 en el microscopio mencionado arriba) usando filtros específicos para fluorogold y rodamina. Ajustamos el brillo y contraste con ImageJ sin retoque alguno de la imagen.

*2.2.2. Lesiones excitotóxicas del BSTM*

En una segunda aproximación, realizamos lesiones excitotóxicas unilaterales del BSTMP sin dañar las fibras de paso, mediante inyección estereotáxica de ácido iboténico. Para ello realizamos cirugía estereotáxica en 12 machos, de forma similar a la administración de cochicina (experimento 1) y FG. Inyectamos 150nl de ácido iboténico 60mM en el BSTMP de uno de los hemisferios cerebrales, mediante presión hidráulica, usando un capilar de vidrio sellado con silicona y unido a una jeringa Hamilton. Para evitar la entrada de ácido iboténico en los ventrículos laterales (próximos al BSTM), entramos con un ángulo antero-posterior de 23 grados e inyectamos la solución a un ritmo de unos 15nL/min (coordenadas desde Bregma, en milímetros: AP-2.25, L0.85, DV4.85 desde meninge).

Tras una semana de supervivencia, sacrificamos y procesamos los animales como en el experimento 1. Procesamos 2 series para el marcador neuronal NeuN (para delimitar la lesión) y para AVP, respectivamente, siguiendo el mismo procedimiento que en el experimento 1 (Tabla 1).

Para analizar los efectos de la lesión, comparamos la densidad de somas en el BSTMP y de fibras en el mvStP, septum lateral y amígdala medial posterodorsal, entre el hemisferio lesionado y el no lesionado, como en el experimento 1. El objetivo era comprobar la hipótesis de que la disminución de somas AVP-ir en el BSTMP del hemisferio lesionado estaba correlacionada con la disminución de fibras en las áreas supuestamente receptoras de sus proyecciones AVP-ir, utilizando el hemisferio no lesionado como control intra-sujeto. Utilizamos un t de Student para medidas relacionadas comparando ambos hemisferios, y una correlación de Pearson entre número de somas y densidad de fibras en los campos terminales.

***2.3. Experimento 3. Distribución de la imunoreactividad para OT***

Obtuvimos preparaciones de inmunohistoquímica para OT en 10 hembras y 2 machos vírgenes de la cepa CD1. Los animales fueron sacrificados y procesados como el en Experimento 1, pero recogimos los cortes en cuatro series paralelas en lugar de cinco. Para la inmunohistoquímica, empleamos el método indirecto ABC como en el Experimento 1 (para anticuerpos y diluciones ver Tabla 2). Estudiamos las preparaciones histológicas y elaboramos las figuras usando la misma metodología que en el experimento 1.

Tabla 2. Anticuerpos y diluciones para inmunohistoquímica en el experimento 3

| Anticuerpo primario | Dilución | Anticuerpo secundario | Dilución |
|---|---|---|---|
| **Mouse anti-oxytocin, monoclonal** (Dr. Harold Gainer, NIH Cat#PS38)<br>Antigen: Oxytocin-specific neurophysin<br>Inmunogen: Rat posterior pituitary extract, KLH coupled | 1:600 | Biotinylated goat anti-mouse IgG (Vector Labs, BA-9200) | 1:200 |
| **Rabbit anti-Oxytocin IgG** (Millipore Cat#AB911)<br>Antigen: Full-length oxytocin<br>Inmunogen: Synthetic oxytocin conjugated to thyroglobulin | 1:25,000 | Biotinylated goat anti-rabbit IgG (Vector Labs, BA-1000) | 1:200 |

### *2.4. Experimento 4. Análisis de la co-localización de OT+AVP*

Para el marcaje simultáneo de oxitocina y vasopresina combinamos la detección de ambos péptidos mediante inmunofluorescencia. Usamos dos de las cuatro series obtenidas de tres machos y tres hembras vírgenes. Brevemente, incubamos las series en borohidruro sódico (para reducir la autofluorescencia tisular), incubamos en solución de bloqueo, anticuerpo primario y secundario marcado con fluoróforo, lavando cuidadosamente entre cada paso (Tabla 3). Para revelar la citoarquitectura en las secciones, contrateñimos con DAPI. Finalmente, montamos los cortes en portaobjetos gelatinizados y cubrimos con medio de montaje para fluorescencia.

Analizamos las preparaciones con un microscopio confocal Olympus FV1000 invertido, escaneando en tres canales para identificar el DAPI, Alexa Fluor 488 (AVP) y Rodamina (OT). Las longitudes de onda de excitación fueron 405 nm para DAPI, 488 nm para Alexa Fluor 488 y 559 nm para Rodamina Red-X. Las longitudes de onda de emisión fueron 461, 520 y 591 respectivamente. Las secciones del plano Z se tomaron separadas entre 1.5 y 4 micras, a x100, x200 y x600 aumentos, en las regiones de interés. Para minimizar el cruce de señal entre canales adquirimos las imágenes de forma secuencial, y las guardamos en formato TIF y OIF. Procesamos los stacks obtenidos con ImageJ para optimizar el brillo y contraste, sin realizar manipulaciones de elementos individuales. Finalmente, elaboramos las figuras con GIMP.

Table 3. Antibodies and immunoprocedure of experiment 4

| Primary antibody | Dilution | Secondary antibody | Dilution |
|---|---|---|---|
| **Mouse anti-oxytocin, monoclonal** (Dr. Harold Gainer, NIH Cat#PS38) | 1:200 | Rhodamine Red X-conjugated goat anti-mouse IgG (Invitrogen R6393) | 1:250 |
| **Rabbit anti-Vasopressin IgG** (Millipore Cat#AB1565) | 1:2,500 | Alexa Fluor 488-conjugated Goat anti-rabbit IgG (Jackson ImmunoResearch, 111-545-003) | 1:300 |

## 3. DISCUSIÓN DE LOS RESULTADOS OBTENIDOS

El presente trabajo constituye la primera descripción completa de los sistemas nonapeptidérgicos del cerebro del ratón. Aparte de los ya bien descritos centros neurosecretores del hipotálamo, nuestros experimentos revelan una serie de grupos celulares localizados principalmente en los hemisferios cerebrales del telencéfalo y en la frontera telencéfalo-diencefálica, que expresan AVP, OT o ambos péptidos simultáneamente. Además, describimos varios campos terminales que revelan la existencia de importantes proyecciones centrales nonapeptidérgicas, con posible papel en la modulación de comportamientos sociales.

### *3.1. Los elementos AVP-ir en los hemisferios cerebrales del ratón*

Al comparar los resultados con la bibliografía, parece que los circuitos AVP-ir se encuentran muy conservados en mamíferos. El cerebro del ratón contiene una población AVP-ir sexualmente dimórfica, que da lugar a la inervación AVP-ir de la mayor parte de los nodos de la SBN. Además, varios centros de la amígdala subpalial muestran inervación AVP-ir no dimórfica. La amígdala medial muestra inervación AVP-ir tanto dimórfica como no dimórfica, probablemente involucradas en la modulación de diferentes componentes del comportamiento social. Por último, nuestros datos nos permiten identificar un nuevo caso de dimorfismo sexual en la inervación AVP-ir del mvStP, lo que apunta a un rol de este centro en el SBN, donde estaría involucrado en el control motivacional de las interacciones sociales.

En líneas generales, nuestros resultados sobre la distribución de elementos AVP-ir en la cepa CD1 de ratón (Fig. 1) concuerdan con los publicados en la cepa C57BL (Ho et al., 2010; Plumari et al., 2002; B D Rood & de Vries, 2011). Además, nuestros datos evidencian una discordancia entre la distribución de fibras AVP-ir y la distribución de receptores para el neuropéptido. Dicha disparidad puede atribuirse en algunos casos (como el de la amígdala medial) a la promiscuidad de receptores (Manning et al., 2012), pudiendo ocurrir que la AVP liberada actúe sobre receptore OTR. Otra explicación es que la AVP liberada podría difundir y actuar sobre receptores V1aR situados a cierta distancia, mediante transmisión de volumen (Landgraf & Neumann, 2004).

Por otro lado, nuestro material revela algunos hallazgos novedosos sobre el sistema AVPérgico. Primero, caracterizamos tres poblaciones AVP-ir además de las tres ya descritas pertenecientes a los núcleos hipotalámicos neuorsecretores (paraventricular, supraóptico y supraquiasmático). Dos de ellas son sexualmente dimórficas (a favor de los machos) y testosterona-dependientes: están localizadas en ambos polos de la amígdala extendida, una en el BST intraamigdalino (BSTIA; Fig. 1k-l y Fig. 2d) y la otra en el BST medial posteriointermedio (BSTMPI; Fig. 1f-g y Fig. 2a; Fig. 3). La tercera, que no muestra dimorfismo sexual (pero una tendencia a mayor dominancia en hembras) se encuentra situada en la región dorsal-anterior del área preóptica medial, flanqueada lateralmente por el BST posterior, dorsalmente por el núcleo de la comisura anterior (AC) y medialmente por el núcleo preóptico antero-dorsal (ADP) que hemos denominado el grupo ADP/AC. Además esta última población co-expresa NADPH-diaforasa (Fig. 1 f-g y Fig. 2 a-c). Como describimos más adelante, la mayoría de estas células co-expresan también oxitocina.

Estos resultados refuerzan el concepto de amígdala medial extendida propuesto por Alheid & Heimer (1988) y muestran la dependencia de testosterona de las poblaciones AVP-ir de esta región cerebral (Fig. 6). Además, los resultados revelan una relación entre el número de células AVP-ir en el BSTMPI y la densidad de la inervación AVP-ir de la amígdala medial posterodorsal, el septum lateral (ya descrita anteriormente), y el mvStP (Experimento 2, Tabla 2). Además, el trazado retrógrado de las proyecciones AVP-ir al mvStP confirma el origen (al menos parcial) de dichas fibras en el BSTMPI (Fig. 7). Las lesiones del BSTMP disminuyen la inervación AVP-ir del mvStP, amígdala medial y septum lateral, indicando que el grupo dimórfico del BST medial origina también (al menos parcialmente) la inervación AVP-ir de la amígdala medial y el septum lateral (Fig. 8).

Utilizando preparaciones inmunohistoquímicas y tinciones histológicas, delimitamos el área inervada por las fibras AVP-ir (Fig. 4). La distribución dimórfica de la inervación AVP-ir en el mvStP es indicativa de su papel en la SBN, ya que además el mvStP cumple con otros los criterios para su inclusión en dicha red, de la que depende el comportamiento socio-sexual (Newman 1999b): está involucrado en varias conductas sociales, como el comportamiento paternal (Akther et al., 2014) y los vínculos de pareja (Larry J Young & Wang, 2004); está interconectada con otras áreas del SBN; y expresa gran cantidad de receptores para esteroides sexuales (Mitra et al., 2003; Shughrue & Merchenthaler, 2001). Esta región parece estar situada en la intersección entre el SBN y el sistema mesolímbico del refuerzo y la motivación, como ocurre con el septum lateral y la amígdala medial extendida, según O'Connell & Hofmann (2011) (Fig. 15).

Por último, en nuestras preparaciones las fibras AVP-ir no dimórficas de la amígdala central muestran una gran variabilidad inter-individual. Dicha variación podría estar relacionada con diferencias en la expresión de comportamientos de miedo, ansiedad, maternales, etc. Como demuestran Knobloch et al. (2012) en el caso de la oxitocina. Otro descubrimiento relevante, es el de la presencia de gruesos procesos AVP-ir (no dimórficos) en la porción ventral de la amígdala medial, aparentemente dendritas procedentes de los somas neurosecretores del núcleo supraóptico anterior (Fig. 5a-b). Smithson et al. (1989; 1992) encontraron estructuras similares en rata, y describieron inputs olfativos directos sobre las células del núcleo supraóptico (Hatton & Yang, 1989). El gran tamaño de estos procesos dendríticos en el cerebro del ratón podría tener importantes implicaciones funcionales si liberaran AVP mediante el mecanismo de liberación dendrítica descrito por Ludwig and Leng (2006).

### *3.2. Los elementos OT-ir en el encéfalo del ratón*

La distribución de elementos OT-ir se asemeja a la observada en otros mamíferos como macacos (Caffé et al., 1989), musarañas arborícolas (Ni et al., 2014), ratas topo lampiñas (Rosen et al., 2008; Valesky et al., 2012), topillos (Z. Wang et al., 1996), hamsters (L. Xu et al., 2010), ratas (Buijs et al., 1978) y diferentes especies de ratón (Castel & Morris, 1988; Hermes et al., 1988). Sin embargo, nuestro trabajo aporta una descripción detallada de la distribución y localización de elementos OT-ir (Fig. 9), que no existía para el ratón, principal especie usada en el estudio de la neurobiología del comportamiento social.

La distribución de células OT-ir sugiere su origen embrionario común, concretamente de la región supraopto-paraventricular del neuroepitelio embrionario (Garcia-Moreno et al., 2010). En nuestro material, las células OT-ir del núcleo supraóptico mostraron menor inmunoreactividad que las del resto del hipotálamo. Esto podría deberse a una menor tasa de síntesis o mayor tasa de transporte anterógrado del péptido. Al estudiar el grupo OT-ir del ADP/AC, destacan sus similitudes con las células AVP-ir de la misma región. Además estas células OT-ir se encuentran a menudo asociadas a vaso sanguíneos (Fig. 10a-b) (ver Muchlinski et al. 1988), lo que posibilita su participación en procesos neurosecretores, aunque no proyecten a la pituitaria (Ross et al., 2009). Esto podría explicar la correlación entre algunos rasgos del comportamiento y los niveles circulantes de oxitocina y daría una respuesta alternativa a la acción de este neuropéptido como hormona moduladora de la conducta, habida cuenta de la impermeabilidad de la barrera hematoencefálica para la oxiti¡ocina.

En cuanto a la inervación OT-ir del encéfalo, la mayoría de fibras observadas corresponden a las fibras neurosecretoras del hipotálamo. Sin embargo, observamos importantes campos terminales con fibras de diferentes morfologías en áreas concretas del sistema nervioso central, lo que sugiere la presencia de varios circuitos OTérgicos originados en las células OT-ir hipotalámico-preópticas.

En el telencéfalo rostral, la inervación OT-ir es escasa y muestra una gran variabilidad inter-individual en términos de abundancia. Es tentador especular que la variabilidad en la inervación nonapeptidérgica en áreas prefrontales pueda estar relacionada con variaciones inter-individuales en comportamiento social.

El BST anterior y las regiones adyacentes del hipotálamo prepótico muestran gruesos procesos OT-ir que podrían provenir de los somas del cercano ADP/AC, y/o ser fibras de paso hacia el núcleo accumbens. En la amígdala central, también encontramos fibras gruesas intensamente inmunoreactivas, que podrían estar implicadas en la regulación del comportamiento maternal (según evidencia obtenida en ratas). Sin embargo, a diferencia de lo descrito por Knobloch et al. (2012) en ratas, nosotros no vemos diferencias en la inervación de las diferentes divisiones de la amígdala central. Esta inervación también muestra gran variabilidad inter-individual, como ocurre en áreas fronto-temporales que se encuentran conectadas con la amígdala, lo que también podría tener implicaciones funcionales.

Otras áreas funcionalmente relevantes presentan inervación OT-ir. El hipotálamo dorsomedial, que participa en reflejos de eyección de leche (Takano et al. 1992), muestra fibras de diferente grosor (Fig. 9k y 10c). La sustancia gris periacueductal presenta una inervación notable (Fig. 9 l, m), que podría mediar en la nocicepción o analgesia (Yang et al. 2011). También hay fibras marcadas en la substancia nigra y área ventral tegmental, donde la OT parece regular funciones como el comportamiento maternal (Pedersen et al. 1997), la ingesta de comida (Mullis et al. 2013) y erección del pene (Melis et al. 2007). Finalmente, el núcleo del rafe magno contiene gran cantidad de fibras OT-ir, que podrían estar regulando los niveles de agresión (Yoshida et al. 2009) y agresividad (Pagani et al. 2015) al actuar sobre neuronas serotoninérgicas (Eaton et al. 2012; Mottolese et al 2014).

### *3.3. Co-expresión de OT y AVP en el cerebro del ratón*

Los primeros estudios inmunohistoquímicos y de hibridación *in situ* sugerían que la OT y AVP se expresan de forma exclusiva en diferentes poblaciones de neuronas (Mohr et al. 1988). Esa visión de los sistemas oxitocinérgicos y vasopresinérgicos como independientes está aún vigente. Sin embargo, el uso de técnicas de PCR cuantitativa en células aisladas (Kiyama & Emson 1990; Glasgow et al. 1999) demuestran que casi todas las células neurosecretoras expresan ambos péptidos, aunque en proporciones diferentes que van desde 1:500, en células consideradas exclusivamente oxitocinérgicas o vasopresinérgicas, a 1:2 en células descritas como co-expresoras de ambos péptidos (Xi et al 1999). Esto refleja las limitaciones de las técnicas de inmunodetección o hibridación *in situ*.

Teniendo en cuenta estas limitaciones, nuestros resultados muestran que la expresión de AVP y OT es complementaria, tanto en células como en fibras, en la mayoría de áreas analizadas. En el núcleo paraventricular nuestros resultados concuerdan con los de estudios previos en rata de Rhodes et al. (1981) y Hou-Yu et al (1986; ver Fig. 12). Sin embargo, la distribución que hemos encontrado en el núcleo supraóptico del ratón (Fig. 12) difiere de la descrita en la rata: en el ratón, las células AVP-ir son mucho más abundantes, y que las OT-ir están restringidas a la porción más rostro-medial del núcleo supraóptico. El núcleo supraóptico de la rata muestra una proporción parecida de células AVP-ir y OT-ir, entremezcladas en lugar de separadas como en el ratón. Un hallazgo muy relevante es la identificación de varias poblaciones que co-expresan OT y AVP a niveles inmunodetectables. En el núcleo paraventricular y en el supraóptico las células doblemente marcadas son una minoría y presentan, en general, niveles similares de immunofluorescencia para ambos nonapéptidos. En los núcleos accesorios del hipotálamo, la proporción de células doblemente marcadas parece mayor, aunque el patrón de marca es similar. Sin embargo, en la porción más rostral del núcleo paraventricular, la mayoría de las células intensamente OT-ir son también ligeramente inmunoreactivas para AVP. También en el ADP/AC, la mayoría de células presentan doble marcaje, con dominancia de OT frente a AVP. Esto refuerza la idea que estas células forman una población neuronal diferenciada dentro del cerebro del ratón, un nuevo núcleo. Algunas células en la amígdala medial también presentan este fenotipo (marca OT intensa y marca AVP débil).

En cuanto a las fibras, encontramos un patrón de inmunoreactividad similar (doble marcaje con predominancia de OT) en la inervación de dos áreas cerebrales: el núcleo accumbens y la amígdala central. Esto sugiere que el origen de dicha inervación podría estar en el ADP/AC y/o el extremo rostral del núcleo paraventricular. La relativa baja abundancia, elevada inmunoreactividad y la ultraestructura de las fibras (Ross et al. 2009), junto a la distribución de receptores, sugiere un papel de dichas fibras en transmisión por volumen de OT y AVP en estos centros del telencéfalo. La liberación simultánea de ambos nonapéptidos y su proporción relativa podría tener importantes implicaciones en las funciones motivacionales y emocionales en las que participan el núcleo accumbens y la amígdala central, respectivamente.

Además, el ADP/AC está localizado en una región clave para la expresión de los comportamientos maternales (Numan & Numan 1996), cuyas proyecciones al núcleo accumbens y a la amígdala central podrían estar modulando los componentes motivacionales y emocionales (Knobloch et al. 2012) del comportamiento maternal.

## 4. CONCLUSIONES FINALES

1. Las células inmunoreactivas para arginina-vasopresina (AVP-ir) están presentes en los núcleos hipotalámicos neurosecretores, además de en varios centros de los hemisferios cerebrales, incluyendo las porciones intra- y extra-amigdalinas del núcleo de la estría terminalis (BST) y la región situada entre el área preóptica anterodorsal y el núcleo de la comisura anterior (ADP/AC). Nuestros datos histoquímicos sugieren que las células situadas en la porción intra-amigdalina del BST habían sido previamente malinterpretadas como pertenecientes a la amígdala medial.
2. Los grupos celulares AVP-ir del BST medial posterointermedio son sexualmente dimórficos, siendo más abundantes en machos que en hembras. Los machos castrados muestran un fenotipo parecido al de las hembras, indicando que la expresión de AVP enm estas células depende de testosterona.
3. Las fibras inmunoreactivas para AVP forman densos campos terminales en varias áreas del cerebro, incluyendo todos los nodos de la red neural que dirige el comportamiento socio-sexual (la SBN).
4. Un análisis cuantitativo de la densidad de fibras AVP-ir en los centros localizados en los hemisferios cerebrales, concretamente en el septum lateral, la amígdala medial posterodorsal y el estriado-pálido medioventral, indica que la densidad de estos campos terminales es mayor en machos que en hembras. En machos, la densidad de esta inervación AVP-ir depende de testosterona.
5. El campo terminal AVP-ir del estriado-pálido medioventral cubre un área mal definida citoarquitectónicamente, localizada entre el núcleo accumbens y la banda diagonal ventral, que no se corresponde con el pálido ventral.
6. Mediante técnicas de trazado de conexiones combinadas con inmunohistoquímica, y el análisis de los efectos de lesiones unilaterales del BST en la densidad de la inervación AVP-ir en el estriado-pálido medioventral, concluimos que dicha inervación proviene del grupo celular sexualmente dimórfico del BST.
7. La evidencia mencionada indica que el estriado-pálido medioventral es un nodo clave en la interfase entre el SBN y el sistema mesolímbico del refuerzo, pudiendo jugar un papel importante en la expresión de comportamientos socio-sexuales motivados.
8. Además del sistema vasopresinérgico sexualmente dimórfico, dos regiones de la amígdala muestran procesos inmunoreactivos no dimórficos, como son las fibras con morfología axónica en la amígdala central y los procesos con aspecto dendrítico en la amígdala medial ventral. Los procesos de la amígdala medial ventral parecen originarse en las células de la porción anterior del núcleo supraóptico.
9. Al igual que para AVP, las células inmunoreactivas para OT (OT-ir) se concentran en los núcleos neurosecretores hipotalámicos, pero encontramos poblaciones adicionales en los núcleos accesorios y en el ADP/AC.
10. En contraste con AVP, los grupos celulares OT-ir no presentan dimorfismo sexual aparente. De la misma forma, los campos terminales OT-ir son similares en machos y hembras.
11. Como regla general, los campos terminales OT-ir son más escasos y menos extensos que sus equivalentes AVP-ir. Salvo contadas excepciones, como la sustancia gris periqueductal, las inervaciones OT- y AVP-ir no se solapan y cubren regiones adyacentes.

12. La doble inmunofluorescencia para OT y AVP revela células doblemente marcadas, que son muy escasas en el hipotálamo neurosecretor, pero se concentran en la región rostral del núcleo paraventricular y en el ADP/AC. Esta población está compuesta mayortariamente por células intensamente inmunoreactivas para OT y débilmente para AVP.
13. Igualmente, los experimentos de doble marcaje revelan fibras marcadas para ambos péptidos en dos localizaciones cerebrales: el núcleo accumbens (shell y core) y las diferentes divisiones de la amígdala central. Estas fibras muestran un patrón de inmunoreactividad similar al de las neuronas preópticas/paraventriculares.
14. Esta evidencia sugiere que la inervación nonapeptidérgica del núcleo accumbens y de la amígdala central puede originarse en las células del ADP/AC y el polo rostral del núcleo paraventricular.
15. La localización y posibles proyecciones nonapeptidérgicas al núcleo accumbens y amígdala central, sugiere que el ADP/AC corresponde a la región ventral al BST que, según Neuman y Neuman (1996), es crítica para la expresión de comportamiento maternal en ratas.

# REFERENCES

Agmo, A. (1997). Male rat sexual behavior. *Brain Research. Brain Research Protocols*, *1*(2), 203–209.

Agustin-Pavon, C., Martinez-Garcia, F., & Lanuza, E. (2014). Focal lesions within the ventral striato-pallidum abolish attraction for male chemosignals in female mice. *Behavioural Brain Research*, *259*, 292–296. doi:10.1016/j.bbr.2013.11.020

Akther, S., Fakhrul, A. a K. M., & Higashida, H. (2014). Effects of electrical lesions of the medial preoptic area and the ventral pallidum on mate-dependent paternal behavior in mice. *Neuroscience Letters*, *570*, 21–5. doi:10.1016/j.neulet.2014.03.078

Alberi, S., Dreifuss, J. J., & Raggenbass, M. (1997). The oxytocin-induced inward current in vagal neurons of the rat is mediated by G protein activation but not by an increase in the intracellular calcium concentration. *European Journal of Neuroscience*, *9*(12), 2605–2612. doi:10.1111/j.1460-9568.1997.tb01690.x

Banczerowski, P., Csaba, Z., Csernus, V., & Gerendai, I. (2003). Lesion of the amygdala on the right and left side suppresses testosterone secretion but only left-sided intervention decreases serum luteinizing hormone level. *Journal of Endocrinological Investigation*, *26*(5), 429–434.

Barbaresi, P., Quaranta, A., Amoroso, S., Mensà, E., & Fabri, M. (2012). Immunocytochemical localization of calretinin-containing neurons in the rat periaqueductal gray and colocalization with enzymes producing nitric oxide: A double, double-labeling study. *Synapse*, *66*(4), 291–307. doi:10.1002/syn.21509

Bartz, J. A., & Hollander, E. (2008). Oxytocin and experimental therapeutics in autism spectrum disorders. *Progress in Brain Research*. doi:10.1016/S0079-6123(08)00435-4

Baumgartner, T., Heinrichs, M., Vonlanthen, A., Fischbacher, U., & Fehr, E. (2008). Oxytocin Shapes the Neural Circuitry of Trust and Trust Adaptation in Humans. *Neuron*, *58*(4), 639–650. doi:10.1016/j.neuron.2008.04.009

Bayerl, D. S., Klampfl, S. M., & Bosch, O. J. (2014). Central V1b Receptor Antagonism in Lactating Rats: Impairment of Maternal Care But Not of Maternal Aggression. *Journal of Neuroendocrinology*, *26*(12), 918–926. doi:10.1111/jne.12226

Beery, A. K., Lacey, E. a., & Francis, D. D. (2008). Oxytocin and vasopressin receptor distributions in a solitary and a social species of tuco-tuco (Ctenomys haigi and Ctenomys sociabilis). *Journal of Comparative Neurology*, *507*(6), 1847–1859. doi:10.1002/cne.21638

Belenky, M., Castel, M., Young, W. S., Gainer, H., & Cohen, S. (1992). Ultrastructural immunolocalization of rat oxytocin-neurophysin in transgenic mice expressing the rat oxytocin gene. *Brain Research*, *583*(1-2), 279–286. doi:10.1016/S0006-8993(10)80034-4

Ben-Barak, Y., Russell, J. T., Whitnall, M. H., Ozato, K., & Gainer, H. (1985). Neurophysin in the hypothalamo-neurohypophysial system. I. Production and characterization of monoclonal antibodies. *The Journal of Neuroscience : The Official Journal of the Society for Neuroscience*, *5*(1), 81–97.

Bielsky, I. F., Hu, S. B., Ren, X., Terwilliger, E. F., & Young, L. J. (2005). The V1a vasopressin receptor is necessary and sufficient for normal social recognition: a gene replacement study. *Neuron*, *47*(4), 503–513. doi:10.1016/j.neuron.2005.06.031

Blanchard, D. C., & Blanchard, R. J. (1988). Ethoexperimental approaches to the biology of emotion. *Annual Review of Psychology*, *39*, 43–68. doi:10.1146/annurev.psych.39.1.43

Bosch, O. J. (2011). Maternal nurturing is dependent on her innate anxiety: the behavioral roles of brain oxytocin and vasopressin. *Hormones and Behavior*, *59*(2), 202–212. doi:10.1016/j.yhbeh.2010.11.012

Breiter, H. C., Etcoff, N. L., Whalen, P. J., Kennedy, W. A., Rauch, S. L., Buckner, R. L., … Rosen, B. R. (1996). Response and habituation of the human amygdala during visual processing of facial expression. *Neuron*, *17*(5), 875–887. doi:10.1016/S0896-6273(00)80219-6

Brock, O., Baum, M. J., & Bakker, J. (2011). The development of female sexual behavior requires prepubertal estradiol. *The Journal of Neuroscience : The Official Journal of the Society for Neuroscience*, *31*(15), 5574–5578. doi:10.1523/JNEUROSCI.0209-11.2011

Brownstein, M. J., Russell, J. T., & Gainer, H. (1980). Synthesis, transport, and release of posterior pituitary hormones. *Science (New York, N.Y.)*, *207*(4429), 373–378. doi:10.1126/science.6153132

Buijs, R. M. (1978). Intra- and extrahypothalamic vasopressin and oxytocin pathways in the rat. Pathways to the limbic system, medulla oblongata and spinal cord. *Cell and Tissue Research*, *192*(3), 423–435.

Buijs, R. M., Swaab, D. F., Dogtermon, J., & van Leeuwen, F. W. (1978). Intra- and Extrahypothalamic Vasopressin and Oxytocin Pathways in the Rat. *Cell and Tissue Research*, *186*, 423–433.

Bupesh, M., Legaz, I., Abellan, A., & Medina, L. (2011). Multiple telencephalic and extratelencephalic embryonic domains contribute neurons to the medial extended amygdala. *The Journal of Comparative Neurology*, *519*(8), 1505–1525. doi:10.1002/cne.22581; 10.1002/cne.22581

Burbach, J. P., Luckman, S. M., Murphy, D., & Gainer, H. (2001). Gene regulation in the magnocellular hypothalamo-neurohypophysial system. *Physiological Reviews*, *81*(3), 1197–1267.

Butovsky, E., Juknat, A., Elbaz, J., Shabat-Simon, M., Eilam, R., Zangen, A., … Vogel, Z. (2006). Chronic exposure to ??9-tetrahydrocannabinol downregulates oxytocin and oxytocin-associated neurophysin in specific brain areas. *Molecular and Cellular Neuroscience*, *31*(4), 795–804. doi:10.1016/j.mcn.2006.01.008

Bychowski, M. E., Mena, J. D., & Auger, C. J. (2013). Vasopressin infusion into the lateral septum of adult male rats rescues progesterone-induced impairment in social recognition. *Neuroscience*, *246*, 52–58. doi:10.1016/j.neuroscience.2013.04.047

Cádiz-Moretti, B., Martínez-García, F., & Lanuza, E. (2013). Neural Substrate to Associate Odorants and Pheromones: Convergence of Projections from the Main and Accessory

Olfactory Bulbs in Mice. In M. L East & M. Dehnhard (Eds.), *Chemical Signals in Vertebrates 12* (pp. 269–275). New York: Springer Science. doi:10.1007/978-1-4614-5927-9

Caffé, A. R., Van Ryen, P. C., Van der Woude, T. P., & Van Leeuwen, F. W. (1989). Vasopressin and oxytocin systems in the brain and upper spinal cord of Macaca fascicularis. *The Journal of Comparative Neurology*, *287*(3), 302–325. doi:10.1002/cne.902870304

Caldwell, H. K., Dike, O. E., Stevenson, E. L., Storck, K., & Young, W. S. (2010). Social dominance in male vasopressin 1b receptor knockout mice. *Hormones and Behavior*, *58*(2), 257–263. doi:10.1016/j.yhbeh.2010.03.008

Caldwell, H. K., Wersinger, S. R., & Young 3rd, W. S. (2008). The role of the vasopressin 1b receptor in aggression and other social behaviours. *Progress in Brain Research*, *170*, 65–72. doi:10.1016/S0079-6123(08)00406-8

Caldwell, H., & Young 3rd, W. S. (2006). Oxytocin and Vasopressin: Genetics and Behavioral Implications. *Handbook of Neurochemistry and Molecular Neurobiology*, 573–607. doi:10.1007/978-0-387-30381-9_25

Campbell, P., Ophir, A. G., & Phelps, S. M. (2009). Central vasopressin and oxytocin receptor distributions in two species of singing mice. *Journal of Comparative Neurology*, *516*(4), 321–333. doi:10.1002/cne.22116

Canteras, N. S. (2002). The medial hypothalamic defensive system: Hodological organization and functional implications. *Pharmacology Biochemistry and Behavior*, *71*(3), 481–491. doi:10.1016/S0091-3057(01)00685-2

Carter, C. S., Grippo, A. J., Pournajafi-Nazarloo, H., Ruscio, M. G., & Porges, S. W. (2008). Oxytocin, vasopressin and sociality. *Progress in Brain Research*. doi:10.1016/S0079-6123(08)00427-5

Castel, M., & Morris, J. F. (1988). The neurophysin-containing innervation of the forebrain of the mouse. *Neuroscience*, *24*(3), 937–966. doi:10.1016/0306-4522(88)90078-4

Caughey, S. D., Klampfl, S. M., Bishop, V. R., Pfoertsch, J., Neumann, I. D., Bosch, O. J., & Meddle, S. L. (2011). Changes in the intensity of maternal aggression and central oxytocin and vasopressin V1a receptors across the peripartum period in the rat. *Journal of Neuroendocrinology*, *23*(11), 1113–1124. doi:10.1111/j.1365-2826.2011.02224.x

Chamero, P., Marton, T. F., Logan, D. W., Flanagan, K., Cruz, J. R., Saghatelian, A., … Stowers, L. (2007). Identification of protein pheromones that promote aggressive behaviour. *Nature*, *450*(7171), 899–902. doi:10.1038/nature05997

Choleris, E., Pfaff, D. W., & Kavaliers, M. (2013). Oxytocin, Vasopressin and Related Peptides in the Regulation of Behavior. In *Oxytocin, Vasopressin and Related Peptides in the Regulation of Behavior* (pp. 379–381). doi:10.1017/CBO9781139017855

Condés-Lara, M., Martínez-Lorenzana, G., Rojas-Piloni, G., & Rodríguez-Jiménez, J. (2007). Branched oxytocinergic innervations from the paraventricular hypothalamic nuclei to

superficial layers in the spinal cord. *Brain Research*, *1160*(1), 20–29. doi:10.1016/j.brainres.2007.05.031

Danalache, B. A., Gutkowska, J., Ślusarz, M. J., Berezowska, I., & Jankowski, M. (2010). Oxytocin-Gly-Lys-Arg: A novel cardiomyogenic peptide. *PLoS ONE*, *5*(10). doi:10.1371/journal.pone.0013643

De Vries, G. J. (2008). Sex differences in vasopressin and oxytocin innervation of the brain. *Progress in Brain Research*. doi:10.1016/S0079-6123(08)00402-0

De Vries, G. J. (2008). Sex differences in vasopressin and oxytocin innervation of the brain. *Progress in Brain Research*, *170*, 17–27. doi:10.1016/S0079-6123(08)00402-0; 10.1016/S0079-6123(08)00402-0

De Vries, G. J., Wang, Z., Bullock, N. A., & Numan, S. (1994). Sex differences in the effects of testosterone and its metabolites on vasopressin messenger RNA levels in the bed nucleus of the stria terminalis of rats. *The Journal of Neuroscience : The Official Journal of the Society for Neuroscience*, *14*(3 Pt 2), 1789–1794.

DeVries, G. J., Buijs, R. M., Van Leeuwen, F. W., Caffe, A. R., & Swaab, D. F. (1985). The vasopressinergic innervation of the brain in normal and castrated rats. *The Journal of Comparative Neurology*, *233*(2), 236–254. doi:10.1002/cne.902330206

DiBenedictis, B. T., Olugbemi, A. O., Baum, M. J., & Cherry, J. A. (2014). 6-Hydroxydopamine lesions of the anteromedial ventral striatum impair opposite-sex urinary odor preference in female mice. *Behavioural Brain Research*, *274*, 243–247. doi:10.1016/j.bbr.2014.08.024

Dölen, G., Darvishzadeh, A., Huang, K. W., & Malenka, R. C. (2013). Social reward requires coordinated activity of nucleus accumbens oxytocin and serotonin. *Nature*, *501*(7466), 179–84. doi:10.1038/nature12518

Domes, G., Heinrichs, M., Michel, A., Berger, C., & Herpertz, S. C. (2007). Oxytocin Improves “Mind-Reading” in Humans. *Biological Psychiatry*, *61*(6), 731–733. doi:10.1016/j.biopsych.2006.07.015

Donaldson, Z. R., & Young, L. J. (2008). Oxytocin, vasopressin, and the neurogenetics of sociality. *Science (New York, N.Y.)*, *322*(5903), 900–904. doi:10.1126/science.1158668

Dong, H. W., & Swanson, L. W. (2006). Projections from bed nuclei of the stria terminalis, dorsomedial nucleus: Implications for cerebral hemisphere integration of neuroendocrine, autonomic, and drinking responses. *Journal of Comparative Neurology*, *494*(1), 75–107. doi:10.1002/cne.20790

Dubois-Dauphin, M., Barberis, C., & De Bilbao, F. (1996). Vasopressin receptors in the mouse (Mus musculus) brain: Sex-related expression in the medial preoptic area and hypothalamus. *Brain Research*, *743*(1-2), 32–39. doi:10.1016/S0006-8993(96)01019-0

Eaton, J. L., Roache, L., Nguyen, K. N., Cushing, B. S., Troyer, E., Papademetriou, E., & Raghanti, M. A. (2012). Organizational effects of oxytocin on serotonin innervation. *Developmental Psychobiology*, *54*(1), 92–97. doi:10.1002/dev.20566

Egashira, N., Tanoue, A., Matsuda, T., Koushi, E., Harada, S., Takano, Y., … Fujiwara, M. (2007). Impaired social interaction and reduced anxiety-related behavior in vasopressin V1a receptor knockout mice. *Behavioural Brain Research*, *178*(1), 123–127. doi:10.1016/j.bbr.2006.12.009

Engelmann, M., Wotjak, C. T., Ebner, K., & Landgraf, R. (2000). Behavioural impact of intraseptally released vasopressin and oxytocin in rats. *Experimental Physiology*, *85 Spec No*, 125S–130S.

Evans, D. W., Lazar, S. M., Boomer, K. B., Mitchel, A. D., Michael, A. M., & Moore, G. J. (2014). Social Cognition and Brain Morphology: Implications for Developmental Brain Dysfunction. *Brain Imaging and Behavior*. doi:10.1007/s11682-014-9304-1

Fallon, J. H. (1983). The islands of Calleja complex of rat basal forebrain II: Connections of medium and large sized cells. *Brain Research Bulletin*, *10*(6), 775–793. doi:10.1016/0361-9230(83)90210-1

Fallon, J. H., Loughlin, S. E., & Ribak, C. E. (1983). The islands of Calleja complex of rat basal forebrain. III. Histochemical evidence for a striatopallidal system. *The Journal of Comparative Neurology*, *218*(1), 91–120. doi:10.1002/cne.902180106

Fallon, J. H., Riley, J. N., Sipe, J. C., & Moore, R. Y. (1978). The islands of Calleja: organization and connections. *The Journal of Comparative Neurology*, *181*(2), 375–395. doi:10.1002/cne.901810209

Feldman, R., Gordon, I., Schneiderman, I., Weisman, O., & Zagoory-Sharon, O. (2010). Natural variations in maternal and paternal care are associated with systematic changes in oxytocin following parent-infant contact. *Psychoneuroendocrinology*, *35*(8), 1133–1141. doi:10.1016/j.psyneuen.2010.01.013

Ferguson, J. N., Aldag, J. M., Insel, T. R., & Young, L. J. (2001). Oxytocin in the medial amygdala is essential for social recognition in the mouse. *The Journal of Neuroscience : The Official Journal of the Society for Neuroscience*, *21*(20), 8278–8285.

Fleming, A. S., Kraemer, G. W., Gonzalez, A., Lovic, V., Rees, S., & Melo, A. (2002). Mothering begets mothering: The transmission of behavior and its neurobiology across generations. *Pharmacology Biochemistry and Behavior*, *73*(1), 61–75. doi:10.1016/S0091-3057(02)00793-1

Francis, D., Diorio, J., Liu, D., & Meaney, M. J. (1999). Nongenomic transmission across generations of maternal behavior and stress responses in the rat. *Science (New York, N.Y.)*, *286*(5442), 1155–1158. doi:10.1126/science.286.5442.1155

Gabor, C. S., Phan, A., Clipperton-Allen, A. E., Kavaliers, M., & Choleris, E. (2012). Interplay of oxytocin, vasopressin, and sex hormones in the regulation of social recognition. *Behavioral Neuroscience*, *126*(1), 97–109. doi:10.1037/a0026464

Garcia-Moreno, F., Pedraza, M., Di Giovannantonio, L. G., Di Salvio, M., Lopez-Mascaraque, L., Simeone, A., & De Carlos, J. A. (2010). A neuronal migratory pathway crossing from diencephalon to telencephalon populates amygdala nuclei. *Nature Neuroscience*, *13*(6), 680–689. doi:10.1038/nn.2556; 10.1038/nn.2556

Gimpl, G., Fahrenholz, F., & Gene, C. (2001). The Oxytocin Receptor System : Structure , Function , and Regulation, *81*(2), 629–684.

Glasgow, E., Kusano, K., Chin, H., Mezey, V. a, Iii, W. S. Y., & Gainer, H. (1999). Single Cell Reverse Transcription-Polymerase Chain Reaction Analysis of Rat Supraoptic Magnocellular Neurons : Neuropeptide Phenotypes and High Voltage-, *140*(11).

Goodson, J. L. (2005). The vertebrate social behavior network: Evolutionary themes and variations. *Hormones and Behavior*, *48*(1 SPEC. ISS.), 11–22. doi:10.1016/j.yhbeh.2005.02.003

Gravati, M., Busnelli, M., Bulgheroni, E., Reversi, A., Spaiardi, P., Parenti, M., … Chini, B. (2010). Dual modulation of inward rectifier potassium currents in olfactory neuronal cells by promiscuous G protein coupling of the oxytocin receptor. *Journal of Neurochemistry*, *114*(5), 1424–1435. doi:10.1111/j.1471-4159.2010.06861.x

Gregory, R., Cheng, H., Rupp, H. A., Sengelaub, D. R., & Heiman, J. R. (2015). Oxytocin increases VTA activation to infant and sexual stimuli in nulliparous and postpartum women. *Hormones and Behavior*, *69*, 82–88. doi:10.1016/j.yhbeh.2014.12.009

Gutierrez-Castellanos, N., Martinez-Marcos, A., Martinez-Garcia, F., & Lanuza, E. (2010). Chemosensory function of the amygdala. *Vitamins and Hormones*, *83*, 165–196. doi:10.1016/S0083-6729(10)83007-9

Gutiérrez-Castellanos, N., Pardo-Bellver, C., Martínez-García, F., & Lanuza, E. (2014). The vomeronasal cortex - afferent and efferent projections of the posteromedial cortical nucleus of the amygdala in mice. *European Journal of Neuroscience*, *39*(1), 141–158. doi:10.1111/ejn.12393

Haga, S., Hattori, T., Sato, T., Sato, K., Matsuda, S., Kobayakawa, R., … Touhara, K. (2010). The male mouse pheromone ESP1 enhances female sexual receptive behaviour through a specific vomeronasal receptor. *Nature*, *466*(7302), 118–122. doi:10.1038/nature09142

Hammock, E. a D., & Levitt, P. (2013). Oxytocin receptor ligand binding in embryonic tissue and postnatal brain development of the C57BL/6J mouse. *Frontiers in Behavioral Neuroscience*, *7*(December), 195. doi:10.3389/fnbeh.2013.00195

Hammock, E. A. D., & Young, L. J. (2005). Microsatellite instability generates diversity in brain and sociobehavioral traits. *Science (New York, N.Y.)*, *308*(5728), 1630–1634. doi:10.1126/science.1111427

Hatton, G. I., Cobbett, P., & Salm, A. K. (1985). Extranuclear axon collaterals of paraventricular neurons in the rat hypothalamus: intracellular staining, immunocytochemistry and electrophysiology. *Brain Research Bulletin*, *14*(2), 123–132. doi:10.1016/0361-9230(85)90072-3

Hatton, G. I., & Yang, Q. Z. (1989). Supraoptic nucleus afferents from the main olfactory bulb--II. Intracellularly recorded responses to lateral olfactory tract stimulation in rat brain slices. *Neuroscience*, *31*(2), 289–297.

Hawthorn, J., Ang, V. T., & Jenkins, J. S. (1985). Effects of lesions in the hypothalamic paraventricular, supraoptic and suprachiasmatic nuclei on vasopressin and oxytocin in rat brain and spinal cord. *Brain Research*, *346*(1), 51–57.

Hermes, M. L. H. J., Buijs, R. M., Masson-Pévet, M., & Pévet, P. (1988). Oxytocinergic Innervation of the Brain of the Garden Dormouse (Eliomys quercinus L.). *The Journal of Comparative Neurology*, *273*, 252–262.

Ho, J. M., Murray, J. H., Demas, G. E., & Goodson, J. L. (2010). Vasopressin cell groups exhibit strongly divergent responses to copulation and male-male interactions in mice. *Hormones and Behavior*, *58*(3), 368–377. doi:10.1016/j.yhbeh.2010.03.021

Honda, K., & Higuchi, T. (2010a). Effects of unilateral electrolytic lesion of the dorsomedial nucleus of the hypothalamus on milk-ejection reflex in the rat. *The Journal of Reproduction and Development*, *56*(1), 98–102. doi:10.1262/jrd.09-090E

Honda, K., & Higuchi, T. (2010b). Electrical activities of neurones in the dorsomedial hypothalamic nucleus projecting to the supraoptic nucleus during milk-ejection reflex in the rat. *The Journal of Reproduction and Development*, *56*(3), 336–340. doi:10.1262/jrd.09-117E

Hou-Yu, a, Lamme, a T., Zimmerman, E. a, & Silverman, a J. (1986). Comparative distribution of vasopressin and oxytocin neurons in the rat brain using a double-label procedure. *Neuroendocrinology*, *44*(2), 235–246. doi:10.1159/000124651

Huber, D., Veinante, P., & Stoop, R. (2005). Vasopressin and oxytocin excite distinct neuronal populations in the central amygdala. *Science (New York, N.Y.)*, *308*(5719), 245–248. doi:10.1126/science.1105636

Insel, T. R. (2010). The challenge of translation in social neuroscience: a review of oxytocin, vasopressin, and affiliative behavior. *Neuron*, *65*(6), 768–779. doi:10.1016/j.neuron.2010.03.005

Insel, T. R., & Harbaugh, C. R. (1989). Lesions of the hypothalamic paraventricular nucleus disrupt the initiation of maternal behavior. *Physiology & Behavior*, *45*(5), 1033–1041. doi:10.1016/0031-9384(89)90234-5

Insel, T. R., Young, L., Witt, D. M., & Crews, D. (1993). Gonadal steroids have paradoxical effects on brain oxytocin receptors. *Journal of Neuroendocrinology*, *5*(6), 619–628. doi:10.1111/j.1365-2826.1993.tb00531.x

Isogai, Y., Si, S., Pont-Lezica, L., Tan, T., Kapoor, V., Murthy, V. N., & Dulac, C. (2011). Molecular organization of vomeronasal chemoreception. *Nature*. doi:10.1038/nature10437

Israel, S., Lerer, E., Shalev, I., Uzefovsky, F., Riebold, M., Laiba, E., … Ebstein, R. P. (2009). The oxytocin receptor (OXTR) contributes to prosocial fund allocations in the Dictator Game and the social value orientations task. *PLoS ONE*, *4*(5). doi:10.1371/journal.pone.0005535

Jin, D., Liu, H.-X., Hirai, H., Torashima, T., Nagai, T., Lopatina, O., … Higashida, H. (2007). CD38 is critical for social behaviour by regulating oxytocin secretion. *Nature*, *446*(7131), 41–45. doi:10.1038/nature05526

Jirikowski, G. F., Ramalho-Ortigao, F. J., & Caldwell, J. D. (1991). Transitory coexistence of oxytocin and vasopressin in the hypothalamo neurohypophysial system of parturient rats. *Hormone and Metabolic Research = Hormon- Und Stoffwechselforschung = Hormones et Metabolisme*, *23*(10), 476–480. doi:10.1055/s-2007-1003733

Kalivas, P. W., Churchill, L., & Klitenick, M. A. (1993). GABA and enkephalin projection from the nucleus accumbens and ventral pallidum to the ventral tegmental area. *Neuroscience*, *57*(4), 1047–1060. doi:10.1016/0306-4522(93)90048-K

Kang, N., Baum, M. J., & Cherry, J. A. (2009). A direct main olfactory bulb projection to the "vomeronasal" amygdala in female mice selectively responds to volatile pheromones from males. *European Journal of Neuroscience*, *29*(3), 624–634. doi:10.1111/j.1460-9568.2009.06638.x

Karlson, P., & Luscher, M. (1959). Pheromones': a new term for a class of biologically active substances. *Nature*, *183*(4653), 55–56.

Kim, S.-J., Young, L. J., Gonen, D., Veenstra-VanderWeele, J., Courchesne, R., Courchesne, E., … Insel, T. R. (2002). Transmission disequilibrium testing of arginine vasopressin receptor 1A (AVPR1A) polymorphisms in autism. *Molecular Psychiatry*, *7*(5), 503–507. doi:10.1038/sj.mp.4001125

Kiyama, H., & Emson, P. C. (1990). Evidence for the co-expression of oxytocin and vasopressin messenger ribonucleic acids in magnocellular neurosecretory cells: simultaneous demonstration of two neurohypophysin messenger ribonucleic acids by hybridization histochemistry. *Journal of Neuroendocrinology*, *2*(3), 257–259. doi:JNE257 [pii]\r10.1111/j.1365-2826.1990.tb00401.x

Knobloch, H. S., Charlet, A., Hoffmann, L., Eliava, M., Khrulev, S., Cetin, A., … Grinevich, V. (2012). Evoked axonal oxytocin release in the central amygdala attenuates fear response. *Neuron*, *73*(3), 553–566. doi:10.1016/j.neuron.2011.11.030

Kosfeld, M., Heinrichs, M., Zak, P. J., Fischbacher, U., & Fehr, E. (2005). *Oxytocin increases trust in humans. Nature* (Vol. 435). doi:10.1038/nature03701

Krisch, B. (1976). Immunohistochemical and electron microscopic study of the rat hypothalamic nuclei and cell clusters under various experimental conditions. Possible sites of hormone release. *Cell and Tissue Research*, *174*(1), 109–127.

Landgraf, R., & Neumann, I. D. (2004). Vasopressin and oxytocin release within the brain: A dynamic concept of multiple and variable modes of neuropeptide communication. *Frontiers in Neuroendocrinology*, *25*(3-4), 150–176. doi:10.1016/j.yfrne.2004.05.001

Lim, M. M., Murphy, A. Z., & Young, L. J. (2004). Ventral Striatopallidal Oxytocin and Vasopressin V1a Receptors in the Monogamous Prairie Vole (Microtus ochrogaster). *Journal of Comparative Neurology*, *468*(4), 555–570. doi:10.1002/cne.10973

Lim, M. M., & Young, L. J. (2004). Vasopressin-dependent neural circuits underlying pair bond formation in the monogamous prairie vole. *Neuroscience*, *125*(1), 35–45. doi:10.1016/j.neuroscience.2003.12.008

Liu, H., Brown, J. L., Jasmin, L., Maggio, J. E., Vigna, S. R., Mantyh, P. W., & Basbaum, A. I. (1994). Synaptic relationship between substance P and the substance P receptor: light and electron microscopic characterization of the mismatch between neuropeptides and their receptors. *Proceedings of the National Academy of Sciences of the United States of America*, *91*(3), 1009–1013. doi:10.1073/pnas.91.3.1009

Ludwig, M., & Leng, G. (2006). Dendritic peptide release and peptide-dependent behaviours. *Nature Reviews. Neuroscience*, *7*(2), 126–136. doi:10.1038/nrn1845

Lukas, M., Toth, I., Veenema, A. H., & Neumann, I. D. (2013). Oxytocin mediates rodent social memory within the lateral septum and the medial amygdala depending on the relevance of the social stimulus: Male juvenile versus female adult conspecifics. *Psychoneuroendocrinology*, *38*(6), 916–926. doi:10.1016/j.psyneuen.2012.09.018

Manning, M., Misicka, a., Olma, a., Bankowski, K., Stoev, S., Chini, B., … Guillon, G. (2012). Oxytocin and Vasopressin Agonists and Antagonists as Research Tools and Potential Therapeutics. *Journal of Neuroendocrinology*, *24*(4), 609–628. doi:10.1111/j.1365-2826.2012.02303.x

Markowitsch, H. J. (1998). Differential contribution of right and left amygdala to affective information processing. *Behavioural Neurology*, *11*(4), 233–244. Retrieved from http://www.ncbi.nlm.nih.gov/pubmed/11568425

Martínez-García, F., Novejarque, A., Gutiérrez-Castellanos, N., & Lanuza, E. (2012). Chapter 6 - Piriform Cortex and Amygdala. In G. P. Charles Watson A2George Paxinos and Luis PuellesA2 Charles Watson & L. Puelles (Eds.), *The Mouse Nervous System* (pp. 140–172). San Diego: Academic Press. doi:10.1016/B978-0-12-369497-3.10006-8

Martinez-Ricos, J., Agustin-Pavon, C., Lanuza, E., & Martinez-Garcia, F. (2007). Intraspecific communication through chemical signals in female mice: reinforcing properties of involatile male sexual pheromones. *Chemical Senses*, *32*(2), 139–148. doi:10.1093/chemse/bjl039

Martinez-Ricos, J., Agustin-Pavon, C., Lanuza, E., & Martinez-Garcia, F. (2008). Role of the vomeronasal system in intersexual attraction in female mice. *Neuroscience*, *153*(2), 383–395. doi:10.1016/j.neuroscience.2008.02.002

McGlone, J. J. (1986). Agonistic behavior in food animals: review of research and techniques. *Journal of Animal Science*.

Melis, M. R., Melis, T., Cocco, C., Succu, S., Sanna, F., Pillolla, G., … Argiolas, A. (2007). Oxytocin injected into the ventral tegmental area induces penile erection and increases extracellular dopamine in the nucleus accumbens and paraventricular nucleus of the hypothalamus of male rats. *European Journal of Neuroscience*, *26*(4), 1026–1035. doi:10.1111/j.1460-9568.2007.05721.x

Mens, W. B. J., Witter, A., & Van Wimersma Greidanus, T. B. (1983). Penetration of neurohypophyseal hormones from plasma into cerebrospinal fluid (CSF): Half-times of disappearance of these neuropeptides from CSF. *Brain Research*, *262*(1), 143–149. doi:10.1016/0006-8993(83)90478-X

Merighi, A., Polak, J. M., Fumagall, G., & Theodosis, D. T. (1989). Ultrastructural localization of neuropeptides and GABA in rat dorsal horn: a comparison of different immunogold labeling techniques. *The Journal of Histochemistry and Cytochemistry : Official Journal of the Histochemistry Society*, *37*(4), 529–540.

Meyer-Lindenberg, A., Domes, G., Kirsch, P., & Heinrichs, M. (2011). Oxytocin and vasopressin in the human brain: social neuropeptides for translational medicine. *Nature Reviews. Neuroscience*, *12*(9), 524–538. doi:10.1038/nrn3044

Mezey, E., & Kiss, J. Z. (1991). Coexpression of vasopressin and oxytocin in hypothalamic supraoptic neurons of lactating rats. *Endocrinology*, *129*(4), 1814–1820. doi:10.1210/endo-129-4-1814 [doi]

Michener, C. D. (1969). Comparative social behaviour of bees. *Annual Review of Entomology*, *14*, 299–342.

Mitra, S. W., Hoskin, E., Yudkovitz, J., Pear, L., Wilkinson, H. A., Hayashi, S., … Alves, S. E. (2003). Immunolocalization of estrogen receptor beta in the mouse brain: comparison with estrogen receptor alpha. *Endocrinology*, *144*(0013-7227; 5), 2055–2067.

Modney, B. K., Yang, Q. Z., & Hatton, G. I. (1990). Activation of excitatory amino acid inputs to supraoptic neurons. II. Increased dye-coupling in maternally behaving virgin rats. *Brain Research*, *513*(2), 270–273.

Mohr, E., Bahnsen, U., Kiessling, C., & Richter, D. (1988). Expression of the vasopressin and oxytocin genes in rats occurs in mutually exclusive sets of hypothalamic neurons. *FEBS Letters*, *242*(1), 144–148.

Moncho-Bogani, J., Lanuza, E., Hernandez, A., Novejarque, A., & Martinez-Garcia, F. (2002). Attractive properties of sexual pheromones in mice: innate or learned? *Physiology & Behavior*, *77*(1), 167–176.

Morris, J. A., Jordan, C. L., & Breedlove, S. M. (2004). Sexual differentiation of the vertebrate nervous system. *Nature Neuroscience*, *7*(10), 1034–1039. doi:10.1038/nn1325

Mottolese, R., Redouté, J., Costes, N., Le Bars, D., & Sirigu, A. (2014). Switching brain serotonin with oxytocin. *Proceedings of the National Academy of Sciences of the United States of America*, *111*(23), 8637–42. doi:10.1073/pnas.1319810111

Muchlinski, a E., Johnson, D. J., & Anderson, D. G. (1988). Electron microscope study of the association between hypothalamic blood vessels and oxytocin-like immunoreactive neurons. *Brain Research Bulletin*, *20*(2), 267–271.

Mullis, K., Kay, K., & Williams, D. L. (2013). Oxytocin action in the ventral tegmental area affects sucrose intake. *Brain Research*, *1513*, 85–91. doi:10.1016/j.brainres.2013.03.026

Nephew, B. C., & Bridges, R. S. (2008). Central actions of arginine vasopressin and a V1a receptor antagonist on maternal aggression, maternal behavior, and grooming in lactating rats. *Pharmacology, Biochemistry, and Behavior*, *91*(1), 77–83. doi:10.1016/j.pbb.2008.06.013

Neumann, I. D., & Landgraf, R. (2012). Balance of brain oxytocin and vasopressin: Implications for anxiety, depression, and social behaviors. *Trends in Neurosciences*, *35*(11), 649–659. doi:10.1016/j.tins.2012.08.004

Newman, S. W. (1999). The medial extended amygdala in male reproductive behavior. A node in the mammalian social behavior network. *Annals of the New York Academy of Sciences*, *877*, 242–257. doi:10.1111/j.1749-6632.1999.tb09271.x

Ni, R. J., Shu, Y. M., Wang, J., Yin, J. C., Xu, L., & Zhou, J. N. (2014). Distribution of vasopressin, oxytocin and vasoactive intestinal polypeptide in the hypothalamus and extrahypothalamic regions of tree shrews. *Neuroscience*, *265*, 124–136. doi:10.1016/j.neuroscience.2014.01.034

Nishimori, K., Takayanagi, Y., Yoshida, M., Kasahara, Y., Young, L. J., & Kawamata, M. (2008). New aspects of oxytocin receptor function revealed by knockout mice: sociosexual behaviour and control of energy balance. *Progress in Brain Research*. doi:10.1016/S0079-6123(08)00408-1

Nodari, F., Hsu, F.-F., Fu, X., Holekamp, T. F., Kao, L.-F., Turk, J., & Holy, T. E. (2008). Sulfated steroids as natural ligands of mouse pheromone-sensing neurons. *The Journal of Neuroscience : The Official Journal of the Society for Neuroscience*, *28*(25), 6407–6418. doi:10.1523/JNEUROSCI.1425-08.2008

Novejarque, A., Gutierrez-Castellanos, N., Lanuza, E., & Martinez-Garcia, F. (2011). Amygdaloid projections to the ventral striatum in mice: direct and indirect chemosensory inputs to the brain reward system. *Frontiers in Neuroanatomy*, *5*, 54. doi:10.3389/fnana.2011.00054

Numan, M., & Callahan, E. C. (1980). The connections of the medial preoptic region and maternal behavior in the rat. *Physiology & Behavior*, *25*(5), 653–665.

Numan, M., Corodimas, K. P., Numan, M. J., Factor, E. M., & Piers, W. D. (1988). Axon-sparing lesions of the preoptic region and substantia innominata disrupt maternal behavior in rats. *Behavioral Neuroscience*, *102*(3), 381–396. doi:10.1037/0735-7044.102.3.381

Numan, M., & Numan, M. (1996). A lesion and neuroanatomical tract-tracing analysis of the role of the bed nucleus of the stria terminalis in retrieval behavior and other aspects of maternal responsiveness in rats. *Developmental Psychobiology*, *29*(1), 23–51. doi:10.1002/(SICI)1098-2302(199601)29:1<23::AID-DEV2>3.0.CO;2-O

Numan, M., & Woodside, B. (2010). Maternity: neural mechanisms, motivational processes, and physiological adaptations. *Behavioral Neuroscience*, *124*(6), 715–741. doi:10.1037/a0021548

O'Connell, L. A., & Hofmann, H. A. (2011). The Vertebrate mesolimbic reward system and social behavior network: A comparative synthesis. *Journal of Comparative Neurology*. doi:10.1002/cne.22735

O'Connell, L. A., & Hofmann, H. A. (2012). Evolution of a Vertebrate Social Decision-Making Network. *Science*. doi:10.1126/science.1218889

O'Riain, M. J., & Faulkes, C. G. (2008). African Mole-Rats: Eusociality, Relatedness and Ecological Constraints. In *Ecology of Social Evolution* (pp. 207–223). Retrieved from http://dx.doi.org/10.1007/978-3-540-75957-7_10

Ogier, R., Tribollet, E., Suarez, P., & Raggenbass, M. (2006). Identified motoneurons involved in sexual and eliminative functions in the rat are powerfully excited by vasopressin and tachykinins. *The Journal of Neuroscience : The Official Journal of the Society for Neuroscience*, *26*(42), 10717–10726. doi:10.1523/JNEUROSCI.3364-06.2006

Olazabal, D. E., Kalinichev, M., Morrell, J. I., & Rosenblatt, J. S. (2002). MPOA cytotoxic lesions and maternal behavior in the rat: effects of midpubertal lesions on maternal behavior and the role of ovarian hormones in maturation of MPOA control of maternal behavior. *Hormones and Behavior*, *41*(2), 126–138. doi:10.1006/hbeh.2001.1753

Olazábal, D. E., & Young, L. J. (2006). Oxytocin receptors in the nucleus accumbens facilitate "spontaneous" maternal behavior in adult female prairie voles. *Neuroscience*, *141*(2), 559–568. doi:10.1016/j.neuroscience.2006.04.017

Olucha-Bordonau, F. E., Fortes-Marco, L., Otero-García, M., Lanuza, E., & Martínez-García, F. (2014). Amygdala: Structure and Function. In G. Paxinos (Ed.), *The Rat Nervous System* (4th ed., pp. 441–490). Academic Press.

Otero-Garcia, M., Martin-Sanchez, A., Fortes-Marco, L., Martínez-Ricós, J., Agustin-Pavón, C., Lanuza, E., & Martínez-García, F. (2014). Extending the socio-sexual brain: Arginine-vasopressin immunoreactive circuits in the telencephalon of mice. *Brain Structure and Function*, *219*(3), 1055–1081. doi:10.1007/s00429-013-0553-3

Pagani, J. H., Williams Avram, S. K., Cui, Z., Song, J., Mezey, E., Senerth, J. M., … Young, W. S. (2015). Raphe serotonin neuron-specific oxytocin receptor knockout reduces aggression without affecting anxiety-like behavior in male mice only. *Genes, Brain, and Behavior*, *14*(2), 167–176. doi:10.1111/gbb.12202

Pardo-Bellver, C., Cadiz-Moretti, B., Novejarque, A., Martinez-Garcia, F., & Lanuza, E. (2012). Differential efferent projections of the anterior, posteroventral, and posterodorsal subdivisions of the medial amygdala in mice. *Frontiers in Neuroanatomy*, *6*, 33. doi:10.3389/fnana.2012.00033

Parmigiani, S., Palanza, P., Rodgers, J., & Ferrari, P. F. (1999). Selection, evolution of behavior and animal models in behavioral neuroscience. *Neuroscience and Biobehavioral Reviews*, *23*(7), 957–970. doi:10.1016/S0149-7634(99)00029-9

Paxinos, G., & Franklin, K. B. J. (2001). *The Mouse Brain in Stereotaxic Coordinates* (Vol. 2nd). San Diego: Academic Press.

Pecina, S., & Berridge, K. C. (2000). Opioid site in nucleus accumbens shell mediates eating and hedonic "liking" for food: map based on microinjection Fos plumes. *Brain Research*, *863*(1-2), 71–86.

Pecina, S., & Berridge, K. C. (2005). Hedonic hot spot in nucleus accumbens shell: where do mu-opioids cause increased hedonic impact of sweetness? *Journal of Neuroscience*, *25*(1529-2401 (Electronic); 50), 11777–11786.

Pedersen, C. A. (1997). Oxytocin control of maternal behavior. Regulation by sex steroids and offspring stimuli. In *Annals of the New York Academy of Sciences* (Vol. 807, pp. 126–145). doi:10.1111/j.1749-6632.1997.tb51916.x

Pedersen, C. A., Caldwell, J. D., Walker, C., Ayers, G., & Mason, G. A. (1994). Oxytocin activates the postpartum onset of rat maternal behavior in the ventral tegmental and medial preoptic areas. *Behavioral Neuroscience*, *108*(6), 1163–1171.

Petrovic, P., Kalisch, R., Singer, T., & Dolan, R. J. (2008). Oxytocin attenuates affective evaluations of conditioned faces and amygdala activity. *The Journal of Neuroscience : The Official Journal of the Society for Neuroscience*, *28*(26), 6607–6615. doi:10.1523/JNEUROSCI.4572-07.2008

Pfaus, J. G. (1999). Neurobiology of sexual behavior. *Current Opinion in Neurobiology*. doi:10.1016/S0959-4388(99)00034-3

Plumari, L., Viglietti-Panzica, C., Allieri, F., Honda, S., Harada, N., Absil, P., … Panzica, G. C. (2002). Changes in the Arginine-Vasopressin immunoreactive systems in male mice lacking a functional aromatase gene. *Journal of Neuroendocrinology*, *14*(12), 971–978. doi:10.1046/j.1365-2826.2002.00866.x

Pobbe, R. L. H., Pearson, B. L., Defensor, E. B., Bolivar, V. J., Young, W. S., Lee, H. J., … Blanchard, R. J. (2012). Oxytocin receptor knockout mice display deficits in the expression of autism-related behaviors. *Hormones and Behavior*, *61*(3), 436–444. doi:10.1016/j.yhbeh.2011.10.010

Pow, D. V., & Morris, J. F. (1989). Dendrites of hypothalamic magnocellular neurons release neurohypophysial peptides by exocytosis. *Neuroscience*, *32*(2), 435–439. doi:10.1016/0306-4522(89)90091-2

Prichard, Z. M., Mackinnon, A. J., Jorm, A. F., & Easteal, S. (2007). AVPR1A and OXTR polymorphisms are associated with sexual and reproductive behavioral phenotypes in humans. Mutation in brief no. 981. Online. *Human Mutation*, *28*(11), 1150. doi:10.1002/humu.9510

Raggenbass, M., Goumaz, M., Sermasi, E., Tribollet, E., & Dreifuss, J. J. (1991). Vasopressin generates a persistent voltage-dependent sodium current in a mammalian motoneuron. *The Journal of Neuroscience : The Official Journal of the Society for Neuroscience*, *11*(6), 1609–1616.

Rhodes, C. H., Morrell, J. I., & Pfaff, D. W. (1981). Immunohistochemical analysis of magnocellular elements in rat hypothalamus: distribution and numbers of cells containing neurophysin, oxytocin, and vasopressin. *The Journal of Comparative Neurology*, *198*(1), 45–64. doi:10.1002/cne.901980106

Roberts, S. A., Simpson, D. M., Armstrong, S. D., Davidson, A. J., Robertson, D. H., McLean, L., … Hurst, J. L. (2010). Darcin: a male pheromone that stimulates female memory and sexual attraction to an individual male's odour. *BMC Biology*, *8*, 75. doi:10.1186/1741-7007-8-75

Rood, B. D., & De Vries, G. J. (2011). Vasopressin innervation of the mouse (Mus musculus) brain and spinal cord. *Journal of Comparative Neurology*, *519*(12), 2434–2474. doi:10.1002/cne.22635

Rood, B. D., & de Vries, G. J. (2011). Vasopressin innervation of the mouse (Mus musculus) brain and spinal cord . *The Journal of Comparative Neurology*. doi:10.1002/cne.22635; 10.1002/cne.22635

Rood, B. D., Stott, R. T., You, S., Smith, C. J. W., Woodbury, M. E., & De Vries, G. J. (2013). Site of origin of and sex differences in the vasopressin innervation of the mouse (Mus musculus) brain. *Journal of Comparative Neurology*, *521*(10), 2321–2358. doi:10.1002/cne.23288

Rosen, G. J., de Vries, G. J., Goldman, S. L., Goldman, B. D., & Forger, N. G. (2008). Distribution of oxytocin in the brain of a eusocial rodent. *Neuroscience*, *155*(3), 809–817. doi:10.1016/j.neuroscience.2008.05.039

Ross, H. E., Cole, C. D., Smith, Y., Neumann, I. D., Landgraf, R., Murphy, a. Z., & Young, L. J. (2009). Characterization of the oxytocin system regulating affiliative behavior in female prairie voles. *Neuroscience*, *162*(4), 892–903. doi:10.1016/j.neuroscience.2009.05.055

Sabatier, N., Shibuya, I., & Dayanithi, G. (2004). Intracellular calcium increase and somatodendritic vasopressin release by vasopressin receptor agonists in the rat supraoptic nucleus: Involvement of multiple intracellular transduction signals. *Journal of Neuroendocrinology*. doi:10.1111/j.0953-8194.2004.01155.x

Sanchez, M. A., & Dominguez, R. (1995). Differential-effects of Unilateral Lesions in the Medial Amygdala on Spontaneous and Induced Ovulation. *Brain Research Bulletin*, *38*(4), 313–317. Retrieved from <Go to ISI>://A1995RV80800002

Sarnyai, Z., & Kovács, G. L. (1994). Role of oxytocin in the neuroadaptation to drugs of abuse. *Psychoneuroendocrinology*, *19*(1), 85–117. doi:10.1016/0306-4530(94)90062-0

Shahrokh, D. K., Zhang, T. Y., Diorio, J., Gratton, A., & Meaney, M. J. (2010). Oxytocin-dopamine interactions mediate variations in maternal behavior in the rat. *Endocrinology*, *151*(5), 2276–2286. doi:10.1210/en.2009-1271

Shipley, M. T., & Adamek, G. D. (1984). The connections of the mouse olfactory bulb: a study using orthograde and retrograde transport of wheat germ agglutinin conjugated to horseradish peroxidase. *Brain Research Bulletin*, *12*, 669–688.

Shughrue, P. J., & Merchenthaler, I. (2001). Distribution of estrogen receptor beta immunoreactivity in the rat central nervous system. *The Journal of Comparative Neurology*, *436*(0021-9967; 1), 64–81.

Simerly, R. B., Chang, C., Muramatsu, M., & Swanson, L. W. (1990). Distribution of androgen and estrogen receptor mRNA-containing cells in the rat brain: an in situ hybridization study. *The Journal of Comparative Neurology*, *294*(1), 76–95. doi:10.1002/cne.902940107

Smithson, K. G., Weiss, M. L., & Hatton, G. I. (1989). Supraoptic nucleus afferents from the main olfactory bulb--I. Anatomical evidence from anterograde and retrograde tracers in rat. *Neuroscience*, *31*(2), 277–287. doi:10.1016/0306-4522(89)90373-4

Smithson, K. G., Weiss, M. L., & Hatton, G. I. (1992). Supraoptic nucleus afferents from the accessory olfactory bulb: evidence from anterograde and retrograde tract tracing in the rat. *Brain Research Bulletin*, *29*(2), 209–220.

Staes, N., Stevens, J. M. G., Helsen, P., Hillyer, M., Korody, M., & Eens, M. (2014). Oxytocin and Vasopressin Receptor Gene Variation as a Proximate Base for Inter- and Intraspecific Behavioral Differences in Bonobos and Chimpanzees. *PLoS ONE*, *9*(11), e113364. doi:10.1371/journal.pone.0113364

Stoesz, B. M., Hare, J. F., & Snow, W. M. (2013). Neurophysiological mechanisms underlying affiliative social behavior: Insights from comparative research. *Neuroscience and Biobehavioral Reviews*. doi:10.1016/j.neubiorev.2012.11.007

Stoop, R. (2012). Neuromodulation by Oxytocin and Vasopressin. *Neuron*, *76*(1), 142–159. doi:10.1016/j.neuron.2012.09.025

Succu, S., Sanna, F., Cocco, C., Melis, T., Boi, A., Ferri, G. L., … Melis, M. R. (2008). Oxytocin induces penile erection when injected into the ventral tegmental area of male rats: role of nitric oxide and cyclic GMP. *Eur J Neurosci*, *28*(4), 813–821. doi:10.1111/j.1460-9568.2008.06385.x

Swanson, L. W., & Kuypers, H. G. (1980). The paraventricular nucleus of the hypothalamus: cytoarchitectonic subdivisions and organization of projections to the pituitary, dorsal vagal complex, and spinal cord as demonstrated by retrograde fluorescence double-labeling methods. *The Journal of Comparative Neurology*, *194*(3), 555–570. doi:10.1002/cne.901940306

Takahashi, A., & Miczek, K. A. (2013). Neurogenetics of Aggressive Behavior: Studies in Rodents. In *Current Topics in Behavioral Neurosciences*. doi:10.1007/7854

Takano, S., Negoro, H., Honda, K., & Higuchi, T. (1992). Lesion and electrophysiological studies on the hypothalamic afferent pathway of the milk ejection reflex in the rat. *Neuroscience*, *50*(4), 877–883. doi:10.1016/0306-4522(92)90211-J

Tang, Y., Chen, Z., Tao, H., Li, C., Zhang, X., Tang, A., & Liu, Y. (2014). Oxytocin activation of neurons in ventral tegmental area and interfascicular nucleus of mouse midbrain. *Neuropharmacology*, *77*, 277–284. doi:10.1016/j.neuropharm.2013.10.004

Telleria-Diaz, A., Grinevich, V. V, & Jirikowski, G. F. (2001). Colocalization of vasopressin and oxytocin in hypothalamic magnocellular neurons in water-deprived rats. *Neuropeptides*, *35*(3-4), 162–167. doi:10.1054/npep.2001.0859

Thompson, R. R., George, K., Walton, J. C., Orr, S. P., & Benson, J. (2006). Sex-specific influences of vasopressin on human social communication. *Proceedings of the National Academy of Sciences of the United States of America*, *103*(20), 7889–7894. doi:10.1073/pnas.0600406103

Tobin, V., Leng, G., & Ludwig, M. (2012). The involvement of actin, calcium channels and exocytosis proteins in somato-dendritic oxytocin and vasopressin release. *Frontiers in Physiology*. doi:10.3389/fphys.2012.00261

Toth, I., & Neumann, I. D. (2013). Animal models of social avoidance and social fear. *Cell and Tissue Research*. doi:10.1007/s00441-013-1636-4

Trueta, C., & De-Miguel, F. F. (2012). Extrasynaptic exocytosis and its mechanisms: A source of molecules mediating volume transmission in the nervous system. *Frontiers in Physiology*, *3 SEP*. doi:10.3389/fphys.2012.00319

Tsukahara, S., Tsuda, M. C., Kurihara, R., Kato, Y., Kuroda, Y., Nakata, M., … Ogawa, S. (2011). Effects of aromatase or estrogen receptor gene deletion on masculinization of the principal nucleus of the bed nucleus of the stria terminalis of mice. *Neuroendocrinology*, *94*(2), 137–147. doi:10.1159/000327541; 10.1159/000327541

Ubeda-Banon, I., Novejarque, A., Mohedano-Moriano, A., Pro-Sistiaga, P., Insausti, R., Martinez-Garcia, F., … Martinez-Marcos, A. (2008). Vomeronasal inputs to the rodent ventral striatum. *Brain Research Bulletin*, *75*(2-4), 467–473. doi:10.1016/j.brainresbull.2007.10.028

Valesky, E. M., Burda, H., Kaufmann, R., & Oelschläger, H. H. a. (2012). Distribution of Oxytocin- and Vasopressin-Immunoreactive Neurons in the Brain of the Eusocial Mole Rat (Fukomys anselli). *Anatomical Record*, *295*(3), 474–480. doi:10.1002/ar.22414

Veenema, A. H., & Neumann, I. D. (2008). Central vasopressin and oxytocin release: regulation of complex social behaviours. *Progress in Brain Research*. doi:10.1016/S0079-6123(08)00422-6

Veinante, P., & Freund-Mercier, M. J. (1997). Distribution of oxytocin- and vasopressin-binding sites in the rat extended amygdala: A histoautoradiographic study. *Journal of Comparative Neurology*, *383*(3), 305–325. doi:10.1002/(SICI)1096-9861(19970707)383:3<305::AID-CNE3>3.0.CO;2-7

Verbalis, J. G. (2010). Vasopressin receptors. In *Hormones, Brain and Behavior Online* (pp. 1599–1610). doi:10.1016/B978-008088783-8.00049-8

Walum, H., Westberg, L., Henningsson, S., Neiderhiser, J. M., Reiss, D., Igl, W., … Lichtenstein, P. (2008). Genetic variation in the vasopressin receptor 1a gene (AVPR1A) associates with pair-bonding behavior in humans. *Proceedings of the National Academy of Sciences of the United States of America*, *105*(37), 14153–14156. doi:10.1073/pnas.0803081105

Wang, W., & Lufkin, T. (2000). The murine Otp homeobox gene plays an essential role in the specification of neuronal cell lineages in the developing hypothalamus. *Developmental Biology*, *227*(2), 432–449. doi:10.1006/dbio.2000.9902

Wang, Z., Zhou, L., Hulihan, T. J., & Insel, T. R. (1996). Immunoreactivity of central vasopressin and oxytocin pathways in microtine rodents: a quantitative comparative study. *The Journal of Comparative Neurology*, *366*(4), 726–737. doi:2-D

Wassink, T. H., Piven, J., Vieland, V. J., Pietila, J., Goedken, R. J., Folstein, S. E., & Sheffield, V. C. (2004). Examination of AVPR1a as an autism susceptibility gene. *Molecular Psychiatry*, *9*(10), 968–972. doi:10.1038/sj.mp.4001503

Wersinger, S. R., Caldwell, H. K., Christiansen, M., & Young 3rd, W. S. (2007). Disruption of the vasopressin 1b receptor gene impairs the attack component of aggressive behavior in mice. *Genes, Brain, and Behavior*, *6*(7), 653–660. doi:10.1111/j.1601-183X.2006.00294.x

Wersinger, S. R., Caldwell, H. K., Christiansen, M., & Young, W. S. (2007). Disruption of the vasopressin 1b receptor gene impairs the attack component of aggressive behavior in mice. *Genes, Brain and Behavior*, *6*(7), 653–660. doi:10.1111/j.1601-183X.2006.00294.x

Wersinger, S. R., Caldwell, H. K., Martinez, L., Gold, P., Hu, S. B., & Young 3rd, W. S. (2007). Vasopressin 1a receptor knockout mice have a subtle olfactory deficit but normal aggression. *Genes, Brain, and Behavior*, *6*(6), 540–551. doi:10.1111/j.1601-183X.2006.00281.x

Wersinger, S. R., Kelliher, K. R., Zufall, F., Lolait, S. J., O'Carroll, A. M., & Young 3rd, W. S. (2004). Social motivation is reduced in vasopressin 1b receptor null mice despite normal performance in an olfactory discrimination task. *Hormones and Behavior*, *46*(5), 638–645. doi:10.1016/j.yhbeh.2004.07.004

Wersinger, S. R., R. Kelliher, K., Zufall, F., Lolait, S. J., O'Carroll, A. M., & Young, W. S. (2004). Social motivation is reduced in vasopressin 1b receptor null mice despite normal performance in an olfactory discrimination task. *Hormones and Behavior*, *46*(5), 638–645. doi:10.1016/j.yhbeh.2004.07.004

Whitnall, M. H., Key, S., Ben-Barak, Y., Ozato, K., & Gainer, H. (1985). Neurophysin in the hypothalamo-neurohypophysial system. II. Immunocytochemical studies of the ontogeny of oxytocinergic and vasopressinergic neurons. *The Journal of Neuroscience : The Official Journal of the Society for Neuroscience*, *5*(1), 98–109.

Wiegand, V., & Gimpl, G. (2012). Specification of the cholesterol interaction with the oxytocin receptor using a chimeric receptor approach. *European Journal of Pharmacology*, *676*(1-3), 12–19. doi:10.1016/j.ejphar.2011.11.041

Wilson, E. O., & Hölldobler, B. (2005). Eusociality: origin and consequences. *Proceedings of the National Academy of Sciences of the United States of America*, *102*(38), 13367–13371. doi:10.1073/pnas.0505858102

Xi, D., Kusano, K., & Gainer, H. (1999). Quantitative analysis of oxytocin and vasopressin messenger ribonucleic acids in single magnocellular neurons isolated from supraoptic nucleus of rat hypothalamus. *Endocrinology*, *140*(10), 4677–4682. doi:10.1210/en.140.10.4677

Xiao, M., Ding, J., Wu, L., Han, Q., Wang, H., Zuo, G., & Hu, G. (2005). The distribution of neural nitric oxide synthase-positive cerebrospinal fluid-contacting neurons in the third ventricular wall of male rats and coexistence with vasopressin or oxytocin. *Brain Research*, *1038*(2), 150–162. doi:10.1016/j.brainres.2005.01.032

Xu, L., Pan, Y., Young, K. a., Wang, Z., & Zhang, Z. (2010). Oxytocin and vasopressin immunoreactive staining in the brains of Brandt's voles (Lasiopodomys brandtii) and greater long-tailed hamsters (Tscherskia triton). *Neuroscience*, *169*(3), 1235–1247. doi:10.1016/j.neuroscience.2010.05.064

Xu, X., Coats, J. K., Yang, C. F., Wang, A., Ahmed, O. M., Alvarado, M., … Shah, N. M. (2012). Modular genetic control of sexually dimorphic behaviors. *Cell*, *148*(3), 596–607. doi:10.1016/j.cell.2011.12.018

Yang, J., Liang, J. Y., Li, P., Pan, Y. J., Qiu, P. Y., Zhang, J., … Wang, D. X. (2011). Oxytocin in the periaqueductal gray participates in pain modulation in the rat by influencing endogenous opiate peptides. *Peptides*, *32*(6), 1255–1261. doi:10.1016/j.peptides.2011.03.007

Yayou, K.-I., Ito, S., & Yamamoto, N. (2015). Relationships between postnatal plasma oxytocin concentrations and social behaviors in cattle. *Animal Science Journal = Nihon Chikusan Gakkaiho*. doi:10.1111/asj.12363

Yoshida, M., Takayanagi, Y., Inoue, K., Kimura, T., Young, L. J., Onaka, T., & Nishimori, K. (2009). Evidence that oxytocin exerts anxiolytic effects via oxytocin receptor expressed in serotonergic neurons in mice. *The Journal of Neuroscience : The Official Journal of the Society for Neuroscience*, *29*(7), 2259–2271. doi:10.1523/JNEUROSCI.5593-08.2009

Young, L. J., Nilsen, R., Waymire, K. G., MacGregor, G. R., & Insel, T. R. (1999). Increased affiliative response to vasopressin in mice expressing the V1a receptor from a monogamous vole. *Nature*, *400*(6746), 766–768. doi:10.1038/23475

Young, L. J., Toloczko, D., & Insel, T. R. (1999). Localization of vasopressin (V1a) receptor binding and mRNA in the rhesus monkey brain. *Journal of Neuroendocrinology*, *11*(4), 291–297.

Young, L. J., & Wang, Z. (2004). The neurobiology of pair bonding. *Nature Neuroscience*, *7*(10), 1048–1054. doi:10.1038/nn1327

Zahm, D. S., Williams, E., & Wohltmann, C. (1996). Ventral striatopallidothalamic projection: IV. Relative involvements of neurochemically distinct subterritories in the ventral pallidum and adjacent parts of the rostroventral forebrain. *Journal of Comparative Neurology*, *364*(2), 340–362. doi:10.1002/(SICI)1096-9861(19960108)364:2<340::AID-CNE11>3.0.CO;2-T

Zoli, M., & Agnati, L. F. (1996). Wiring and volume transmission in the central nervous system: The concept of closed and open synapses. *Progress in Neurobiology*. doi:10.1016/S0301-0082(96)00020-2